

Contract No:

This document was prepared in conjunction with work accomplished under Contract No. 89303321CEM000080 with the U.S. Department of Energy (DOE) Office of Environmental Management (EM).

Disclaimer:

This work was prepared under an agreement with and funded by the U.S. Government. Neither the U.S. Government or its employees, nor any of its contractors, subcontractors or their employees, makes any express or implied:

- 1) warranty or assumes any legal liability for the accuracy, completeness, or for the use or results of such use of any information, product, or process disclosed; or
- 2) representation that such use or results of such use would not infringe privately owned rights; or
- 3) endorsement or recommendation of any specifically identified commercial product, process, or service.

Any views and opinions of authors expressed in this work do not necessarily state or reflect those of the United States Government, or its contractors, or subcontractors.



**Savannah River
National Laboratory®**

A U.S. DEPARTMENT OF ENERGY NATIONAL LAB • SAVANNAH RIVER SITE • AIKEN, SC • USA

Characterization of the Soluble and Insoluble Portions of Solids from the Salt Waste Processing Facility Tank 201 and Tank 202 Samples

L. N. Oji

F. Fondeur

January 2023

SRNL-STI-2022-00145, Revision 2

SRNL.DOE.GOV

DISCLAIMER

This work was prepared under an agreement with and funded by the U.S. Government. Neither the U.S. Government or its employees, nor any of its contractors, subcontractors or their employees, makes any express or implied:

1. warranty or assumes any legal liability for the accuracy, completeness, or for the use or results of such use of any information, product, or process disclosed; or
2. representation that such use or results of such use would not infringe privately owned rights; or
3. endorsement or recommendation of any specifically identified commercial product, process, or service.

Any views and opinions of authors expressed in this work do not necessarily state or reflect those of the United States Government, or its contractors, or subcontractors.

Printed in the United States of America

**Prepared for
U.S. Department of Energy**

Keywords: *SWPF Feed chemistry, Tank Farm, Tanks 201 and 202 solids*

Retention: *Permanent*

Characterization of the Soluble and Insoluble Portions of Solids from the Salt Waste Processing Facility Tank 201 and Tank 202 Samples

L. N. Oji
F. Fondeur

January 2023

Savannah River National Laboratory is operated by Battelle Savannah River Alliance for the U.S. Department of Energy under Contract No. 89303321CEM000080.



| LIST OF REVISIONS | | |
|--------------------------|---------------------------------------------------------------------------------------------------------------------------------------------------------|------------|
| Revision Number | Summary of Changes | Date |
| 0 | Initial Issue | April 2022 |
| 1 | The analytical result for total mercury was updated to 4.89E+04 mg/L as shown in Table 1, page 14, conclusion, and executive summary sections. | May 2022 |
| 2 | SEM/EDX Spectra for the “as-received” March 2022 Tank 202 solids WITHOUT acid Leaching- section 4.0 | June 2022 |
| 2 | XRD and SEM characterization of March 2022 Tank 202 Acid Leached Residual Solids section 5.0 | June 2022 |
| 2 | FT-IR and ¹ H NMR characterization of the March 2022 Tank 202 solids Acid Leached Residual Solids section 5.1.1 | June 2022 |
| 2 | March 2022 Tank 202 Acid Leached Residual Solids: Particle Size Analysis and Elemental Compositions. Section 5.1.2 | June 2022 |
| 2 | Apparent buoyancy of organic solvent leached April 2022 Tank 202 Solids fraction in “mother liquor”-Section 6.0 | May 2022 |
| 2 | ¹ H NMR/FT-IR characterization of organic emulsion layer for the April 2022 Tank 202 sample section 6.1.1 | June 2022 |
| 2 | Elemental composition of the organic emulsion layer for the April 2022 Tank 202 solids sample 6.1.2 | June 2022 |
| 2 | Tank 202 solid fraction sample in water, and dichloromethane Section 6.1.3 | June 2022 |
| 2 | Miscellaneous analysis of the “as-received” March 2022 Tank 202 sample and RCRA metals-Section 7.0 | June 2022 |
| 2 | Updated information on the analytical results for Ag, W and Pb based on ICP-MS data for March 2022 Tank 202 elemental composition section 5.0, Table 4. | June 2022 |

ACKNOWLEDGEMENTS

The authors extend thanks to several members of the SRNL Shielded Cell Operation and Analytical Development (AD) programs who assembled the test equipment, ran the experiments, and provided analytical results, specifically Henry Ajo, Catherine Housley, Julie Fawbush, and Shirley McCollum.

EXECUTIVE SUMMARY

The Salt Waste Processing Facility (SWPF) Tank 201 and Tank 202 samples have been characterized using X-ray diffraction (XRD), scanning electron microscope/energy dispersive x-ray (SEM/EDX), particle size analysis (PSA-Microtrac), Fourier transform-infrared (FT-IR) and nuclear magnetic resonance (^1H NMR) spectroscopic techniques to characterize and identify organic and inorganic components in Tanks 201 and 202 as part of efforts to understand the problems occurring at SWPF due to the presence of solids in the recovered solvent.

The key characterization results from the Tank 201 and Tank 202 includes the following.

- The December 2021 Tank 201 sample, collected from the Tank 201 decontaminated salt solution coalescer, was a small amount of grey slurry (paste), with no observed free-standing liquid, while the December 2021 Tank 202 sample, came in a glass vial with two phases: a liquid layer at the bottom and a floating organic emulsion layer at the top.
- The lower liquid phase of the December 2021 Tank 202 sample was a caustic solution with a pH of 14 or greater (pH is ≥ 14) and a density of 1.05 g/mL (0.32 %RSD).
- The March and April 2022 Tank 202 samples were slurry samples, which eventually settled to a solid fraction and a liquid fraction, consisting of mostly caustic side solvent extraction solvent at the top.
- XRD data for the December 2021 Tank 201 and Tank 202 samples show the presence of both amorphous and crystalline mineral phases. For the Tank 201 sample, the identified crystalline minerals include titanium oxide (TiO_2), bayerite [$\text{Al}(\text{OH})_3$], and sodium nitrate (NaNO_3). The identified crystalline minerals in the Tank 202 air-dried organic emulsion were sodium nitrate (NaNO_3), thermonitrite ($\text{Na}_2\text{CO}_3 \cdot \text{H}_2\text{O}$), and trona ($\text{Na}_3\text{H}(\text{CO}_3)_2 \cdot 2\text{H}_2\text{O}$).
- The SEM/EDX elemental compositions for the December 2021 Tank 201 sample include F (seen almost everywhere and believed to be coming from the modifier), Hg, and Ti, from many locations within the SEM photo images. Additionally, elements found in previous SWPF samples Na, Al, Si, Fe, and Cu are present with Fe and Cu only in relatively small amounts. The predominant SEM/EDX elements present in the December 2021 Tank 202 sample were F, Na, Al, Mg, Si, Hg, Ca, Ti, Fe, and W (tungsten).
- The XRD mineral content for both the March 2022 acid leached Tank 202 solids and the “as-received” March 2022 Tank 202 solids were identical and showed the presence of gibbsite, quartz, and tungsten carbide.
- The principal SEM/EDX elemental compositions for the March 2022 Tank 202 sample also include F, Na, Al, Mg, Si, Hg, Cr, Ca, Ti, Fe, and W.
- The presence elemental tungsten (W) and tungsten mineral (tungsten carbide) in the Tank 202 samples (December 2021, and March 2022 samples) were also confirmed by SEM/EDX, XRD and ICP-MS characterizations and the source of this elemental tungsten or its carbide mineral is not known.
- The particle size distribution for the December 2021 Tank 201 solids show a near gaussian distribution of particles with particle sizes ranging from 2.75 microns to 31.11 microns and the mean particle size at 14.8 microns, with the most abundant particle size being the 18.5 microns. The particle size distribution for the March 2022 Tank 202 acid leached residual solid samples were like that of the December 2021 Tank 201 sample. The particle size distribution also showed a near gaussian distribution of particles with the particle range from 0.972 to 31.11 microns. The mode or highest peak in the distribution is 15.56 microns and the mean particle size of 11.56 micron (SD = 6.33 microns).

- The particle size characterization for the December 2021 Tank 202 liquid portion indicated that no measurable particles were detected in the liquid, which means the particles present, if any, were below the instrument detection limit of 0.243 microns.
- Three of the RCRA elements (Cd, at 5.95 mg/L, Cr at 337 mg/L and Hg at 4.89E+04 mg /L) for the December 2021 Tank 201 sample were above their RCRA limits of 1.0 mg/L, 5 mg/L, and 0.2 mg/L, respectively.
- Of the eight RCRA monitored metals (As, Ba, Cd, Cr, Pb, Hg, Se, Ag), only total mercury at a concentration of 49.1 mg/L was above the RCRA metals concentration limits of 0.2 mg/L in the December 2021 Tank 202 liquid sample portion.
- All but three of the RCRA metals for the March 2022 Tank 202 sample were above RCRA/TCLP limit. The concentrations for Ba, Cd, Cr, Pb, and total mercury in the March 2022 Tank 202 sample were all higher than their RCRA limits and measured 2.24E+02 mg/L, 3.74E+01 mg/L, 4.24E+03 mg/L, < 3.03E+02 mg/L, and 1.56E+05 mg/L, respectively. The RCRA limits for these metals (Ba, Cd, Cr, Pb, and total mercury) are 100 mg/L, 1.0 mg/L, 5 mg/L, 5 mg/L and 0.2 mg/L, respectively. Only Ag (< 7.85E-01 mg/L), As (5.62E-01 mg/L), and Se (< 2.73E-01 mg/l) were below the RCRA limit requirement of 5 mg/L, 5 mg/L and 1.0 mg/L, respectively.
- Based on the elemental concentrations and molar ratios for select elements (Na/Ti, Na/Al, Na/Fe, Ti/Al, Ti/Fe and Al/Fe), the December 2021 Tank 201 sample solids is different from the March 2022 Tank 202 sample solids.
- Infrared (FT-IR) characterization of the December 2021 Tank 201 identified the presence of inorganic compounds, mainly bayerite/ gibbsite ($\text{Al}(\text{OH})_3$), carbonates, and nitrates, while the FT-IR characterization of the December 2021 Tank 202 air-dried organic emulsion sample identified a mixture of multi-cations (Na, Ca, Mg, Fe and Al) and double anions salts (CO_3^{2-} , NO_3^-).
- The ^1H NMR characterization of the December 2021 Tank 201 sample confirmed the presence of two main organic components. These organic compounds include the modifier (Cs-7SB) and ordinary non silicon grease, while the identified ^1H NMR spectra components for the partially water-soluble organic components of the Tank 201 sample included the modifier and sec. butylphenol, which is a known radiolytic decomposition product of the modifier.
- The ^1H NMR characterization of the air-dried December 2021 Tank 202 emulsion sample, with chloroform extraction, identified mainly the modifier (Cs-7SB). ^1H NMR spectra for water extracted air-dried Tank 202 emulsion sample showed two water soluble components, mainly sec. butyl phenol, and formate. Additionally, traces of BOBCalixC6, and aliphatic fluorides were also identified. The sec. butyl phenol and formates are probably decomposition products from the modifier.
- The 1.0 M nitric acid leaching of the March 2022 Tank 202 sample did not show any measurable effect on the mineral structure of the identified minerals tungsten carbide (WC), gibbsite [$\text{Al}(\text{OH})_3$], and quartz (SiO_2).
- The three Tanks 201 and Tank 202 samples (December Tank 201, December Tank 202, and March 2022 Tank 202) are different in their XRD patterns and mineralogy. The March 2022 Tank 202 sample contained more crystalline minerals and thus less amorphous phases.
- The XRD spectrum for the acid leached March Tank 202 solid fraction showed a smaller background shift due to the presence amorphous minerals when compared to the background shift in the XRD spectrum for the “as-received” March 2022 Tank 202 solid fraction, which would seem to indicate that the amorphous layers (organic layers) of the Tank 202 sample may be degraded in the acid leaching process.
- The ^1H NMR spectra for the nitric acid leached March 2022 Tank 202 solids fraction unexpectedly showed that the 1.0 M nitric acid leaching of the March 2022 Tank 202 solid fraction resulted in significant modification/degradation of the molecular structure of the Cs-7SB modifier. The fluorinated tails of the molecule and the ter-butyl groups were now missing with the nitric acid leaching of the Tank 202 solid fraction. This observation is contrary to other study results, based

on simulant salt solutions, which indicate marginal degradation of the modifier at 30 and 60 °C for extended contact times. At this time, it is uncertain what causes the degradation of solvent components (Cs-7SB modifier) in nitric acid; however, it is possible that the degradation observed in nitric acid leaching is due to irregular chemistry (i.e., transition metal catalytic reactions).

- Three components were identified in the FT-IR data for nitric acid leached March 2022 Tank 202 residual solids, and these include the modifier, sec. butyl phenol (a decomposition product) and heavy metal nitrates (possibly from the nitric acid leaching) and carbonates.
- The ^1H NMR spectra for the organic (dichloromethane) leached March 2022 Tank 202 sample showed mainly decomposition products for the modifier and BobcalixC6, which includes propylene glycol group, grease, and ter-butyl alcohol, while the ^1H NMR spectra for the water extracted March 2022 Tank 202 sample identified the presence of the modifier and decomposition products, sec. butyl phenol and acetic acid/ acetone.
- The SEM/EDX identified elemental compositions for the acid leached March 2022 Tank 202 sample is not different from that of the “as- received” March 2022 Tank 202. The principal elemental compositions are similar and include F, Na, W, Ti, Fe, Al, Si, and total Hg.
- The leaching of the organic components in the April 2022 Tank 202 sample with dichloromethane resulted in the formation of an organic emulsion layer, which floated on the dichloromethane organic solvent and a slurry solids layer at the bottom of the container.
- The elemental components for the “as-received” April 2022 Tank 202 solids fraction are also present in measurable quantities in the organic emulsion layer and interstitial liquids, although in relatively lower concentrations. The concentrations for select elements, namely Al, Cd, Fe, Cr, Na, Ni, S, Ti, Zn, W and Hg are 1.19E+01mg/L, 2.07E-01 mg/L, 1.77E+01mg/L, 1.23E+02 mg/L, 6.04E+02 mg/L, 9.98E+00 mg/L, 3.65E+00 mg/L, 6.18E+02 mg/L, 9.22E-01 mg/L, 7.40E+01 mg/L, and 1.76E+03 mg/L, respectively.
- The April 2022 Tank 202 organic solvent leached solids, when introduced into a 50 mL capacity graduated cylinder containing Tank 202 filtrate (mother liquor) did not show any signs of floating and readily sank to the bottom of the graduated cylinder. This confirms that the organic solvent leached Tank 202 solids density was greater than the density of the mother liquor.
- The April 2022 Tank 202 solid fraction was immiscible with water probably due to the high mercury and organic material content of the solids fraction.
- The blending of water with the April 2022 Tank 202 solid fraction sample and dichloromethane, after 24 hours of settling of the mixture, resulted in the formation of two extra phases: an organic phase on top of the water (possibly an organic decomposition product), and an organic phase at the water-dichloromethane interface layer and considered to be the modifier or decomposition products.

The main insoluble inorganic submicron particles identified in the SWPF Tanks 201, and 202 samples include mercuric oxide (HgO), titanium oxide (TiO_2), iron oxides/hydroxides ($\text{Fe}_3\text{O}_4/\text{Fe}_2\text{O}_3$), gibbsite [$\text{Al}(\text{OH})_3$], zinc oxide (ZnO), and even tungsten carbide (WC). These inorganic particles are not only present in the solid and liquid fractions of these Tank 201 and Tank 202 samples, but also in the organic emulsions in each SWPF tank samples sent for characterization. Mercuric oxide (HgO), titanium oxide (TiO_2) and iron oxides/hydroxides ($\text{Fe}_3\text{O}_4/\text{Fe}_2\text{O}_3$), particles are the most abundant particles based on their weight percent composition in each sample. These insoluble inorganic submicron particles may be responsible for the occasional plugging of the SWPF crossflow filtration system.

Aqueous media soluble salts, mostly sodium salts identified in these tank samples, include sodium nitrate, sodium carbonate, and sodium bicarbonate, while the caustic side solvent extraction organic compounds

identified include the modifier (Cs-7B), BobCalixC6, Isopar-L, and radiolytic decomposition products including formates, sec. butyl phenol, fluorinated aliphatic compounds, acetic acid, acetone, and propylene ether.

The aqueous chemistry for the SWPF tank contents suggests that insoluble mercuric oxide particles (HgO), and transition metal particles (Fe_3O_4 and TiO_2), which can foul the crossflow filtrations systems, may be readily formed in the SWPF tanks. Thus, since the potential for the formation of these insoluble mercury submicron particles, especially mercuric oxide, and titanium oxide exists in the SWPF tanks, it is recommended that both the mercury and monosodium titanate (MST) loadings in the feeds be evaluated to determine if it is possible to lower their concentrations/quantity to minimize the formation of HgO and TiO_2 .

TABLE OF CONTENTS

| | |
|---------------------------------------------------------------------------------------------------------------------------------------------------------------------------------------|----|
| 1.0 Introduction..... | 1 |
| 2.0 Experimental Setups/Sample description..... | 1 |
| 3.0 Results and Discussion | 5 |
| 3.1.1 December 2021 Tank 201 XRD and SEM characterizations..... | 5 |
| 3.1.2 FT-IR and ¹ H NMR characterization of the December 2021 Tank 201 solids | 9 |
| 3.1.3 Particle Size Analysis and Elemental Composition for the December 2021 Tank 201 Solids .. | 12 |
| 3.1.4 Characterization of Tank 202 Organic Emulsion Layer and liquid portion (December 2021 sample)..... | 15 |
| 3.1.5 XRD and SEM characterization of the December 2021 Tank 202 solids..... | 15 |
| 3.1.6 FT-IR and ¹ H NMR characterization of the December 2021 Tank 202 emulsion layer | 18 |
| 3.1.7 Particle Size Analysis and Elemental Composition for the December 2021 Tank 202 Liquid Fraction | 21 |
| 4.0 SEM/EDX Spectra for the “as-received” March 2022 Tank 202 solids WITHOUT acid Leaching | 22 |
| 5.0 Characterization of March 2022 Tank 202 Solids-Acid Leached Samples | 26 |
| 5.1 <i>XRD and SEM characterization of March 2022 Tank 202 Acid Leached Residual Solids</i> | 26 |
| 5.1.1 FT-IR and ¹ H NMR characterization of the March 2022 Tank 202 solids Acid Leached Residual Solids..... | 31 |
| 5.1.2 March 2022 Tank 202 Acid Leached Residual Solids: Particle Size Analysis and Leachate Elemental Compositions | 34 |
| 6.0 Apparent buoyancy of organic solvent leached April 2022 Tank 202 Solids fraction in “mother liquor” and ¹ H NMR/FT-IR characterization of organic emulsion layer | 38 |
| 6.1.1 ¹ H NMR/FT-IR characterization of organic emulsion layer for the April 2022 Tank 202 sample | 41 |
| 6.1.2 Elemental composition for the organic emulsion layer for the April 2022 Tank 202 sample ... | 44 |
| 6.1.3 Tank 202 solids fraction in water and dichloromethane | 45 |
| 7.0 Miscellaneous analysis of the “as-received” March 2022 Tank 202 Sample-Elemental Composition | 48 |
| 7.1.1 Data quality presentations for FT-IR and ¹ H NMR based organic analyses..... | 53 |
| 8.0 Conclusions..... | 53 |
| 9.0 Quality Assurance..... | 56 |
| 10.0 References..... | 57 |
| Appendix A: SRNL Scope for the Characterization of the soluble and insoluble portions of solids from SWPF Tank 201 and Tank 202 samples. | 58 |

| | |
|---------------------------------------------------------------------------------------------------------------------------------------------------------------------------------------------|----|
| Appendix B. Molecular structure of Cs-7SB and BobCalixC6..... | 60 |
| Appendix C. FT-IR spectra for gibbsite control blanks showing the presence of extra organic peaks coming from the Shielded Cell oxidized oil grease (in red) and cellulose (in purple)..... | 61 |
| Appendix D. Mass Spectral Analyses of March 2022 Tank 202 Solid fraction..... | 62 |
| Appendix D. Mass Spectral Analyses of March 2022 Tank 202 Solid fraction Continued..... | 63 |
| Appendix D. Mass Spectral Analyses of March 2022 Tank 202 Solid fraction Continued..... | 64 |
| Appendix D2. Mass Spectral Analyses of April 2022 Tank 202 Emulsion Layer..... | 65 |
| Appendix E. Analytical Methods | 68 |

LIST OF TABLES

| | |
|-------------------------------------------------------------------------------------------------------------------|----|
| Table 1. Elemental composition/RCRA metals for the December 2021 Tank 201 acid digested solids. ... | 14 |
| Table 2. Elemental composition and RCRA metals for the December 2021 Tank 202 liquid portion..... | 21 |
| Table 3. Elemental composition for the March 2022 Tank 202 Acid Leachate Solids. | 37 |
| Table 4. Elemental composition for the April 2022 Tank 202 Emulsion Layer..... | 44 |
| Table 5. Elemental composition and RCRA metals for the “as-received” March 2022 Tank 202 solids... | 49 |
| Table 6. Elemental composition comparison between the December 2021 Tank 201 and March 2022 Tank 202 samples..... | 51 |
| Table 7. Summary Information on December 2021 Tank 201 and March 2022 Tank 202 Samples..... | 52 |

LIST OF FIGURES

| | |
|-------------------------------------------------------------------------------------------------------------------------------------------------------------------------------------------------------------------------------------|----|
| Figure 1. Tank 201 and Tank 202 samples (“as-received”)..... | 3 |
| Figure 2. Photo Images of the March 2022 Tank 202 sample. | 4 |
| Figure 3. XRD Spectra for the December 2021 Tank 201 solid particles. | 6 |
| Figure 4. Representative SEM photo image of the December 2021 Tank 201 solid particles, | 7 |
| Figure 5. Representative SEM/EDX elemental composition for SWPF December 2021 Tank 201 solid material. | 8 |
| Figure 6. Representative SEM/EDX elemental composition for SWPF December 2021 Tank 201 solid material. | 9 |
| Figure 7. Overlay FT-IR spectra: “as-received” December 2021 Tank 201 sample: modifier-Cs-7SB (bottom spectrum), grease with modifier (middle spectrum), and inorganics (top spectrum)..... | 10 |
| Figure 8. Overlay ¹ H NMR Spectra for the December 2021 Tank 201 solids after leaching with dichloromethane: organic soluble components include modifier and grease (top spectrum). | 11 |
| Figure 9. Overlay ¹ H NMR Spectra for the December 2021 Tank 201 solids after leaching with Water (water soluble species include modifier (Cs-7SB; bottom spectrum), formate, and sec. butyl phenol (top spectrum))..... | 12 |
| Figure 10. Particle size distribution for the December 2021 Tank 201 solids..... | 13 |
| Figure 11. XRD spectra of the air-dried December 2021 Tank 202 emulsion layer. | 15 |

| | |
|--------------------------------------------------------------------------------------------------------------------------------------------------------------------------------------------------------------------------------|----|
| Figure 12. XRF elemental composition for the December 2021 Tank 202 emulsion phase (X-ray fluorescence (XRF) elementals include elemental peaks for Ti, Hg, Fe, and Cr). | 16 |
| Figure 13. Representative SEM photo image of the December 2021 Tank 202 dry emulsion layer..... | 17 |
| Figure 14. SEM/EDX elemental composition for SWPF December 2021 Tank 202 dry organic emulsion layer. | 17 |
| Figure 15. SEM/EDX elemental composition for SWPF December 2021 Tank 202 dry organic emulsion layer. | 18 |
| Figure 16. Overlay FT-IR spectra for the air-dried December 2021 Tank 202 organic emulsion layer..... | 19 |
| Figure 17. Overlay ^1H NMR spectra: air-dried December 2021 Tank 202 emulsion; organics extracted with chloroform and water extracted peaks (bottom spectrum)..... | 20 |
| Figure 18. Overlay ^1H NMR Spectra: December 2021 Tank 202 air-dried emulsion layer sample-Water extraction (Spectral baseline expanded to show smaller peaks). | 20 |
| Figure 19. Representative SEM photo image for March 2022 “as-received” Tank 202 sample. | 23 |
| Figure 20. Representative SEM/EDX elemental composition for March 2022 “as-received” Tank 202 Sample. | 24 |
| Figure 21. Representative SEM/EDX elemental composition for the March 2022 “as-received” Tank 202 Sample. | 24 |
| Figure 22. Representative SEM/EDX elemental composition for the March 2022 “as-received” Tank 202 Sample. | 25 |
| Figure 23. XRD Spectrum for the “as-received” March 2022 Tank 202 solids WITHOUT acid Leaching. | 26 |
| Figure 24. XRD Spectrum for the March 2022 Tank 202 solids: Acid Leached Residual Solids with minimum baseline shifts due to the absence of more amorphous minerals. | 27 |
| Figure 25. Representative SEM photo image for the March 2022 Tank 202 Acid Leached Residual Solids. | 28 |
| Figure 26. Representative SEM/EDX elemental composition for the March 2022 Tank 202 acid leached residual solids..... | 29 |
| Figure 27. Representative SEM/EDX elemental composition for the March 2022 Tank 202 acid leached residual solids..... | 30 |
| Figure 28. Representative SEM/EDX elemental composition for the March 2022 Tank 202 acid leached residual solids..... | 31 |
| Figure 29. Overlay FT-IR Spectra: Dichloromethane leached March 2022 Tank 202 solids-Post acid Leached Residual Tank 202 solids..... | 32 |
| Figure 30. ^1H NMR Spectra for the March 2022 Tank 202 solids Acid Leached Residual Solids- The modifier has been modified with acid leaching (chloroform soluble organic species)..... | 33 |
| Figure 31. Overlay ^1H NMR Spectra of the March 2022 Tank 202 Acid Leached Residual Solids: Main water-soluble organic species include modifier peaks (bottom spectrum), acetic acid, and acetone (top spectrum)..... | 34 |
| Figure 32. Particle size distribution of the March 2022 Tank 202 solids Acid Leached Residual Solids. . | 36 |
| Figure 33. Post dichloromethane leaching of Tank 202 solids (April 2022 sample)..... | 39 |
| Figure 34. Apparent Buoyancy Test: Dichloromethane leached Tank 202 April 2022 sample in Tank 202 filtrate (Mother liquor)..... | 40 |
| Figure 35. FT-IR spectra of the original emulsion layer (top layer) as seen in Figure 33, insert C..... | 41 |

| | |
|--------------------------------------------------------------------------------------------------------------------------------------------------------------------------------------------------------------------------|----|
| Figure 36. FT-IR spectra of the partitioned three-layer extract of the emulsion layer as seen in Figure 33, insert D..... | 42 |
| Figure 37. Overlay ¹ H NMR spectrum for reference Isopar-L, reference modifier and Tank 202 yellow tinted partition layer (second layer) of the extracted emulsion layer as seen in Figure 33, insert D. | 43 |
| Figure 38. April 2022 Tank 202 solids fraction in water and dichloromethane without agitation. | 46 |
| Figure 39. April 2022 Tank 202 solids fraction in water and dichloromethane with mixing and agitation. | 47 |

LIST OF ABBREVIATIONS

| | |
|--------------------|---------------------------------------------------------|
| AQR | aqua regia digestion |
| CSSX | caustic side solvent extraction |
| DMA | Direct mercury analysis |
| FT-IR | Fourier transform infrared |
| ICP-AES | inductively coupled plasma atomic emission spectroscopy |
| ICP-MS | inductively coupled plasma mass spectrometry |
| IDL | instrument detection limit |
| MST | Monosodium titanate |
| ¹ H NMR | Nuclear magnetic resonance (Proton NMR) |
| PSA | Particle size analysis |
| RCRA | Resource Conservation and Recovery Act |
| SaM | Sensing and Metrology |
| SEM/EDX | scanning electron microscope/energy dispersive x-ray |
| SRMC | Savannah River Mission Completion |
| SRNL | Savannah River National Laboratory |
| SRR | Savannah River Remediation |
| SRS | Savannah River Site |
| SWPF | Salt Waste Processing Facility |
| TCLP | Toxicity Characteristic Leaching Procedure |
| XRD | x-ray diffraction |
| DMA | Direct mercury analysis |

1.0 Introduction

The Savannah River Site (SRS) Salt Waste Processing facility (SWPF) is designed to process batches of radioactive salt solutions with monosodium titanate (MST) acting as the actinide removal adsorbent. This process is followed by crossflow filtration to concentrate and remove the MST solids and the resulting filtrate is processed through the contactors to remove cesium prior to eventual disposal in the SRS Salt-Stone grout.

The work scope for these SWPF samples involves the characterization/observation of specific physical changes of the “as-received” (raw sample solids) from the December 2021 Tanks 201 and 202 samples, the March, and April 2022 Tank 202 samples. Where required, these SWPF Tank samples were to be characterized using x-ray diffraction (XRD),* scanning electron microscope/energy dispersive x-ray (SEM/EDX), particle size analysis (PSA-Microtrac), Fourier transform-infrared (FT-IR) and nuclear magnetic resonance (^1H NMR) spectroscopic techniques and inductively coupled plasma atomic emission spectroscopy/ inductively coupled plasma mass spectrometry (ICP-AES/ICP-MS) to characterize and identify organic and inorganic components in the SWPF Tanks 201 and 202 samples as part of efforts to understand the problems occurring at SWPF due to the presence of solids in the recovered solvent. In late December 2021, Parsons sent Savannah River National Laboratory (SRNL) two SWPF samples from Tank 201 and Tank 202 for these spectroscopic characterizations. Two other Tank 202 samples, one in March and the other in April of 2022, were also sent to SRNL for further characterizations and processing evaluations such as acid leaching (March 2022 Tank 202 sample), apparent buoyancy test and interaction with ordinary water and an organic solvent using the April 2022 Tank 202 sample solids.

Objectives

The SWPF customer requested the characterization of the “as-received” Tanks 201 and 202 samples (December 2021, March 2022, and April 2022 samples) as summarized in tasks 1a, 1b, 1c, 1d, and 2a in Appendix A. Tasks 2b-2d were not performed because of insufficient December 2021 Tank 201 sample solids.

2.0 Experimental Setups/Sample description

The December 2021 Tank 202 sample (S-211201-0021) was collected in SWPF by sampling Tank-202 via Isolok sampler after transferring the contents from Tank-208. The “emulsion” layer containing solids was concentrated by removing some of the clear aqueous sample from the bottom of eight individual vials, which were then combined into one sample vial. Due to the configuration of this tank/pump, the liquid matrix was mostly aqueous. On the other hand, the December 2021 Tank 201 sample was collected from the Tank 201 decontaminated salt solution (DSS) coalescer.

The March 2022 Tank 202 sample (S-220224-00235) was collected directly from a spent filter basket from FLT-250. The FLT-250 solvent adjustment filter was used to remove the solids from the solvent with a 10-micron filter. The liquid matrix in these samples was mostly caustic side solvent extraction (CSSX) solvent. The April 2022 Tank 202 sample apparently came from the same sample batch as the March 2022 Tank 202 sample.

* See Appendix E for analytical method definitions.

Figure 1 is a picture of the “as-received” SWPF Tank 201 and Tank 202 samples. The Tank 201 sample was a small gray slurry sample with no free-standing liquid (Figure 1, insert A), and the Tank 202 sample showed two phases; a liquid layer at the bottom and suspended organic emulsion layer at the top layer (Figure 1, insert B). The Tank 201 sample dose was 5 mRem per hour, while Tank 202 sample dose was 25 mRem per hour. As a result of the high whole-body dose for the Tank 202 sample, its processing for characterizations were performed in the SRNL Shielded Cells. Separation of the suspended fine solids (organic emulsion layer) in the Tank 202 sample was attained by carefully pipetting the bottom layer away from the emulsion layer (see sample photo in Figure 1, insert B and insert C). Figure 1, inserts C and D, show the image of the organic emulsion layer before and after air-drying. The organic emulsion layer contained about 80% interstitial liquid before air drying.

Prior to the preparation of the Tank 202 air-dried emulsion sample for FT-IR analysis, an in-cell gibbsite control mineral in a weighing boat was placed at a strategic location in the Shielded Cells to ensure that the control gibbsite sample was exposed to the same cell environments as the Tank 202 air-drying emulsion sample. The control gibbsite sample container held about 10 grams of the material. The gibbsite control mineral container was opened when the Tank 202 emulsion sample was being air dried or processed and closed at the end of each day of work in the Shielded Cells. At the end of the Tank 202 emulsion drying cycle (96 hours), the gibbsite control material was also prepared in the same manner as the preparation of Tank 202 air-dried emulsion sample and submitted for the same FT-IR analyses as the actual air-dried Tank 202 sample.

The “as-received” March 2022 Tank 202 sample photo images in the SRNL Shielded Cells are shown in Figure 2. Figure 2, insert A, is the picture of the “as-received” March 2022 Tank 202 Sample, while Figure 2, insert B, shows the Tank 202 sample after 24 hours settling. Figure 2, insert C, shows the March 2022 Tank 202 Sample solid fraction solid fraction, ~ 8.9 grams of “wet cake”.

The “as-received” April 2022 Tank 202 sample was only used for the buoyancy test of the solids fraction from the Tank 202 sample after leaching with dichloromethane. Photo images for the “as-received” April 2022 Tank 202 sample and associated buoyancy test are presented in section 6.0.

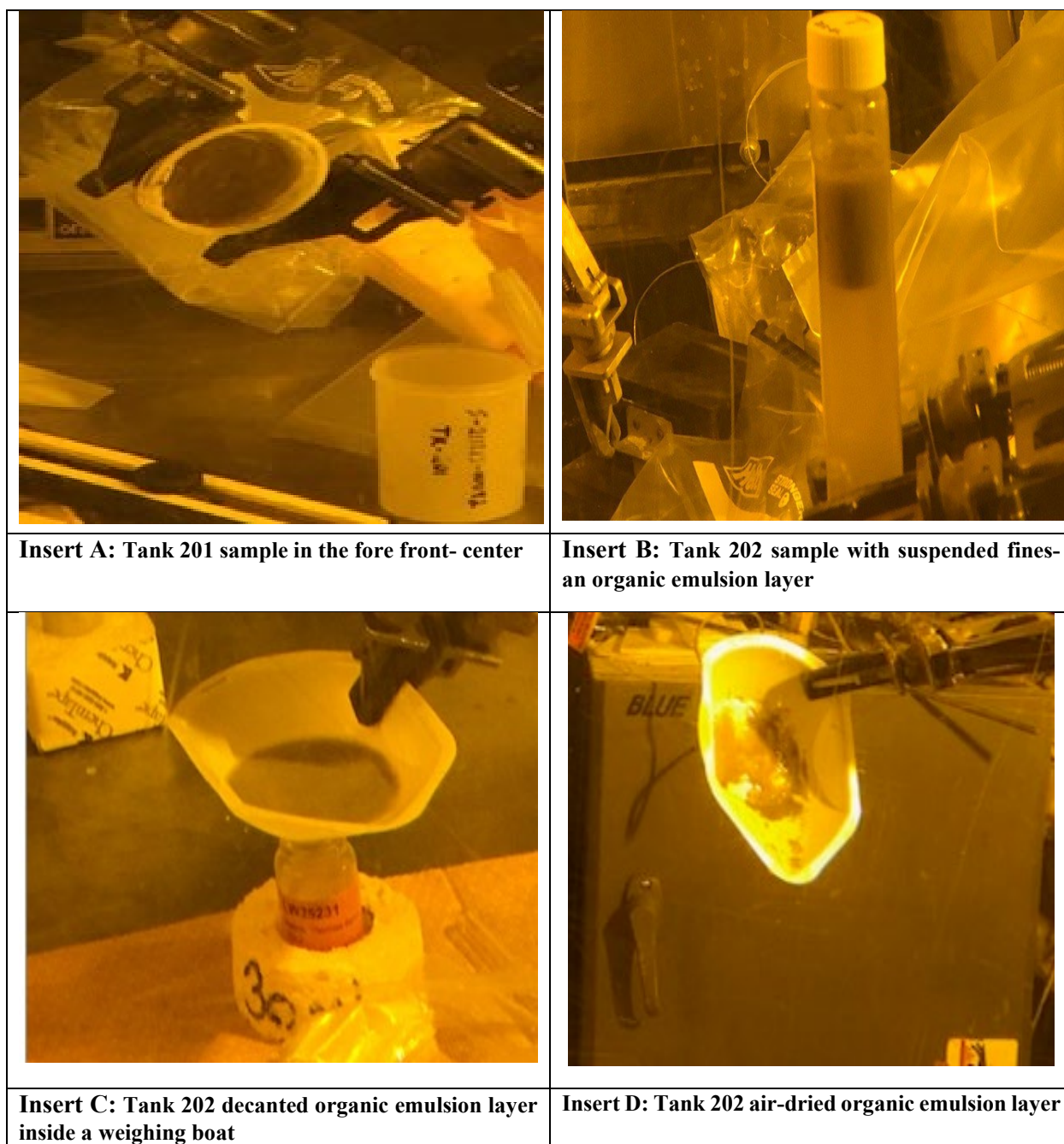


Figure 1. Tank 201 and Tank 202 samples (“as-received”).




| | |
|-------------------------------------------------------------------------------------------------------------|------------------------------------------------------------------------------------|
|  |  |
| <p>Insert A: “As-received” March 2022 Tank 202 Sample</p> | <p>Insert B: Tank 202 sample after 24 hrs. settling. March 2022 sample</p> |
|  | <p>Intentionally left blank</p> |
| <p>Insert C: March 2022 Tank 202 Sample solid fraction solid fraction ~ 8.9 grams of “wet cake”.</p> | |

Figure 2. Photo Images of the March 2022 Tank 202 sample.

3.0 Results and Discussion

No physical measurements such as density was determined for the December 2021 Tank 201 sample because of the limited sample size of the material sent for characterization.

3.1.1 December 2021 Tank 201 XRD and SEM characterizations

The XRD spectra and SEM/EDX images for the SWPF Tank 201 “as-received” sample solids are presented in Figures 3, 4, 5, and 6. The XRD spectra for the SWPF Tank 201 solid, as shown in Figure 3, indicate the presence of a large background shift due to the presence of amorphous and non-crystalline materials along with matching peaks for crystalline inorganic minerals like bayerite $[\text{Al}(\text{OH})_3]$, titanium oxide (TiO_2), and sodium nitrate (NaNO_3). Monosodium titanate (MST), which is the pre-cursor to titanium oxide (TiO_2) is an amorphous, non-crystalline material and thus has a poor XRD spectral signature and is partially responsible for the large background shift in the XRD spectra in Figure 3.

As shown in the representative SEM photographs in Figure 4, the SWPF Tank 201 solids show porous solid materials, which are probably a mixture of the crystalline inorganic salts and CSSX modifier.

The principal SEM/EDX elemental compositions for this SWPF Tank 201 sample, as shown in Figures 5, and 6, are fluorine (F), sodium, (Na), aluminum (Al), silicon (Si), mercury (Hg), titanium (Ti), iron (Fe) and copper (Cu). Elemental fluorine (F) is seen almost everywhere in the solids SEM/EDX photo images of the sample and are probably decomposition products from the modifier (Cs-7SB). Mercury (Hg) and titanium (Ti) are also present in all the SEM/EDX photo images, while both Fe, and Cu are seen occasionally in the images.

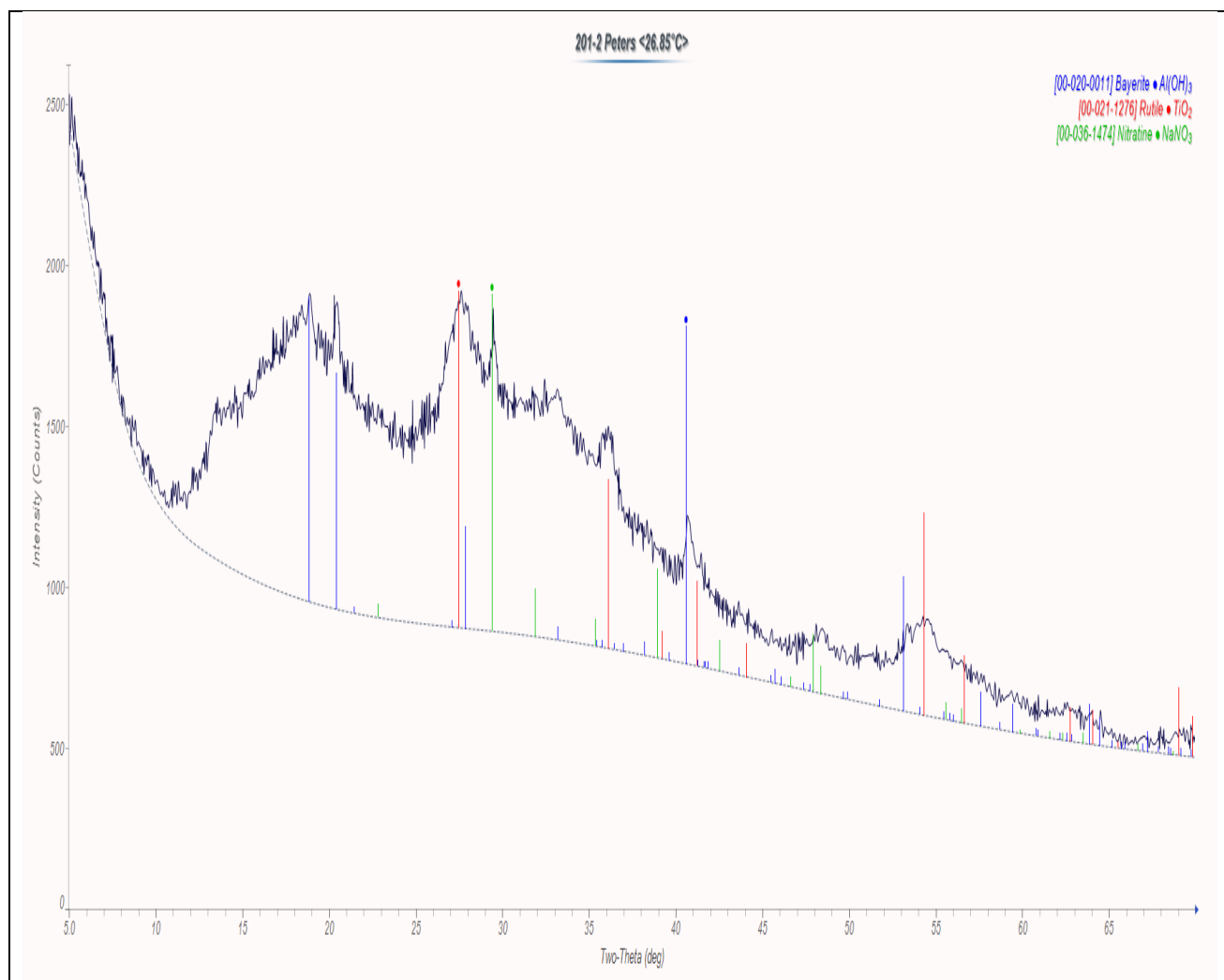


Figure 3. XRD Spectra for the December 2021 Tank 201 solid particles.

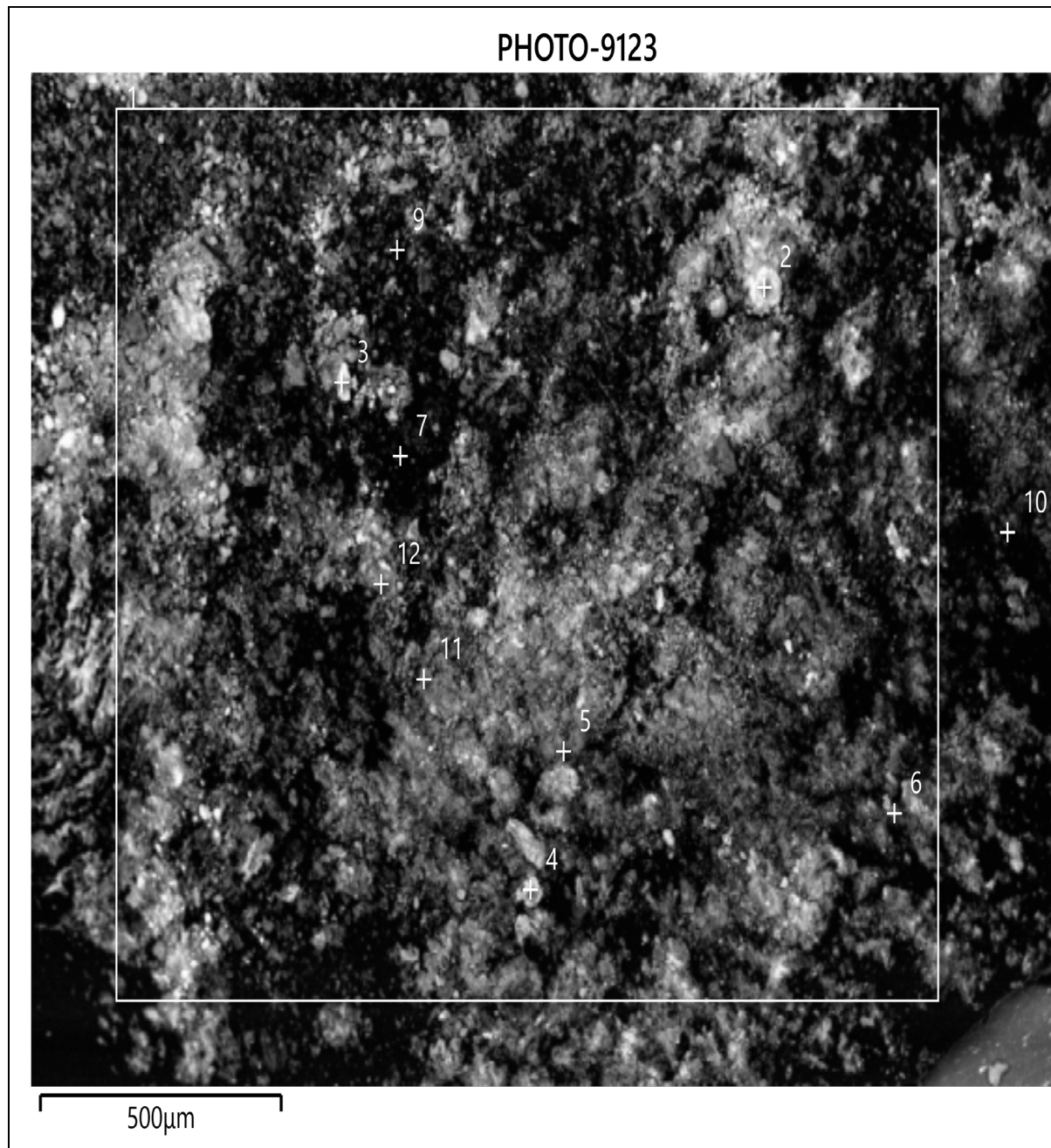


Figure 4. Representative SEM photo image of the December 2021 Tank 201 solid particles,

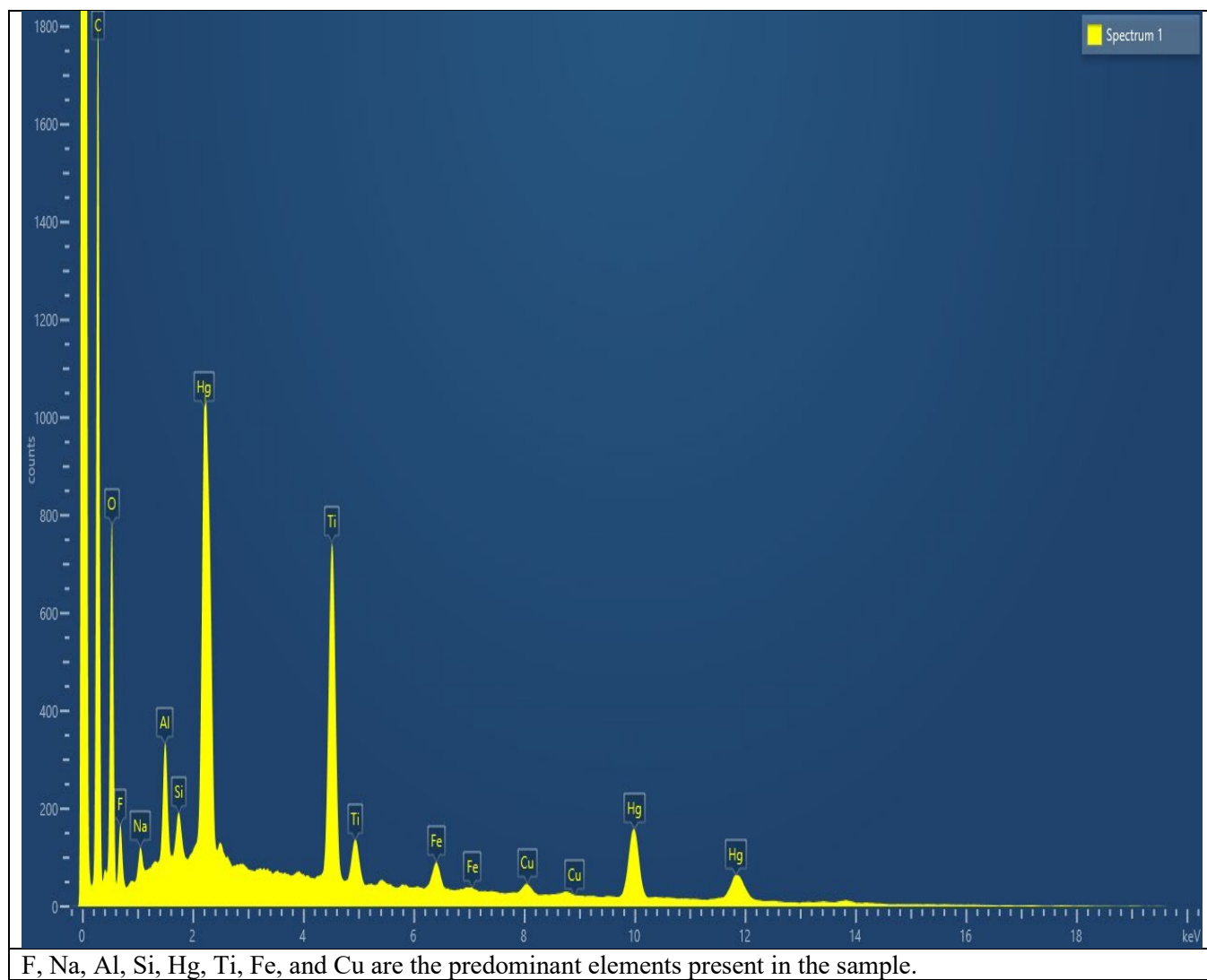


Figure 5. Representative SEM/EDX elemental composition for SWPF December 2021 Tank 201 solid material.

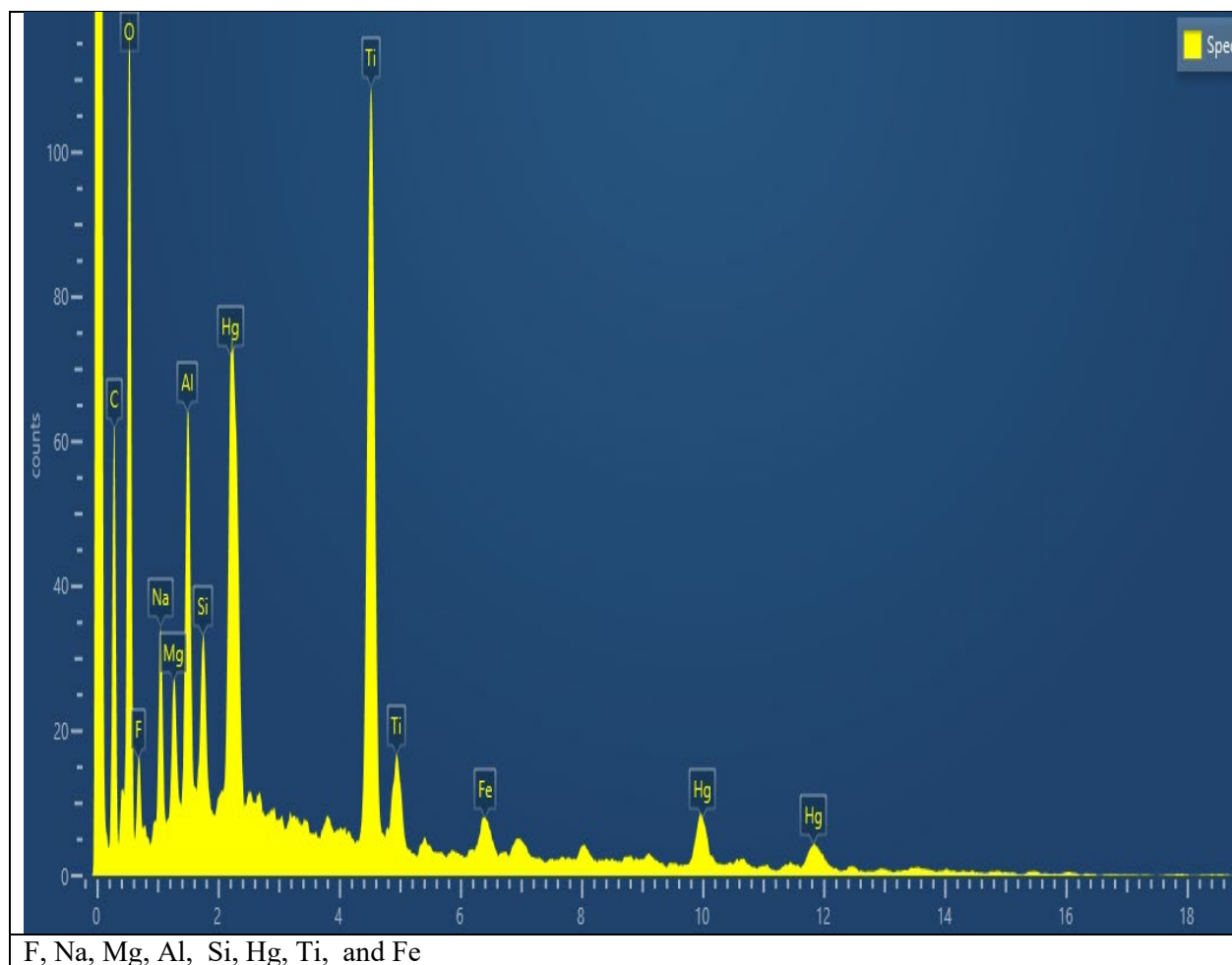


Figure 6. Representative SEM/EDX elemental composition for SWPF December 2021 Tank 201 solid material.

3.1.2 FT-IR and ^1H NMR characterization of the December 2021 Tank 201 solids

The Fourier transform infrared (FT-IR) spectra for the Tank 201 “as-received” sample solid is presented in Figure 7 and it shows the presence of two organic components as well as inorganic compounds. The organic compounds identified include the modifier (Cs-7SB-bottom spectrum) and ordinary grease with modifier (middle spectrum), while the inorganic components are mainly bayerite/ gibbsite ($\text{Al}(\text{OH})_3$), carbonates, and nitrates (top spectrum). The source of the grease in the sample is not known because it does not come from the Shielded Cell environment, where the control blank does not show any detectable grease material. On the other hand, the idea that the radiolytic decomposition/rearrangement of the many organic moieties present in the sample to form a grease-like material cannot be discounted either.

The presence of the modifier in the Tank 201 solids is also confirmed by the presence of elemental fluorine in the SEM/EDX data for the Tank 201 solids; fluorine is part of the molecular structure and thus a decomposition product from the modifier (Appendix B, insert A).

Two approaches were used in the ^1H NMR characterization of the Tank 201 solids. In the first approach, the “as-received” Tank 201 solids material was first leached with an organic solvent (dichloromethane) to isolate and identify by ^1H NMR those organic components which were soluble in an organic solvent. In the second approach, the “as-received” Tank 201 solids were leached with water to isolate and identify by ^1H NMR those components of the “as-received” Tank 201 solids which were water soluble.

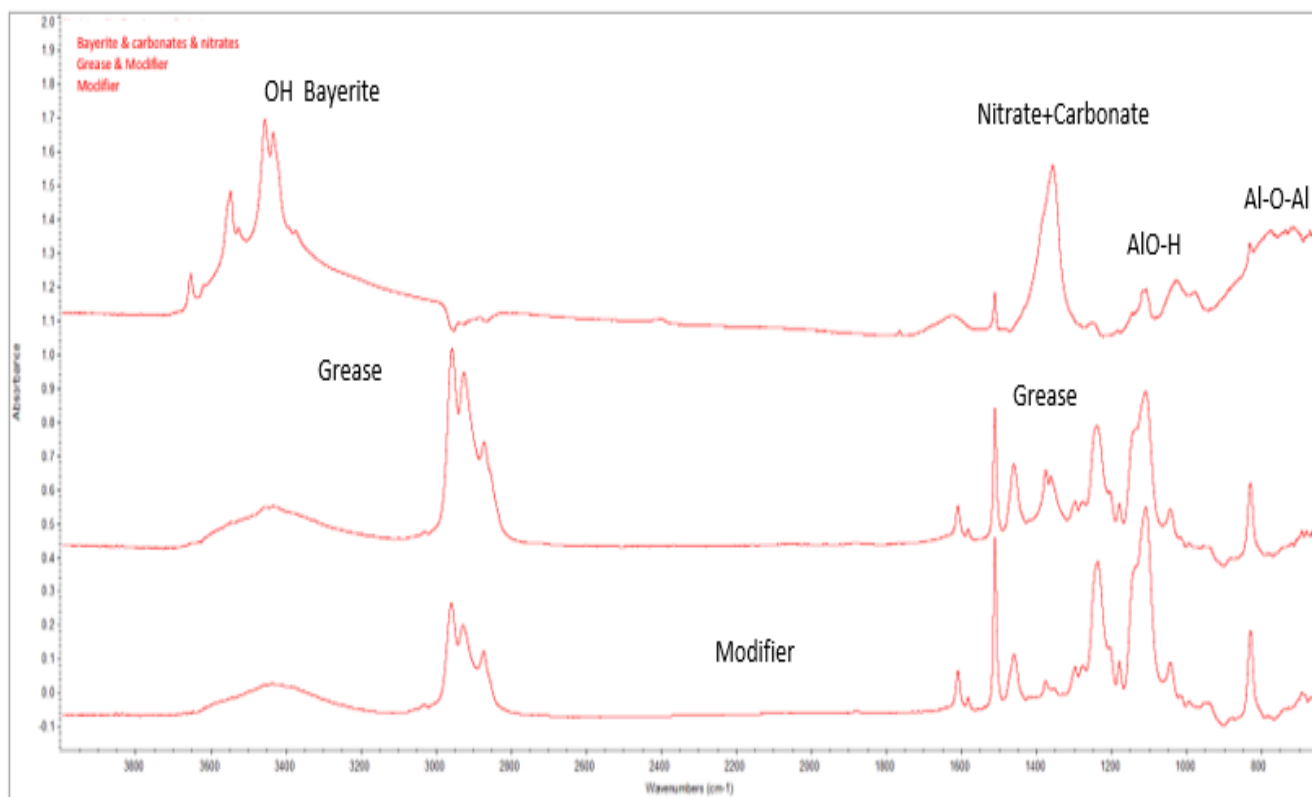


Figure 7. Overlay FT-IR spectra: “as-received” December 2021 Tank 201 sample: modifier-Cs-7SB (bottom spectrum), grease with modifier (middle spectrum), and inorganics (top spectrum).

The ^1H NMR spectral data for the dichloromethane leached Tank 201 solids is presented in Figure 8. The identified matching peaks for the organic soluble components include the modifier and ordinary grease (top spectrum). The bottom spectrum is reference Cs-7SB modifier spectrum. The water-soluble components of the “as-received” Tank 201, as presented in the ^1H NMR spectra peaks in Figure 9 include the modifier (Cs-7SB and traces of the leaching organic dichloromethane peak below 7 ppm). bottom spectrum) and sec. butyl phenol (top spectrum), which may be a decomposition product of the modifier and possibly the cesium extractant BOBCalix6 (although not identified in the figure). The molecular structure of both the modifier and BOBCalixC6 are shown in Appendix B.

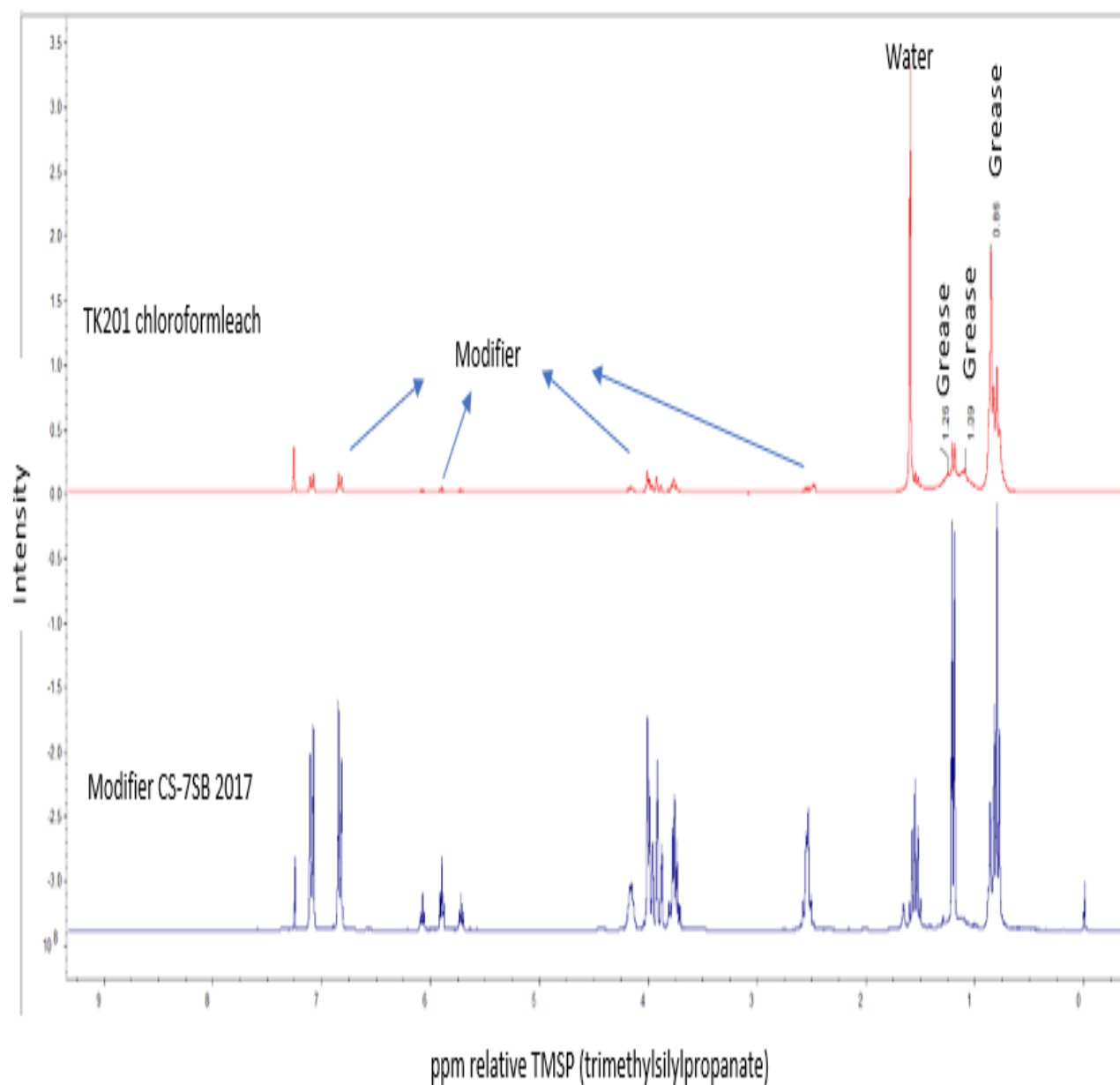


Figure 8. Overlay ^1H NMR Spectra for the December 2021 Tank 201 solids after leaching with dichloromethane: organic soluble components include modifier and grease (top spectrum). Bottom spectrum is reference modifier CS-7SB.

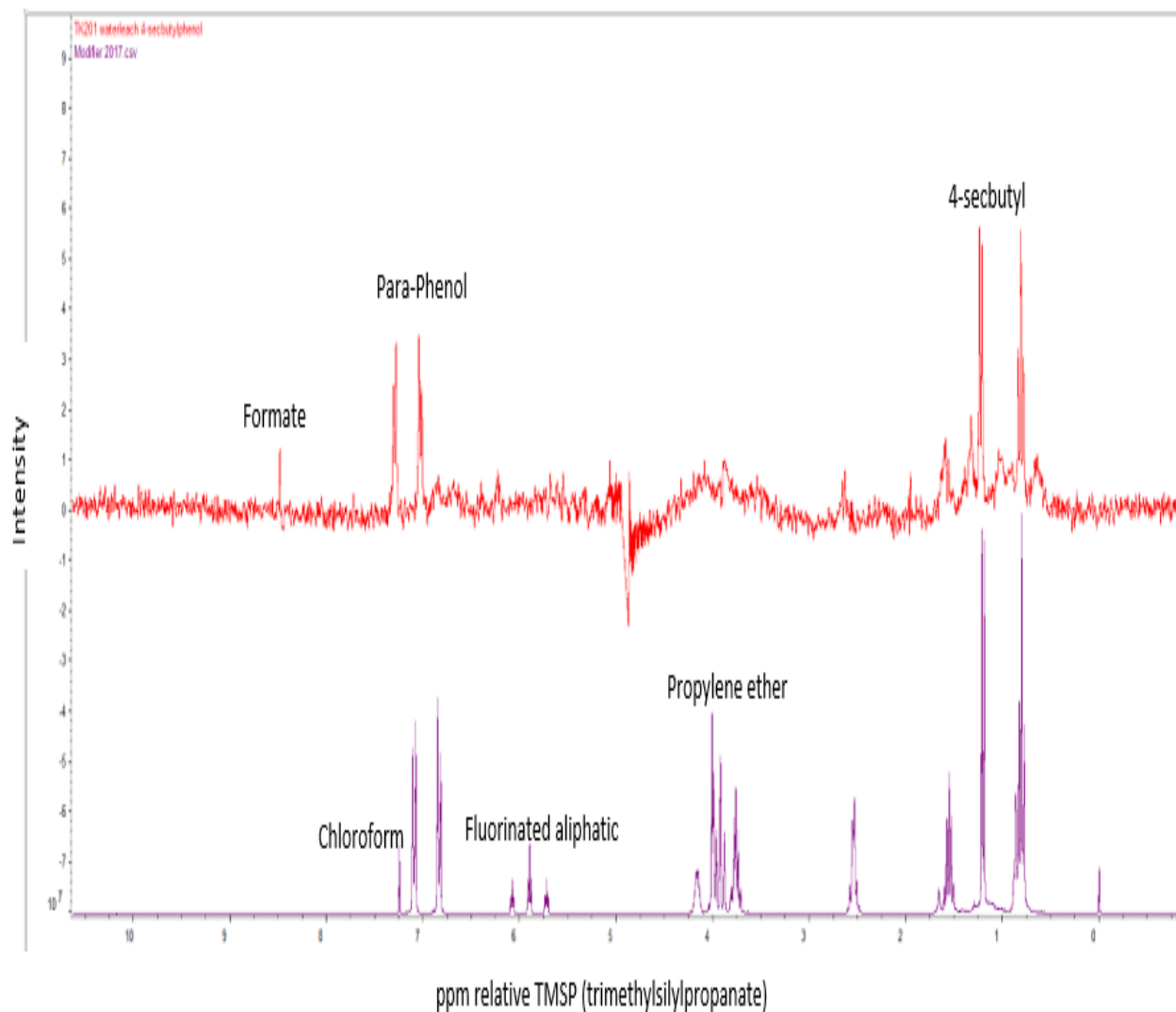


Figure 9. Overlay ^1H NMR Spectra for the December 2021 Tank 201 solids after leaching with Water (water soluble species include modifier (Cs-7SB and dichloromethane (DCM)); bottom spectrum), formate, and sec. butyl phenol (top spectrum).

3.1.3 Particle Size Analysis and Elemental Composition for the December 2021 Tank 201 Solids

As presented in Figure 10, the particle distribution for the Tank 201 solids shows a near gaussian distribution of particles with particle sizes ranging from 2.75 microns to 31.11 microns and the mean particle size at 14.79 microns (SD = 4.87 microns), with the highest peak (mode) in the distribution being 18.5 microns. Please note that the minimum detectable particle size with the Microtrac instrument is 0.243 microns; inorganic particles below this instrument detection limit, if present in these samples, are submicron particles.

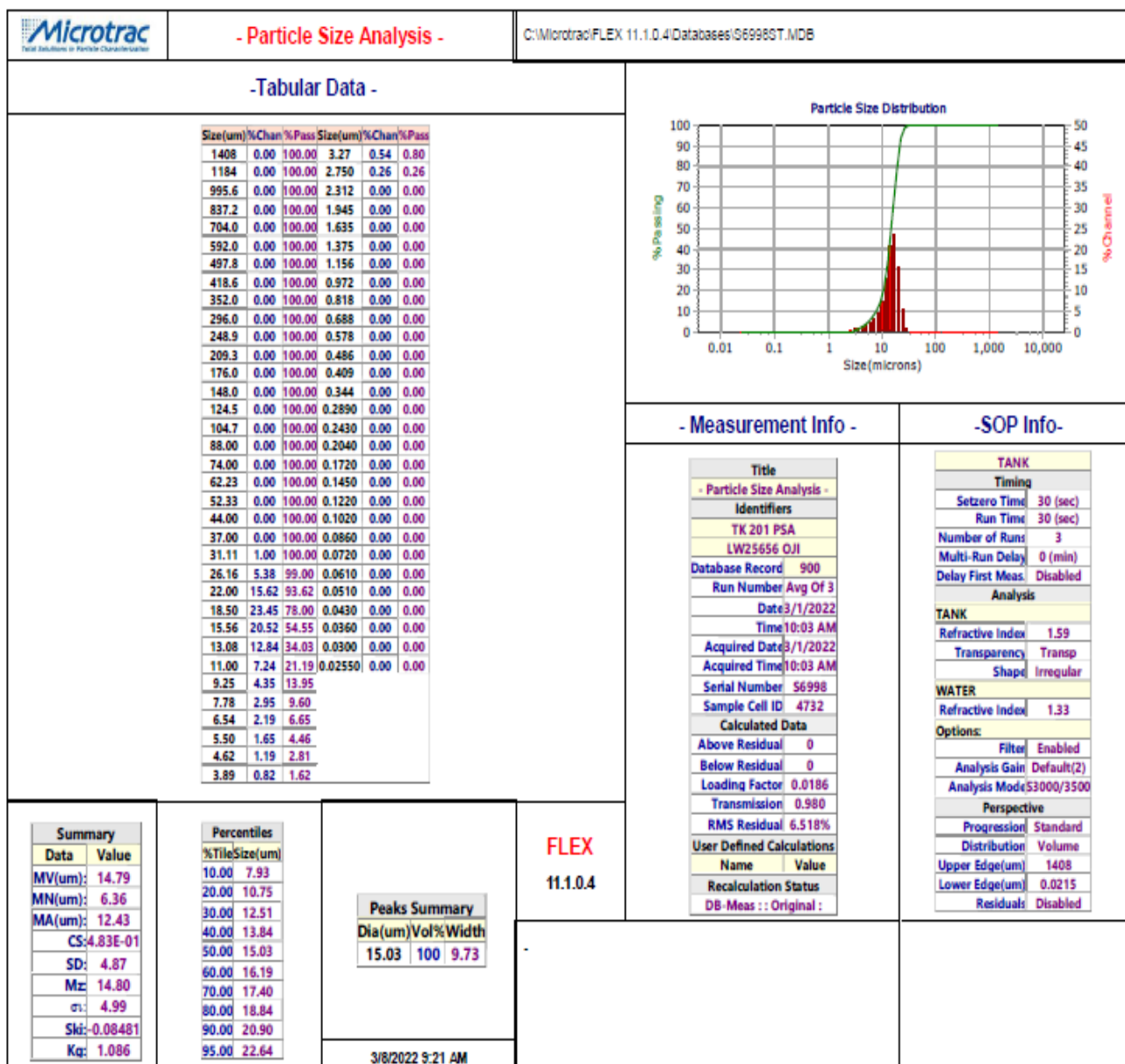


Figure 10. Particle size distribution for the December 2021 Tank 201 solids.

In the characterization of the Tank 201 solids for elements, the Tank 201 solid paste was digested in acid [aqua regia digestion (AQR)] and the resulting liquid analyzed for elements [inductively coupled plasma atomic emission spectroscopy (ICP-AES)], total mercury [direct mercury analysis (DMA)], arsenic, selenium [inductively coupled plasma mass spectrometry (ICP-MS)].

The elemental compositions and other Resource Conservation and Recovery Act (RCRA) metals for the Tank 201 solids are presented in Table 1. The density of the “as-received” Tank 201 was not determined

in this characterization of the material and thus an approximate density of 1.1 mg/L was used in the AQR digestion conversions from mg/g to mg/L based on plant experience with tank farm materials.

Table 1. Elemental composition/RCRA metals for the December 2021 Tank 201 acid digested solids.

| Elemental composition | Concentration Ug/g- solids | @Wt. % | Concentration, mg/L* | [†] TCLP Regulatory limit, mg/L | RCRA Code |
|------------------------------|-----------------------------------|---------------|-----------------------------|-------------------------------------------------|------------------|
| Ag | <4.36E-01 | <4.36E-05 | <4.80E-01 | 5 | D011 |
| Al | 3.07E+03 | 3.07E-01 | 3.38E+03 | na | na |
| B | <4.71E+00 | <4.71E-04 | <5.18E+00 | na | na |
| Ba | 1.58E+01 | 1.58E-03 | 1.74E+01 | 100 | D005 |
| Be | <2.74E-01 | <2.74E-05 | <3.01E-01 | na | na |
| Ca | 6.96E+01 | 6.96E-03 | 7.66E+01 | na | na |
| Cd | 5.41E+00 | 5.41E-04 | 5.95E+00 | 1 | D006 |
| Ce | <2.03E+00 | <2.03E-04 | <2.23E+00 | na | na |
| Co | 3.37E+02 | 3.37E-02 | 3.71E+02 | na | na |
| Cr | 3.06E+02 | 3.06E-02 | 3.37E+02 | 5 | D007 |
| Cu | <1.16E+01 | <1.16E-03 | <1.28E+01 | na | na |
| Fe | 2.07E+03 | 2.07E-01 | 2.28E+03 | na | na |
| Gd | <9.82E-01 | <9.82E-05 | <1.08E+00 | na | na |
| K | <1.05E+02 | <1.05E-02 | <1.16E+02 | na | na |
| La | <5.83E-01 | <5.83E-05 | <6.41E-01 | na | na |
| Li | <9.81E+00 | <9.81E-04 | <1.08E+01 | na | na |
| Mg | 6.28E+01 | 6.28E-03 | 6.91E+01 | na | na |
| Mn | 2.62E+01 | 2.62E-03 | 2.88E+01 | na | na |
| Mo | 1.54E+01 | 1.54E-03 | 1.69E+01 | na | na |
| Na | 1.79E+03 | 1.79E-01 | 1.97E+03 | na | na |
| Ni | 1.06E+02 | 1.06E-02 | 1.17E+02 | na | na |
| P | 9.10E+01 | 9.10E-03 | 1.00E+02 | na | na |
| Pb | <2.89E+01 | <2.89E-03 | <3.18E+01 | 5 | D008 |
| S | 8.36E+02 | 8.36E-02 | 9.20E+02 | na | na |
| Sb | <5.26E+00 | <5.26E-04 | <5.79E+00 | na | na |
| Si | 1.05E+02 | 1.05E-02 | 1.16E+02 | na | na |
| Sn | <3.30E+01 | <3.30E-03 | <3.63E+01 | na | na |
| Sr | <2.31E+00 | <2.31E-04 | <2.54E+00 | na | na |
| Th | <5.27E+00 | <5.27E-04 | <5.80E+00 | na | na |
| Ti | 1.83E+04 | 1.83E+00 | 2.01E+04 | na | na |
| U | 2.03E+02 | 2.03E-02 | 2.23E+02 | na | na |
| V | <6.63E+00 | <6.63E-04 | <7.29E+00 | na | na |
| Zn | 2.79E+01 | 2.79E-03 | 3.07E+01 | na | na |
| Zr | 1.43E+01 | 1.43E-03 | 1.57E+01 | na | na |
| Hg-total | 4.44E+04 | 4.44E+00 | 4.89E+04 | 0.2 | D009 |
| As | < 3.31E-01 | < 3.31E-05 | <3.67E-01 | 5 | D004 |
| Se | < 3.31E-01 | < 3.31E-05 | <3.67E-01 | 1 | D010 |

*It is assumed that the density of the Tank 201 sludge is 1.1 g/mL, @10,000 ug/g-solid = 1 Wt.%, na = not applicable.

[†]Toxicity Characteristic Leaching Procedure [Environmental Protection Agency (EPA) method 1311].

Of the eight RCRA metals, three of them (Cd, Cr, and Hg) were above the Toxicity Characteristic Leaching Procedure (TCLP) regulatory limits as shown in Table 1. The measured concentrations for Cd, Cr and Hg were 5.95 mg/L with TCLP regulatory limit of 1 mg/L, 337 mg/L with TCLP regulatory limit of 5 mg/L and 4.89E+04 mg/L with TCLP regulatory limit of 0.2 mg/L, respectively. The analytical result for Pb (<31.8 mg/L) was an upper limit and the RCRA limit is 5. The analysis for Pb may need to be performed

by another analytical method for better quantification. The RCRA limits (TCLP regulatory limit) are listed in the third column of Table 1, along with the RCRA codes in the last column for these metals.

3.1.4 Characterization of Tank 202 Organic Emulsion Layer and liquid portion (December 2021 sample)

As shown in Figure 1, insert B, the Tank 202 sample consisted of two phases; a liquid phase on the bottom and what looked like suspended fine solids on the top. This second phase at the top turned out to be an organic emulsion. The lower liquid phase of the Tank 202 sample was tested for pH and determined to have a pH of 14 or greater ($\text{pH} \geq 14$). The density of the liquid phase of the Tank 202 sample was determined to be 1.05 g/mL (0.32 %RSD). The organic emulsion was successfully decanted (the slurry- decant contained about 80% interstitial liquid.), and the resulting slurry decant (Figure 1, insert C), after air drying in the Shielded Cell for more than 96 hours, characterized as described below.

The Tank 202 air-dried organic emulsion sample was used for FT-IR and ^1H NMR analyses and the Tank 202 wet emulsion used for XRD and SEM/EDX characterizations. The Tank 202 liquid portion only was used for ICP-AES for elementals and RCRA metal analyses.

3.1.5 XRD and SEM characterization of the December 2021 Tank 202 solids

The crystalline minerals identified in the XRD spectra for this Tank 202 air-dried organic emulsion, as shown in Figure 11, included (NaNO_3), thermonatrite ($\text{Na}_2\text{CO}_3 \cdot \text{H}_2\text{O}$), and trona ($\text{Na}_3\text{H}(\text{CO}_3)_2 \cdot 2\text{H}_2\text{O}$) along with a large background shift possibly due to the amorphous organic layer. X-ray fluorescence (XRF) of this sample, Figure 12, also showed elemental peaks for mainly Ti, Hg, Fe, and Cr.

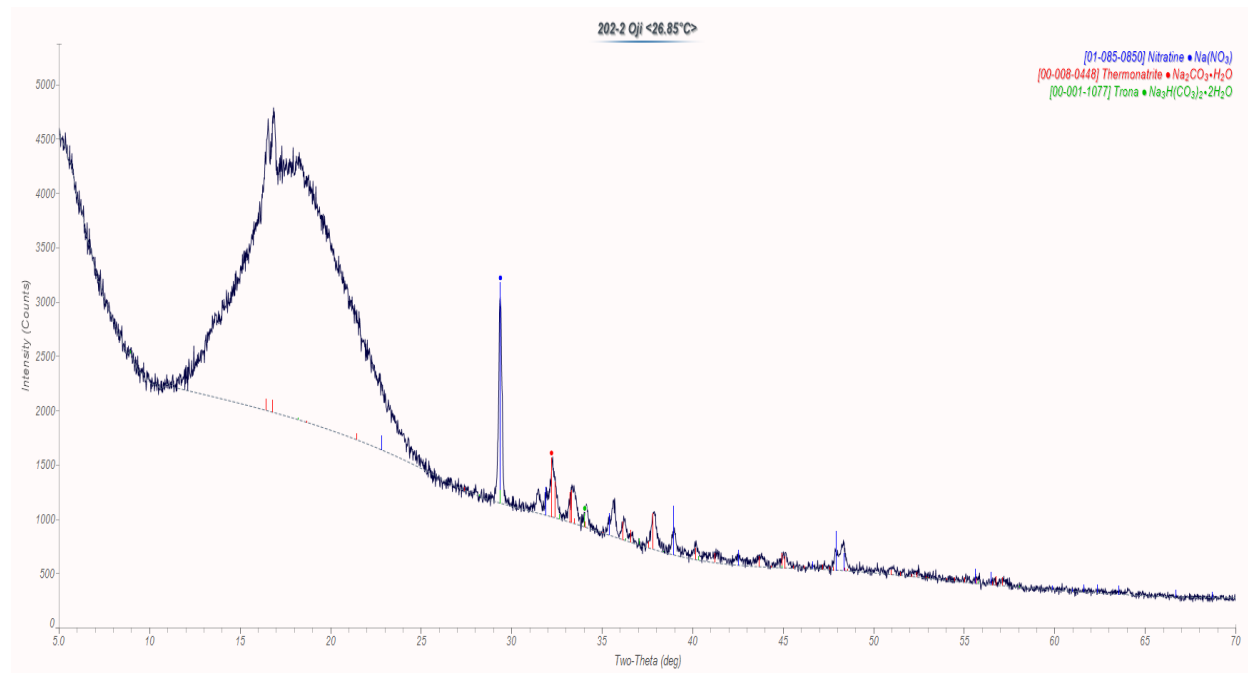


Figure 11. XRD spectra of the air-dried December 2021 Tank 202 emulsion layer.

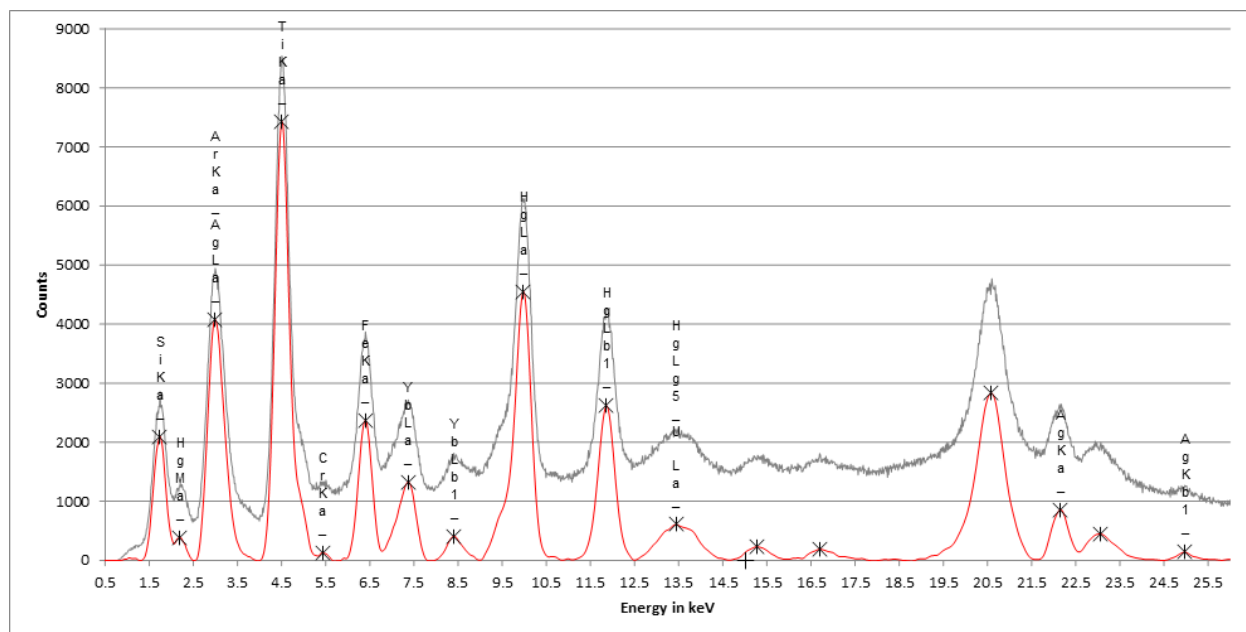


Figure 12. XRF elemental composition for the December 2021 Tank 202 emulsion phase (X-ray fluorescence (XRF) elements include elemental peaks for Ti, Hg, Fe, and Cr).

The scanning electron microscope/ energy dispersive x-ray (SEM/EDX) characterization results for the Tank 202 dry organic emulsion layer are presented in Figures 13 (sample photo image), 14, and 15. The predominant elemental components of this material were F, Na, Al, Mg, Si, Hg, Ca, Ti, Fe, and traces of W. The presence of detectable amounts of elemental tungsten is disconcerting because it is not one of the usual detectable elements in the SWPF tanks. It is worth noting that even the dry organic emulsion layer of this Tank 202 sample also has trapped elements and thus inorganic oxides like HgO , TiO_2 and Fe_3O_4 .

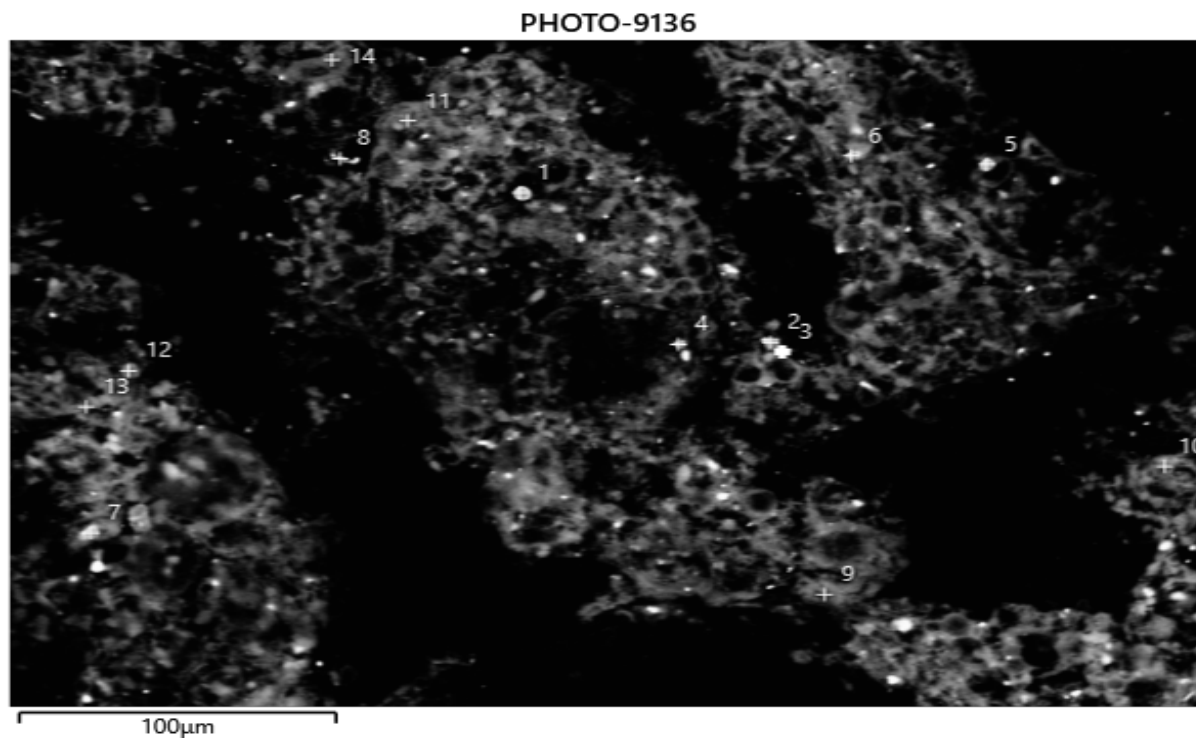


Figure 13. Representative SEM photo image of the December 2021 Tank 202 dry emulsion layer.

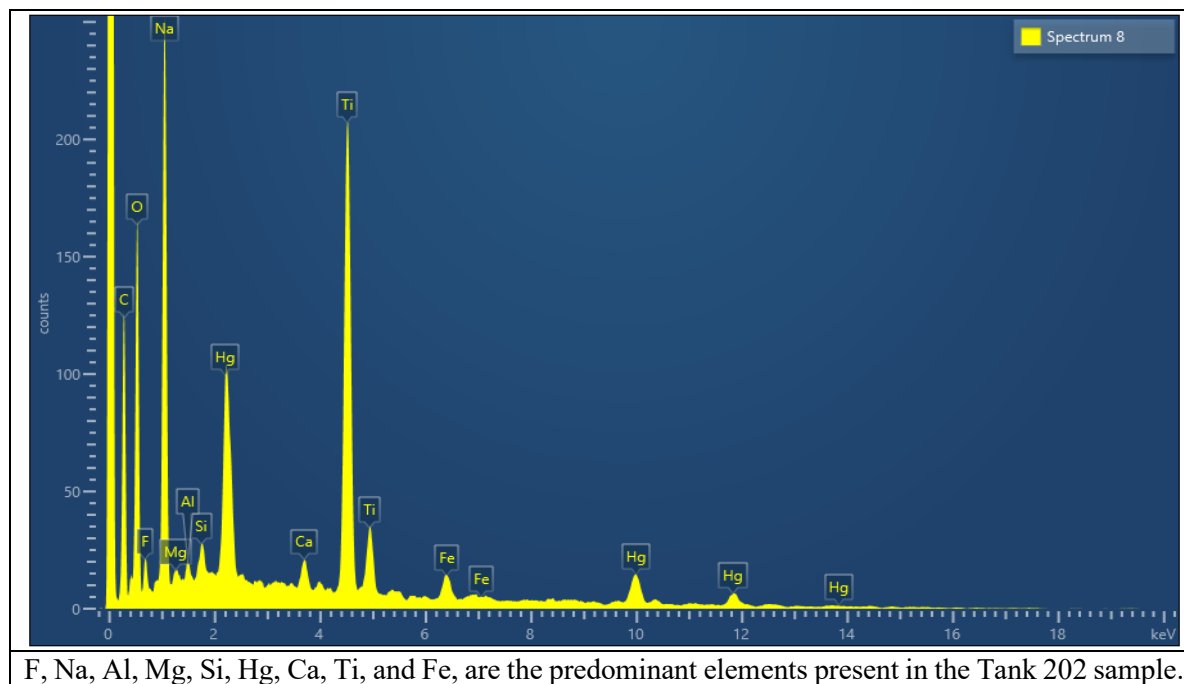


Figure 14. SEM/EDX elemental composition for SWPF December 2021 Tank 202 dry organic emulsion layer.

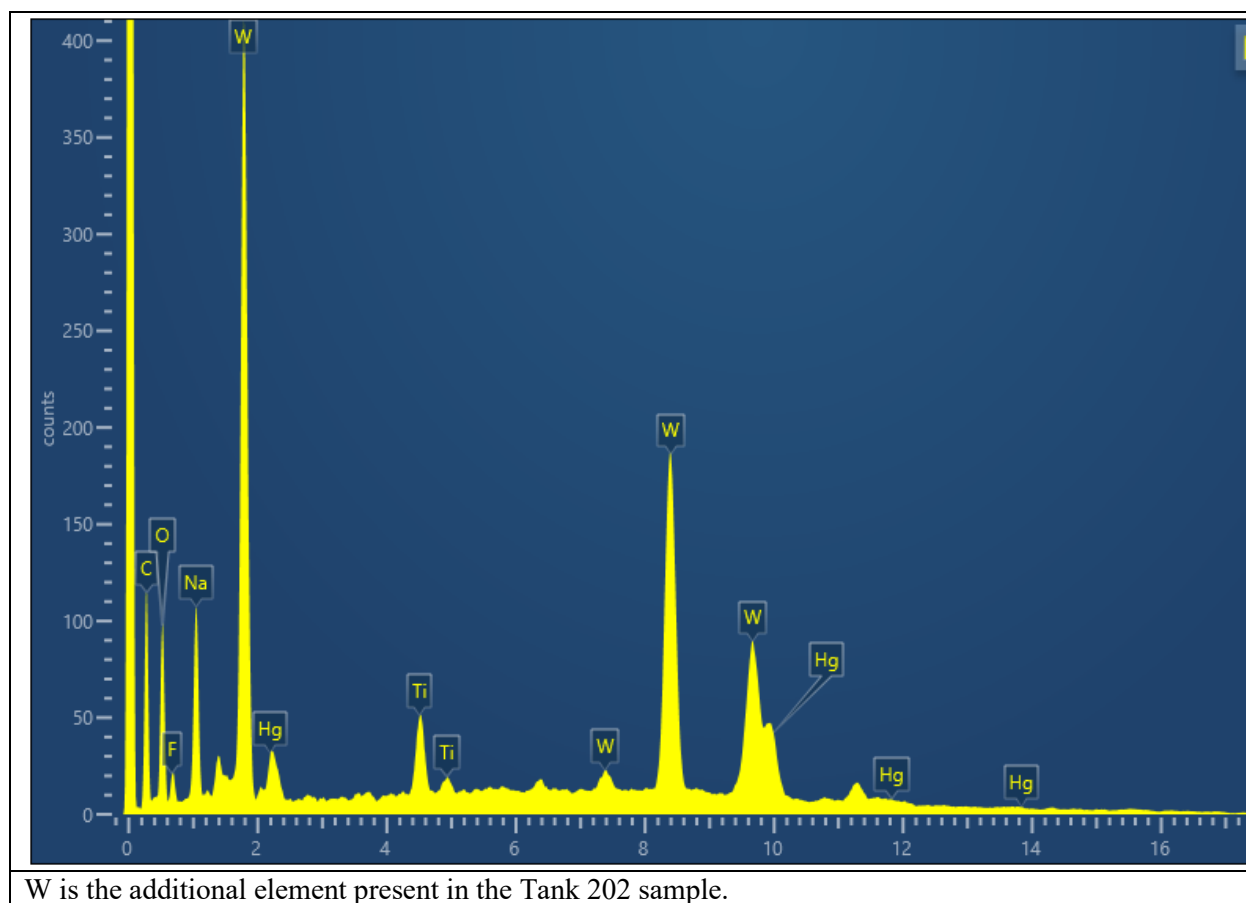


Figure 15. SEM/EDX elemental composition for SWPF December 2021 Tank 202 dry organic emulsion layer.

3.1.6 FT-IR and ^1H NMR characterization of the December 2021 Tank 202 emulsion layer

The FT-IR: spectra, as presented in Figure 16, for the Tank 202 air-dried emulsions confirmed presence of a mixture of multi-cations (Na, Ca, Mg, Fe and Al) and double anions sodium salts of the carbonates and nitrates like sodium nitrate, sodium carbonate and sodium bicarbonate. The presence of these inorganic ions is also confirmed by XRD, as shown earlier in Figure 11.

The bulk of the ^1H NMR organic components (Figure 17) for this air-dried Tank 202 emulsion layer, after extraction with chloroform, is an organic modifier (CS-7SB) currently used in the SWPF process along with BoBCalix for cesium extraction. The hydrogen in the -OH group of the modifier is not exchanging with other hydrogens but is instead coupling with the -CH- in the propylene group of the modifier.

Extraction with water produced two minor water-soluble components for the air-dried Tank 202 emulsion: mainly sec. butyl phenol and formate. The sec. butyl phenol and formates are water soluble organic moieties, which are probably decomposition products from the modifier. In Figure 18, the ^1H NMR spectra for the water leached Tank 202 air-dried organic emulsion are further expanded down to the base line to

show the presence of small minor matching peaks for other water-soluble components, which may include aliphatic fluorides, phthalates, BoBCalix, and acetates. These minor components seem to constitute less than 0.02 weight percent of the total material by weight. The first two peaks at the bottom of Figure 18 are reference peaks for sec. butyl phenol and BoBCalixC6, respectively.

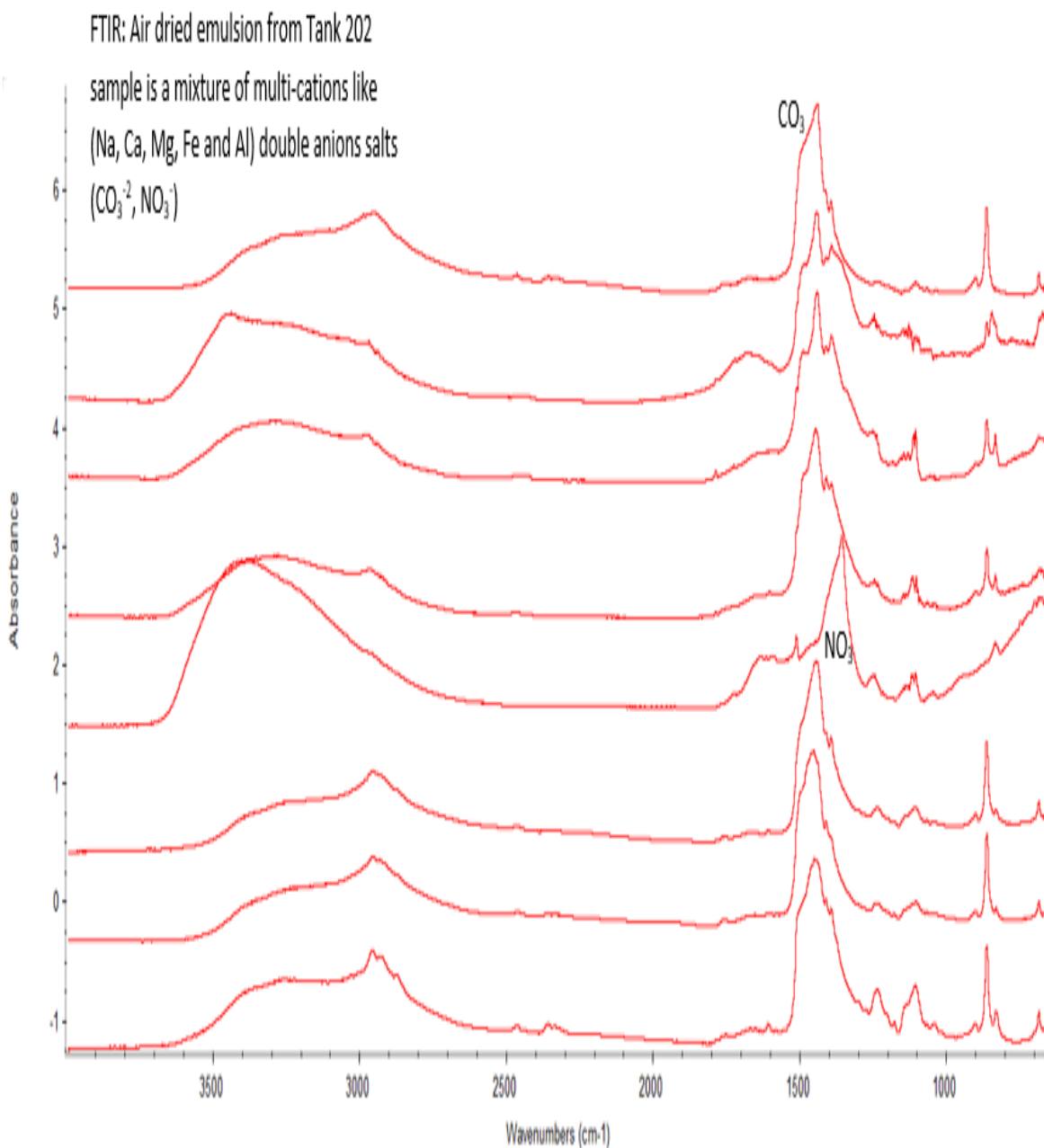


Figure 16. Overlay FT-IR spectra for the air-dried December 2021 Tank 202 organic emulsion layer.

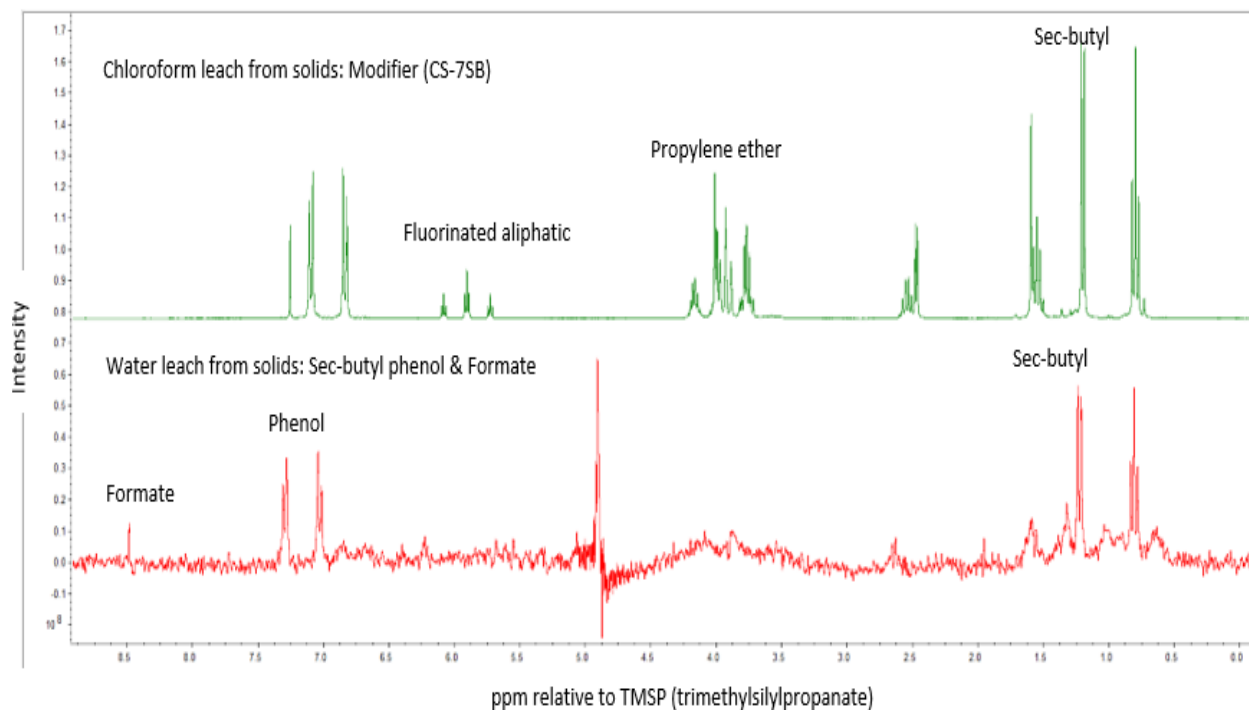


Figure 17. Overlay ^1H NMR spectra: air-dried December 2021 Tank 202 emulsion; organics extracted with chloroform and water extracted peaks (bottom spectrum).

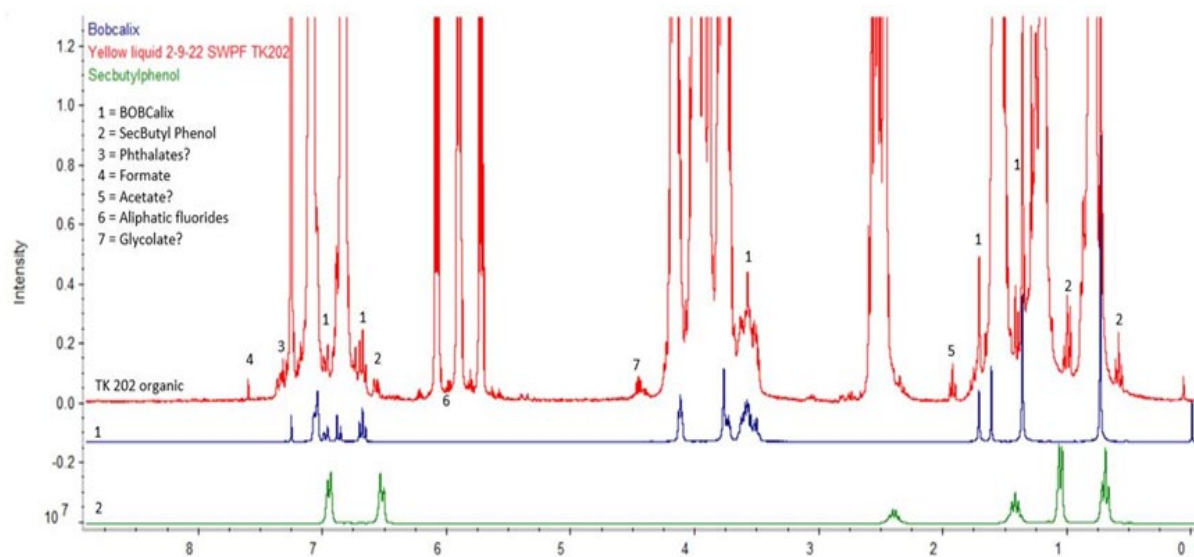


Figure 18. Overlay ^1H NMR Spectra: December 2021 Tank 202 air-dried emulsion layer sample-Water extraction (Spectral baseline expanded to show smaller peaks).

3.1.7 Particle Size Analysis and Elemental Composition for the December 2021 Tank 202 Liquid Fraction

The particles size characterization of the December 2021 Tank 202 liquid portion indicated that no measurable particles were detected in the liquid, which means the particles present, if any, were below the instrument detection limit of 0.243 microns for the Microtrac instrument, in other words the particles may be in the submicron range.

The Tank 202 liquid portion was also submitted for elemental analysis. The elemental composition for this liquid Tank 202 portion is presented in Table 2.

Table 2. Elemental composition and RCRA metals for the December 2021 Tank 202 liquid portion.

| Elemental composition | Concentration, mg/L | [†] TCLP Regulatory limit, mg/L | RCRA Code |
|------------------------------|----------------------------|-------------------------------------------------|------------------|
| Ag | <3.79E-02 | 5 | D011 |
| Al | 6.57E+01 | na | na |
| B | 4.64E+00 | | na |
| Ba | 4.14E-01 | 100 | D005 |
| Be | <2.38E-02 | na | na |
| Ca | 1.69E+00 | na | na |
| Cd | <3.10E-02 | 1 | D006 |
| Ce | <9.67E-01 | na | na |
| Co | 9.39E-01 | na | na |
| Cr | 2.99E+00 | 5 | D007 |
| Cu | <6.35E-01 | na | na |
| Fe | 3.37E+00 | na | na |
| Gd | <8.53E-02 | na | na |
| K | <1.16E+01 | na | na |
| La | <5.07E-02 | na | na |
| Li | <8.52E-01 | na | na |
| Mg | 4.51E-01 | na | na |
| Mn | 1.75E-01 | na | na |
| Mo | <2.95E-01 | na | na |
| Na | 9.85E+03 | na | na |
| Ni | <2.86E-01 | na | na |
| P | <2.74E+00 | na | na |
| Pb | <2.03E-01 | 5 | D008 |
| S | 1.49E+01 | na | na |
| Sb | <4.57E-01 | na | na |
| Si | 9.39E+01 | na | na |
| Sn | <2.87E+00 | na | na |
| Sr | 9.21E-02 | na | na |
| Th | <3.19E+00 | na | na |
| Ti | 2.15E+01 | na | na |
| U | <1.19E+00 | na | na |
| V | <4.49E-01 | na | na |
| Zn | 6.54E-01 | na | na |
| Zr | <7.66E-02 | na | na |
| Hg-total | 4.91E+01 | 0.2 | D009 |
| As | <7.840E-03 | 5 | D004 |
| Se | <7.840E-03 | 1 | D010 |

[†]Toxicity Characteristic Leaching Procedure [Environmental Protection Agency (EPA) method 1311].

As presented in Table 2, only 16 of the elements in the sample were above instrument detection limit, and these elements include sodium ($9.85\text{E}+03$ mg/L), silicon ($9.39\text{E}+01$ mg/L), aluminum ($6.57\text{E}+01$ mg/L), titanium ($2.15\text{E}+01$ mg/L), sulfur ($1.49\text{E}+01$ mg/L), boron ($4.64\text{E}+00$ mg/L), iron ($3.37\text{E}+00$ mg/L), chromium ($2.99\text{E}+00$ mg/L), Ca ($1.69\text{E}+00$ mg/L), Cobalt ($9.39\text{E}-01$ mg/L), Zinc ($6.54\text{E}-01$ mg/L), magnesium ($4.51\text{E}-01$ mg/L), barium ($4.14\text{E}-01$ mg/L), manganese ($1.75\text{E}-01$ mg/L), strontium ($9.21\text{E}-02$ mg/L), and Hg_{-total} (49.08 mg/L). The other elements were below instrument detection limits.

The RCRA metal (As, Ba, Cd, Cr, Pb, Hg, Se, Ag) limits are listed in the third column of Table 2, along with the RCRA codes in the last column for these metals. Of these eight RCRA monitored metals, only total mercury (Hg) is above the TCLP Regulatory limit requirements of 0.2 mg/L. The measured Hg concentration in the December 2021 Tank 202 liquid sample is 49.1 mg/L.

4.0 SEM/EDX Spectra for the “as-received” March 2022 Tank 202 solids WITHOUT acid Leaching

The SEM/EDX data for the “as-received” March 2022 Tank 202 samples, without acid leaching, are presented in Figures 19-22. As shown in Figures 20-22, the SEM/EDX identified predominant elements in the photo images include F, Na, W, Ti, Fe, Al, Si, Hg, Mg, Ca, Cr, and Ni. It is worth mentioning that in the SEM/EDX characterization data, elemental tungsten (W) is seen in the March 2022 Tank 202 sample (Figure 21) as well as in the December 2021 Tank 202 sample (Figure 15) and not in the December 2021 Tank 201 sample. The presence of tungsten is also confirmed in the XRD mineral content for the March 2022 Tank 202 sample (Figures 23 and 24) by the presence of the mineral tungsten carbide (WC), although not seen in the XRD spectra for the December 2021 Tank 202 sample (Figure 11), possible because of the large background shift and lower concentration of the WC mineral in the December 2021 Tank 202 air-dried organic emulsion sample.

PHOTO-9338

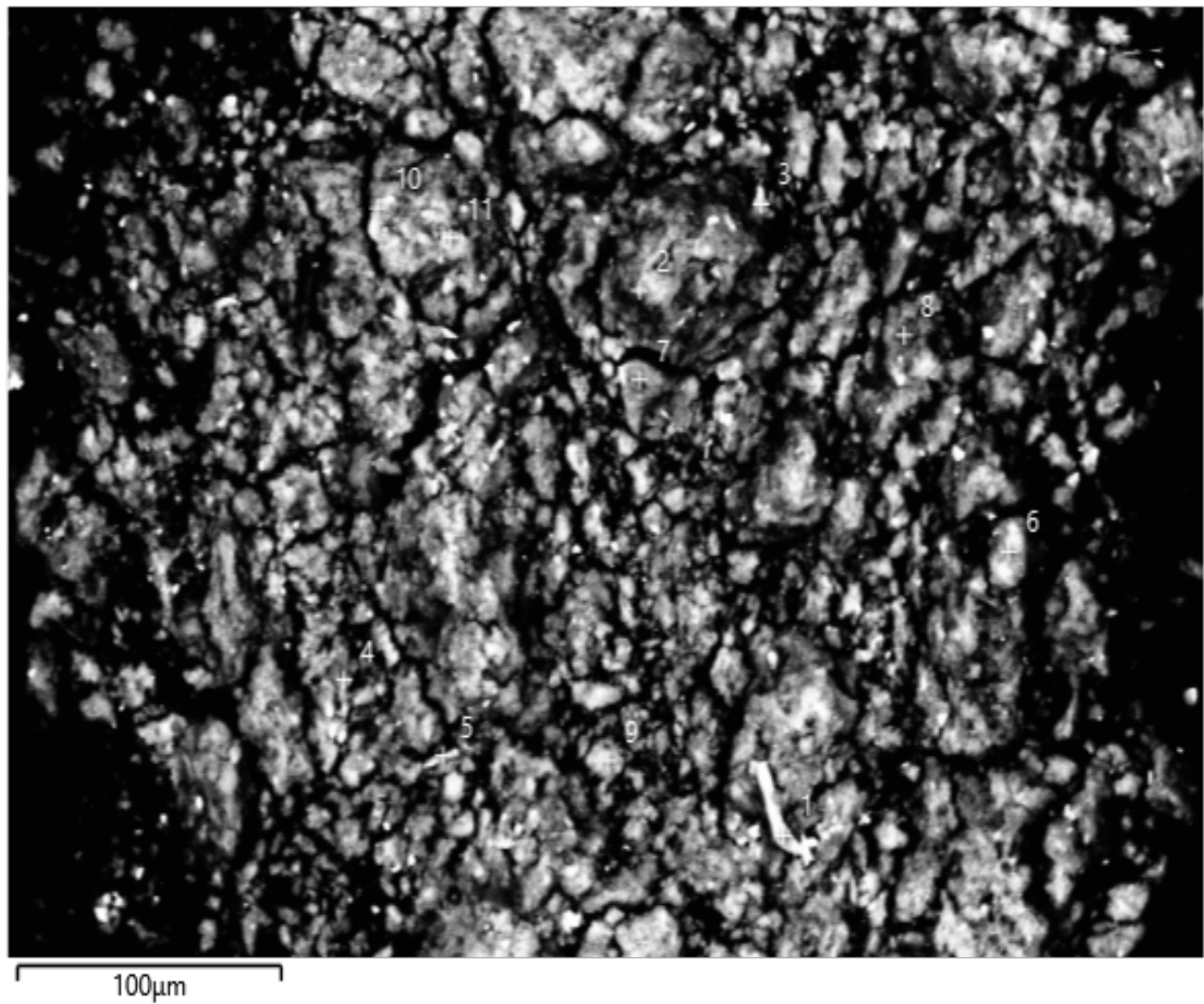


Figure 19. Representative SEM photo image for March 2022 “as-received” Tank 202 sample.

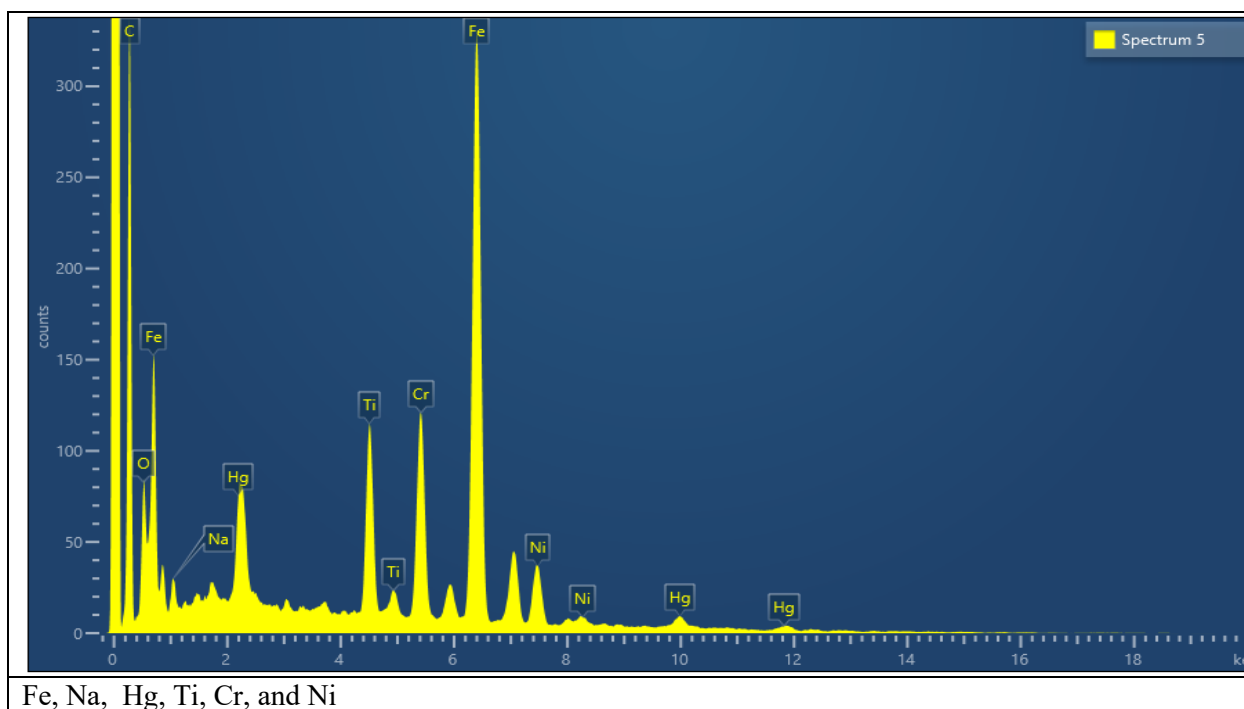


Figure 20. Representative SEM/EDX elemental composition for March 2022 “as-received” Tank 202 Sample.

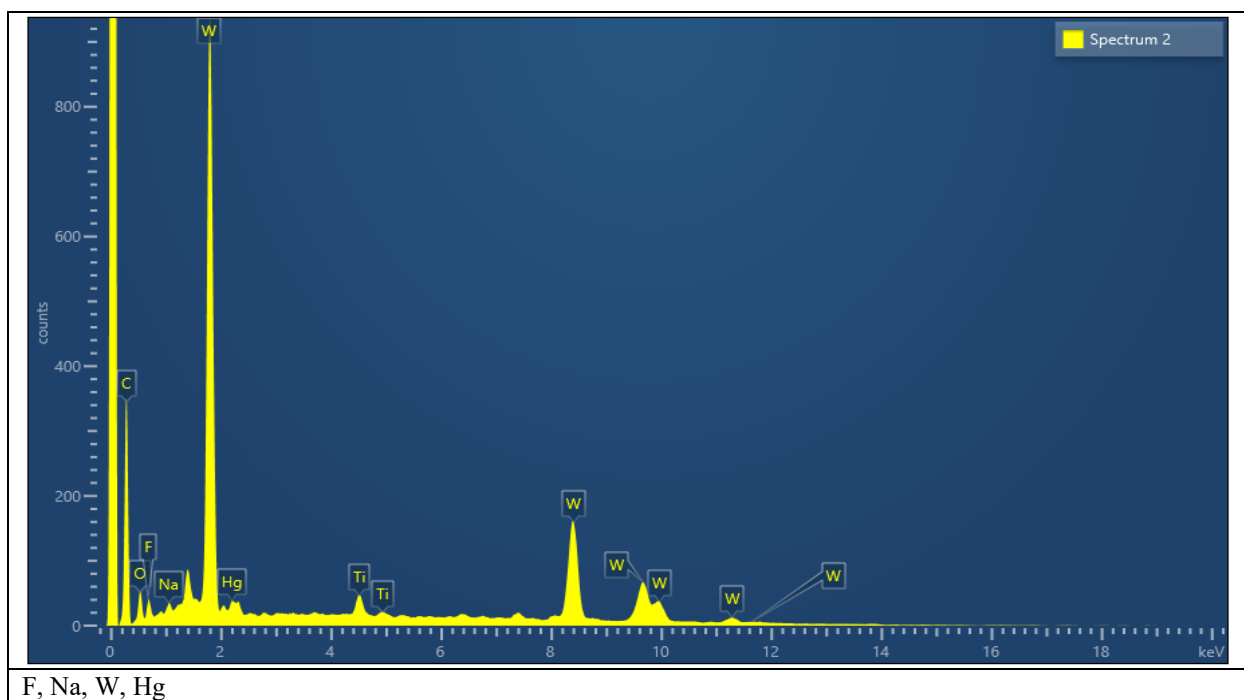


Figure 21. Representative SEM/EDX elemental composition for the March 2022 “as-received” Tank 202 Sample.

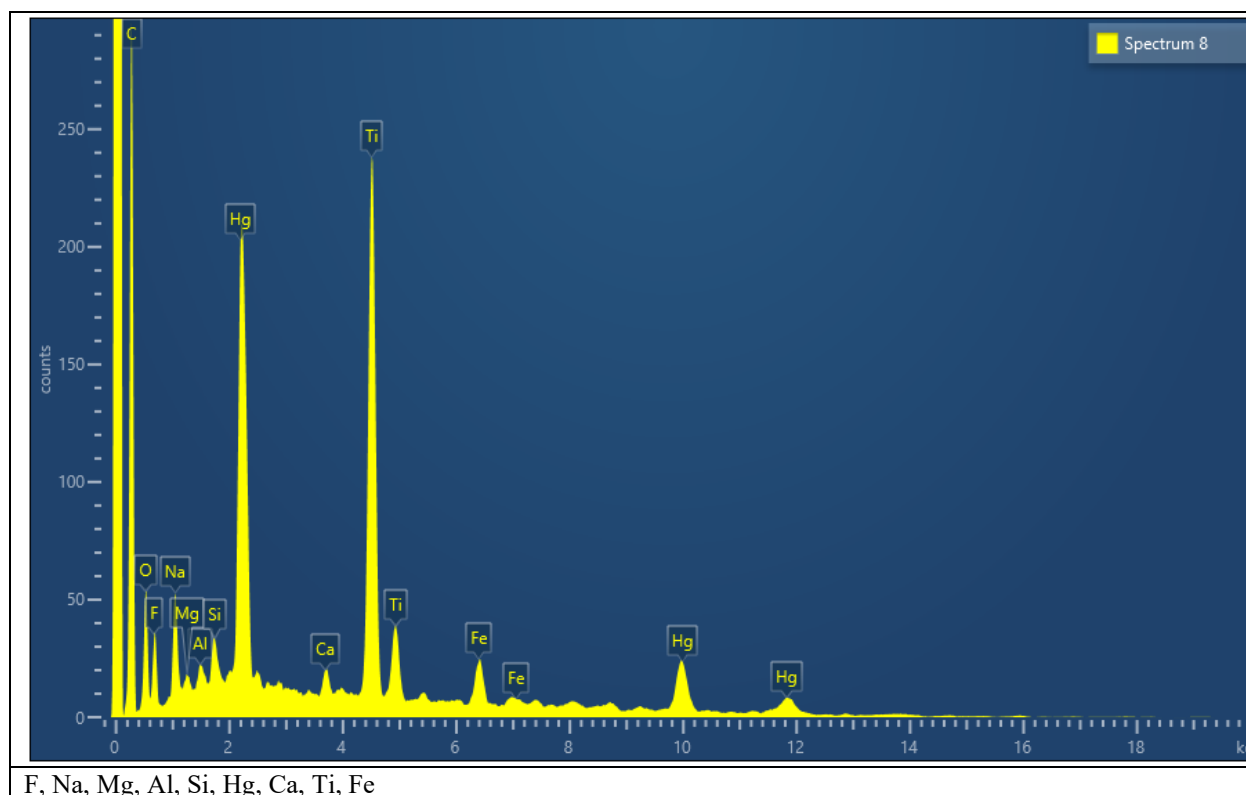


Figure 22. Representative SEM/EDX elemental composition for the March 2022 “as-received” Tank 202 Sample.

The XRD spectrum for the “as-received” March 2022 Tank 202 solids is also presented in Figure 23. Identified minerals in the XRD spectrum include gibbsite [$\text{Al}(\text{OH})_3$], quartz (SiO_2), and tungsten carbide (WC).

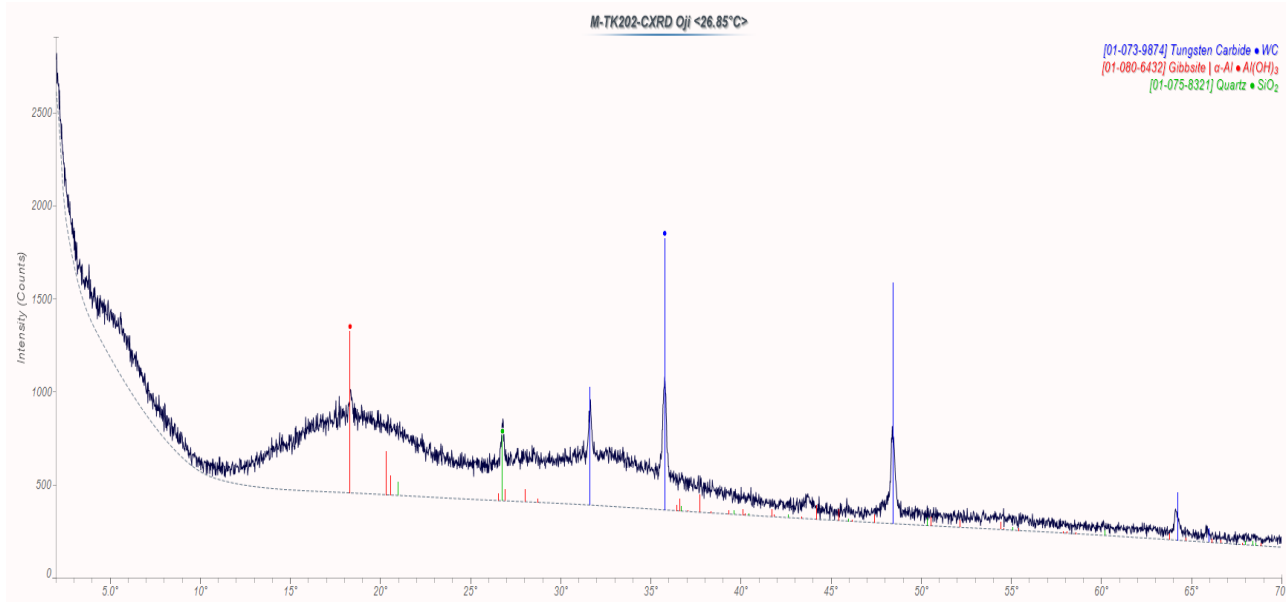


Figure 23. XRD Spectrum for the “as-received” March 2022 Tank 202 solids WITHOUT acid Leaching.

5.0 Characterization of March 2022 Tank 202 Solids-Acid Leached Samples

About 7.8 grams of the March 2022 Tank 202 solid fraction was leached with 1.0 M HNO_3 , with agitation, in a liquid-to solid ratio (phase ratio) of 12.8 mL/g. The acid leaching time was 60 minutes. The wet residual solids from the acid leaching were used for the characterizations in sections 5.1, 5.1.1 and 5.1.2 below.

5.1 XRD and SEM characterization of March 2022 Tank 202 Acid Leached Residual Solids

The XRD spectrum for the March 2022 Tank 202 acid leached residual solids, as shown in Figure 24, shows the presence of the following minerals nitratine (NaNO_3), gibbsite [$\text{Al}(\text{OH})_3$], quartz (SiO_2), and tungsten carbide (WC). Mineral nitratine (NaNO_3) seen in the acid leached Tank 202 sample comes from the nitric acid leaching of the solids and that is why nitratine is below instrument detection limit in the “as-received” March 2022 Tank 202 XRD spectrum (Figure 23). Otherwise, the two XRD spectra in Figures 23 and 24, for the “as-received” sample and the acid leached sample, respectively, are similar in their crystalline mineral content. These XRD spectra for the March 2022 Tank 202 samples show minimum background shift due to limited quantities of amorphous minerals. Therefore, the 1.0 M nitric acid (HNO_3) leaching of this March 2022 Tank 202 sample did not show any measurable effect on the mineral structure or chemistry of the identified minerals tungsten carbide (WC), gibbsite [$\text{Al}(\text{OH})_3$], and quartz (SiO_2).

However, the XRD spectra for other Tank 201 and Tank 202 “as-received” samples from the December 2021 batch of samples sent to SRNL for XRD characterization, as presented in Figures 3 (December 2021 Tank 201 solids) and Figure 11 (December 2021 Tank 202 organic emulsion layer), show measurable background shifts in both spectra due to the presence of significant amounts of amorphous, non-crystalline materials present in these December 2021 samples in comparison with the XRD spectra for the March 2022

Tank 202 sample types (“as-received samples and acid leached sample as seen Figures 23 and 24). However, XRD spectrum for the acid leached March Tank 202 solid fraction (Figure 24) shows a smaller background shift due to the presence amorphous minerals when compared to the background shift in the XRD spectrum for the “as-received” March 2022 Tank 202 solid fraction as presented in Figure 23.

Therefore, these three types of Tanks 201 and Tank 202 samples (December Tank 201, December Tank 202, and March 2022 Tank 202 sample) may be different in terms of their amorphous layers and crystalline mineral contents.

The SEM/EDX data for the acid leached March 2022 Tank 202 samples are presented in Figures 25-28. As, shown in Figures 24-26, the SEM/EDX identified predominant elements in the photo images include F, Na, W, Ti, Fe, Al, Si, and Hg. The SEM/EDX identified elemental composition for the acid leached March 2022 Tank 202 sample is not different from that of the “as-received” March 2022 Tank 202 samples as shown in Figures 20-22.

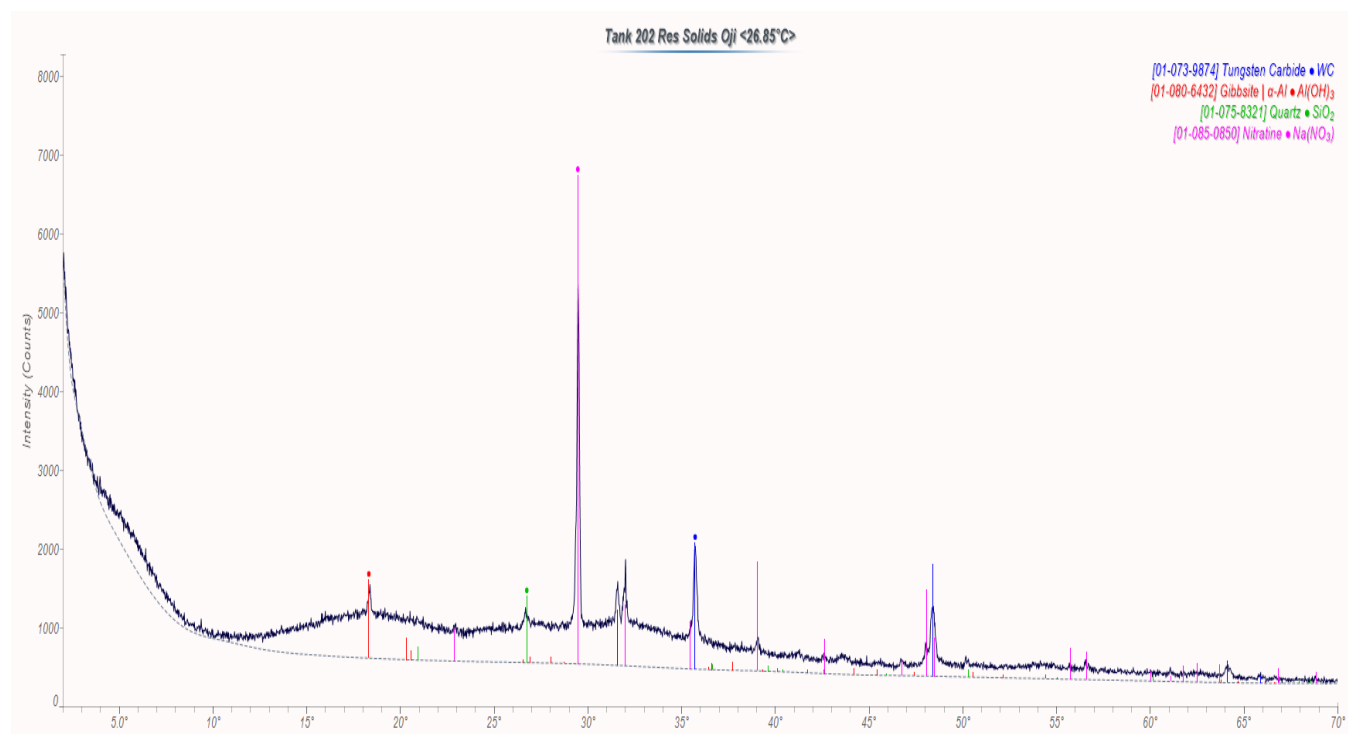


Figure 24. XRD Spectrum for the March 2022 Tank 202 solids: Acid Leached Residual Solids with minimum baseline shifts due to the absence of more amorphous minerals.

9227

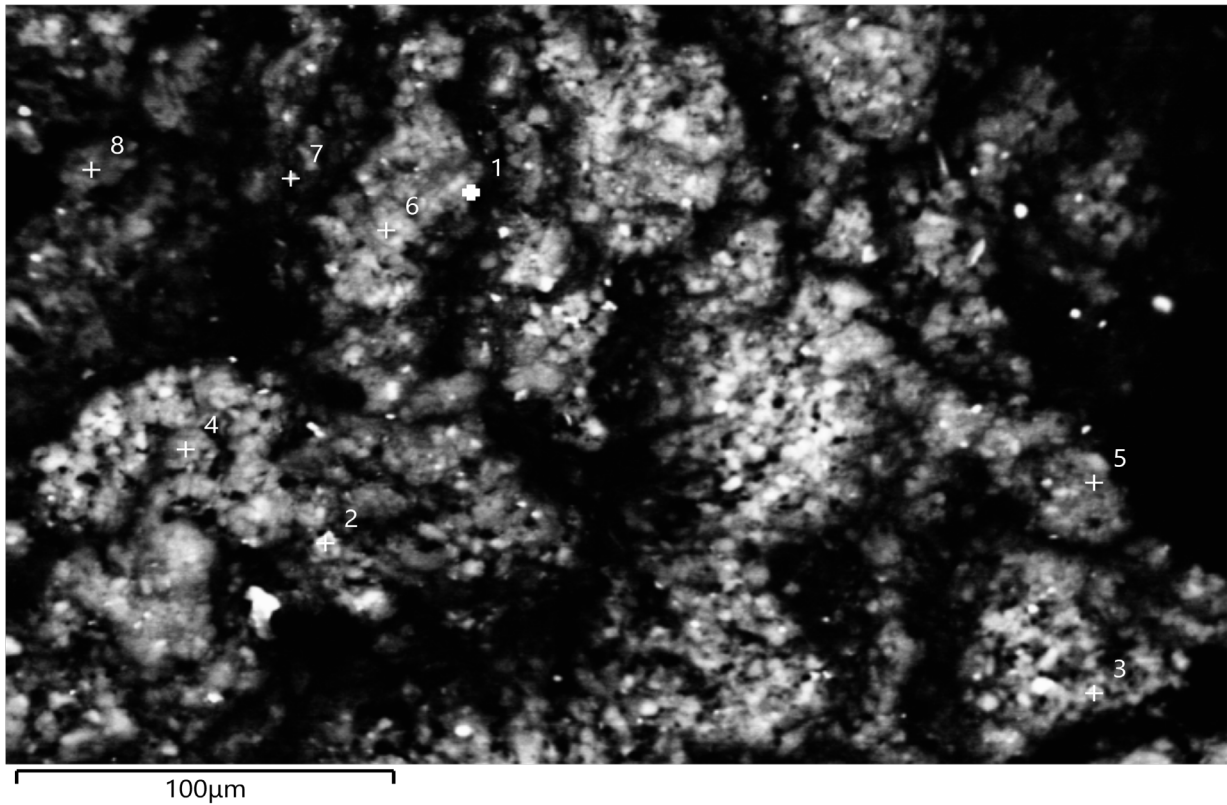


Figure 25. Representative SEM photo image for the March 2022 Tank 202 Acid Leached Residual Solids.

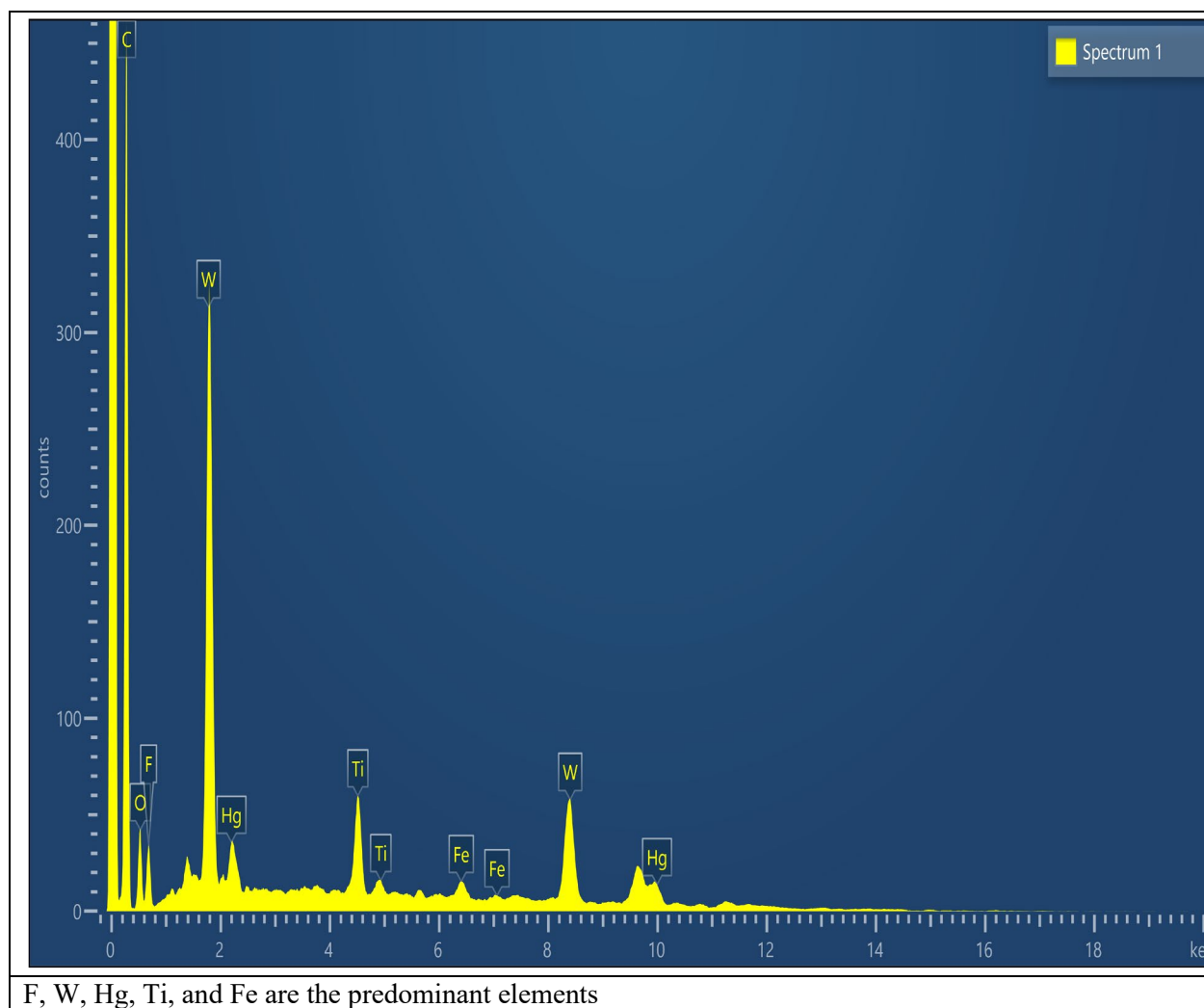


Figure 26. Representative SEM/EDX elemental composition for the March 2022 Tank 202 acid leached residual solids.

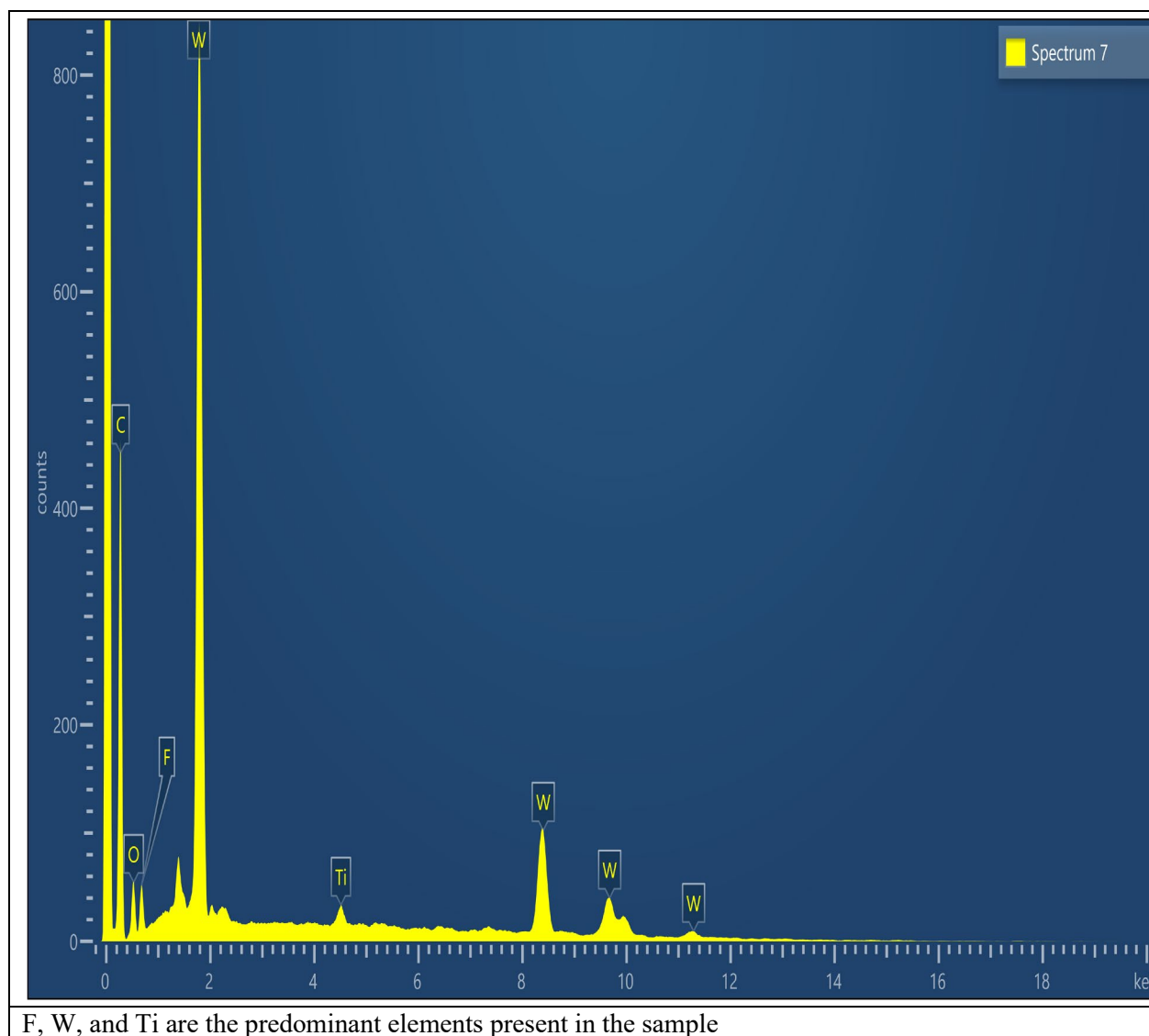


Figure 27. Representative SEM/EDX elemental composition for the March 2022 Tank 202 acid leached residual solids.

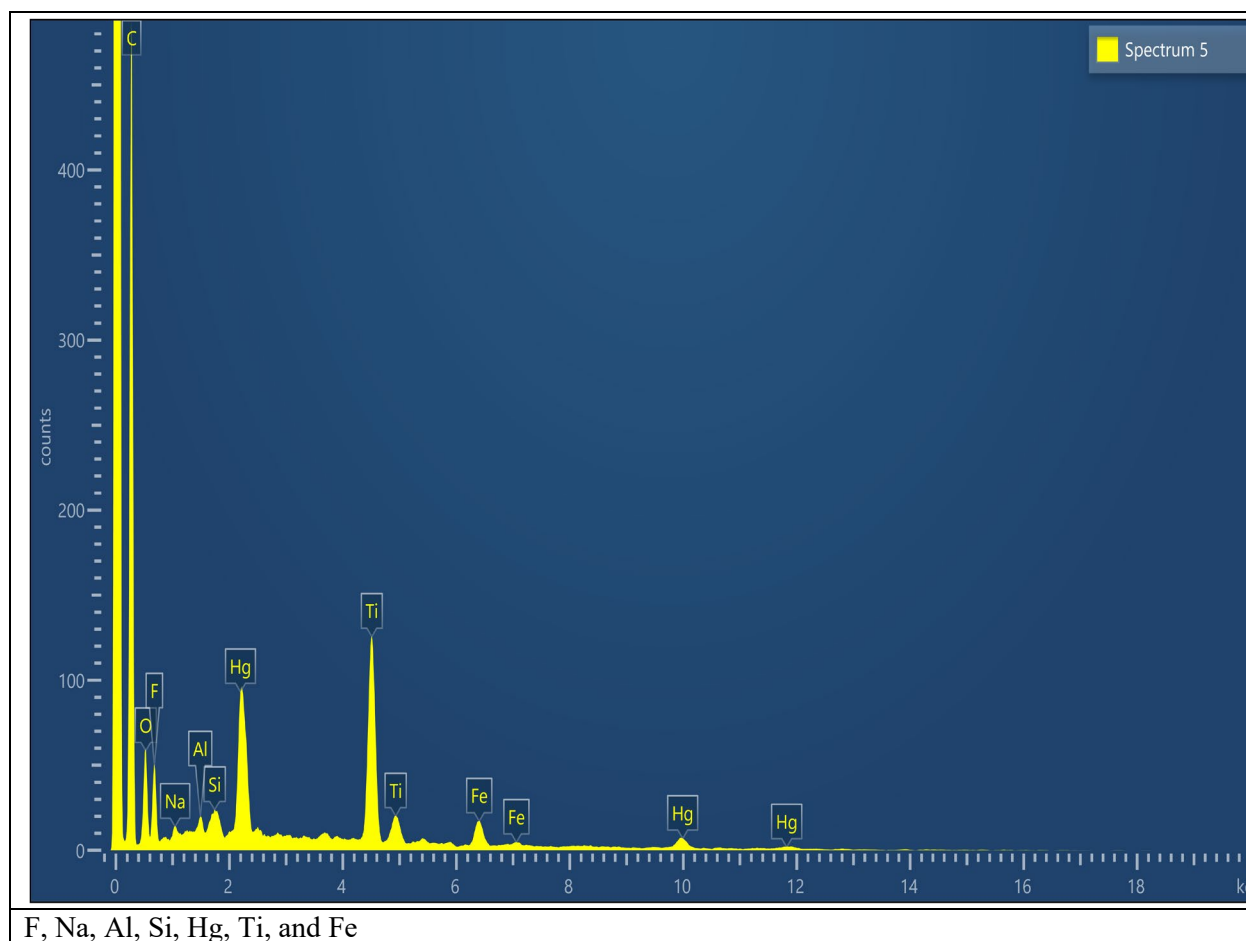
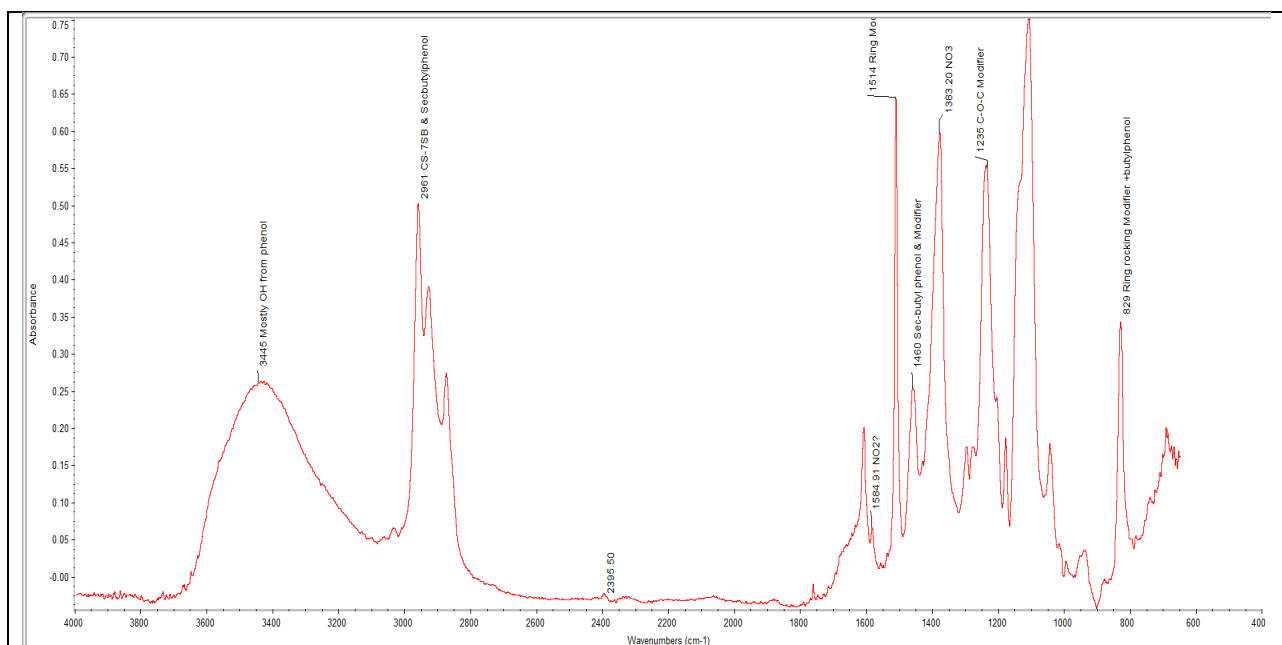


Figure 28. Representative SEM/EDX elemental composition for the March 2022 Tank 202 acid leached residual solids.

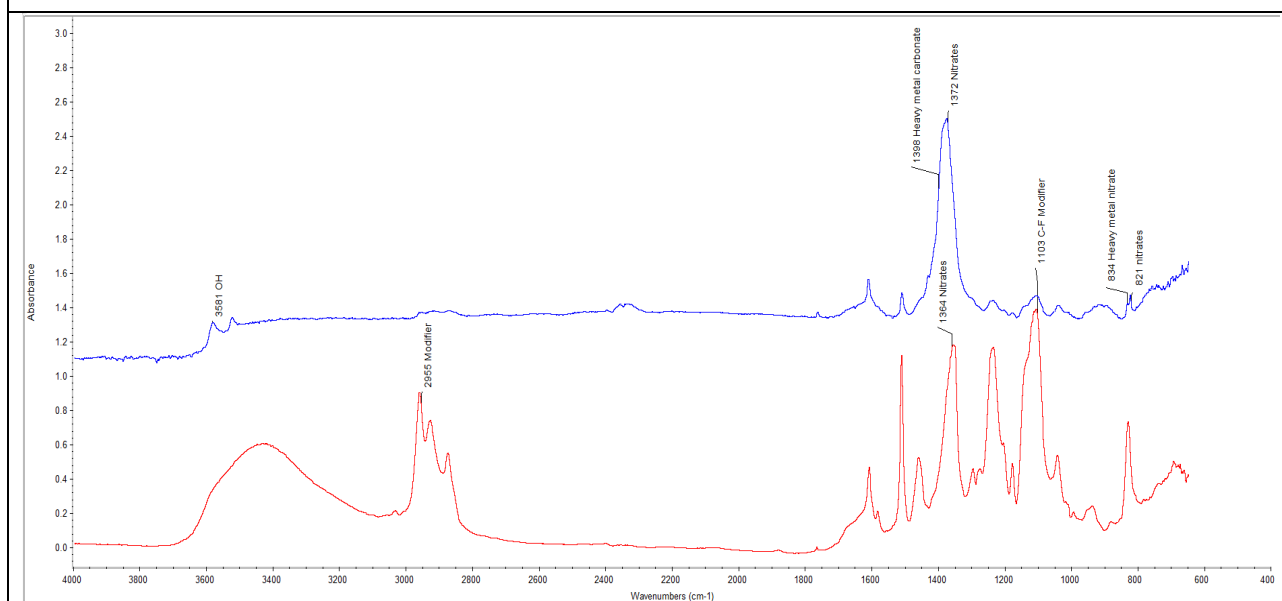
5.1.1 FT-IR and ^1H NMR characterization of the March 2022 Tank 202 solids Acid Leached Residual Solids

The acid leached solids were characterized by FT-IR and ^1H NMR after 3 days and 7 days after the leaching of the solids with nitric acid, respectively. Three components were identified in the FT-IR data for nitric acid leached Tank 202 residual solids (Figure 29, insert A), and these include the modifier, sec. butyl phenol (a decomposition product) and heavy metal nitrates mainly from the nitric acid leaching. The acid leached residual solids were further leached with dichloromethane (DCM) to account for organic soluble species by FT-IR.

The resulting sample solution from DCM leaching of the residual Tank 202 solids prior to FT-IR characterization was heterogenous and contained solid fines. The FT-IR spectra of one solid spot on the sample is shown in Figure 29, insert B (top spectrum). The infrared spectra identified the presence of mostly heavy metal nitrates and carbonates, which may be products from the reaction of nitric acid with the Tank 202 mineral solids. The liquid fraction from the post dichloromethane leaching of the Tank 202 residual solids [Figure 29, insert B (bottom spectrum)] showed the presence of mostly the modifier, sec. butyl phenol and heavy metal nitrates.



Insert A: Nitric acid leached Tank 202 solids: peaks are those for sec-butyl phenol, CS-7SB, and nitrates.



Insert B: Dichloromethane-leached residual Tank 202 solids fines; heavy metal nitrates and carbonate peaks with traces of the modifier (Top spectrum), Dichloromethane leached residual Tank 202 solids-spectrum of liquid fraction (Bottom spectrum)

Figure 29. Overlay FT-IR Spectra: Dichloromethane leached March 2022 Tank 202 solids-Post acid Leached Residual Tank 202 solids.

As shown in Figure 30, the ^1H NMR spectra appears to indicate that the nitric acid leaching of the Tank 202 sample results in the degradation/modification of the molecular structure of the modifier. The fluorinated tails of the molecule and ter-butyl groups are now missing with acidification [compare Figure 17, top spectrum (chloroform leach) with Figure 30]. After nitric acid leaching of the sample, only the propylene glycol group remains along with the grease and possibly ter-butyl alcohol (see appendix B).

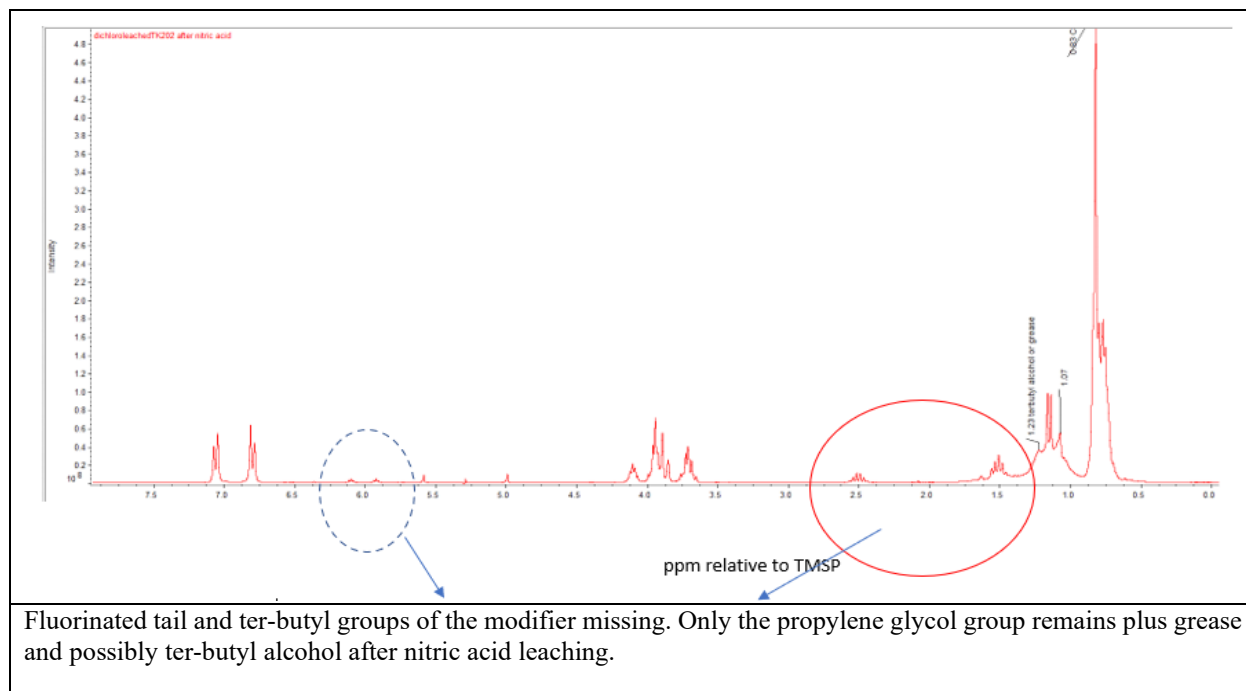


Figure 30. ^1H NMR Spectra for the March 2022 Tank 202 solids Acid Leached Residual Solids- The modifier has been modified with acid leaching (DCM soluble organic species).

The extent of the modification/degradation of the modifier, as shown in Figure 30, does not appear to be consistent or in agreement with previous literature information¹ on the stability of Cs-7SB modifier in contact with 1.0 molar nitric acid in a simulant salt solution. In the cited study above, the modifier was found to be moderately stable in the presence of 1.0 molar nitric acid at 30 and 60 °C for up to 26 days contact time. Meanwhile, it is worth noting that in the cited study, the stability of the modifier in nitric acid was not performed in the presence of transition metal oxides or with radioactive waste sample and no pH shock due to cycling of materials as seen in SWPF processing for cesium or actinide removal. Therefore, it cannot be firmly confirmed that the nitrification observed here was solely responsible for the modification of the molecular structure of the modifier, because the presence of traces of transition metal oxides in the SWPF radioactive waste solids and solutions may also be responsible for the measurable changes in molecular structure of the modifier due to their catalytic activities. In addition, the modifier degradation products, as reported here, are different from the degradation products for the modifier as reported in the cited literature above. This would seem to suggest that degradation mechanisms may be different and may depend on whether a real radioactive waste material is used versus the use of salt simulant solution.

Figure 31 shows the ^1H NMR spectra for the water-soluble species from the post acid leaching of the Tank 202 solids and these include the modifier (bottom spectrum), acetic acid, and acetone (top spectrum).

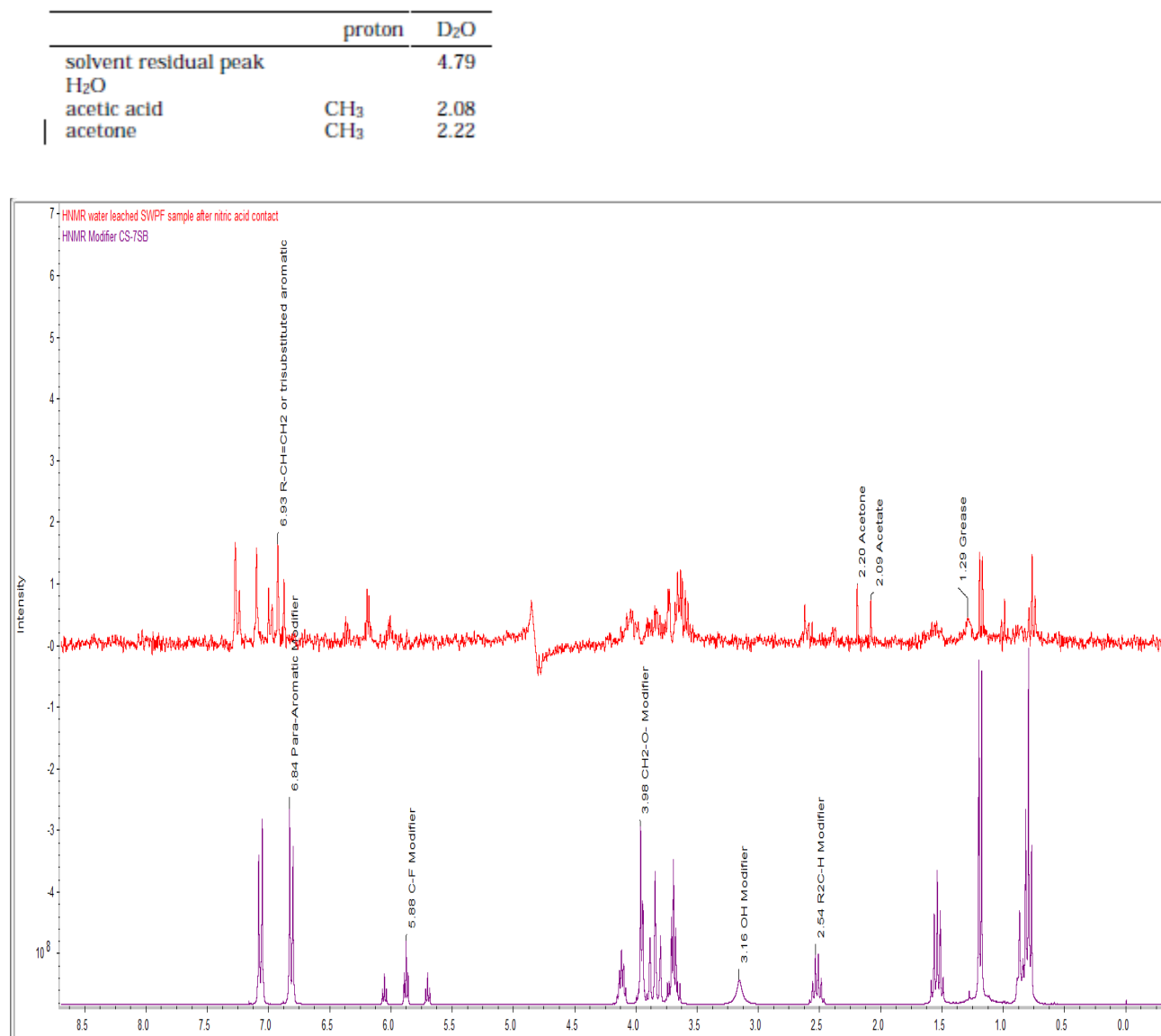


Figure 31. Overlay ^1H NMR Spectra of the March 2022 Tank 202 Acid Leached Residual Solids: Main water-soluble organic species include modifier peaks (bottom spectrum), acetic acid, and acetone (top spectrum).

5.1.2 March 2022 Tank 202 Acid Leached Residual Solids: Particle Size Analysis and Leachate Elemental Compositions

The particle size distribution (PSA) for the nitric acid leached Tank 202 solids material is shown in Figure 32. The PSA shows a near gaussian distribution of particles with the particle range from 0.972 to 31.11

microns. The mode or highest peak in the distribution is 15.56 microns and the mean particle size of 11.55 micron (SD = 6.33 microns).

The particle size distribution profile for the Tank 201 and the March 2022 Tank 202 solids samples, Figures 10, and 32, respectively, are similar. They both show a near gaussian distribution of particles. Although the particle size ranges are almost identical, the Tank 201 sample had larger particles sizes in the lower range (2.75 microns to 31.11) than those in the Tank 202 solids (0.97 to 31.11).

The elemental composition for the acid leachate for the Tank 202 sample is presented in Table 3, and three RCRA metals (Ba, Cd and Cr) in the ICP-AES analytical data at 0.689 mg/L, 0.131 mg/L, and 2.77 mg/L were all below the RCRA limit of 100 mg/L, 1 mg/L and 5 mg/L, respectively.

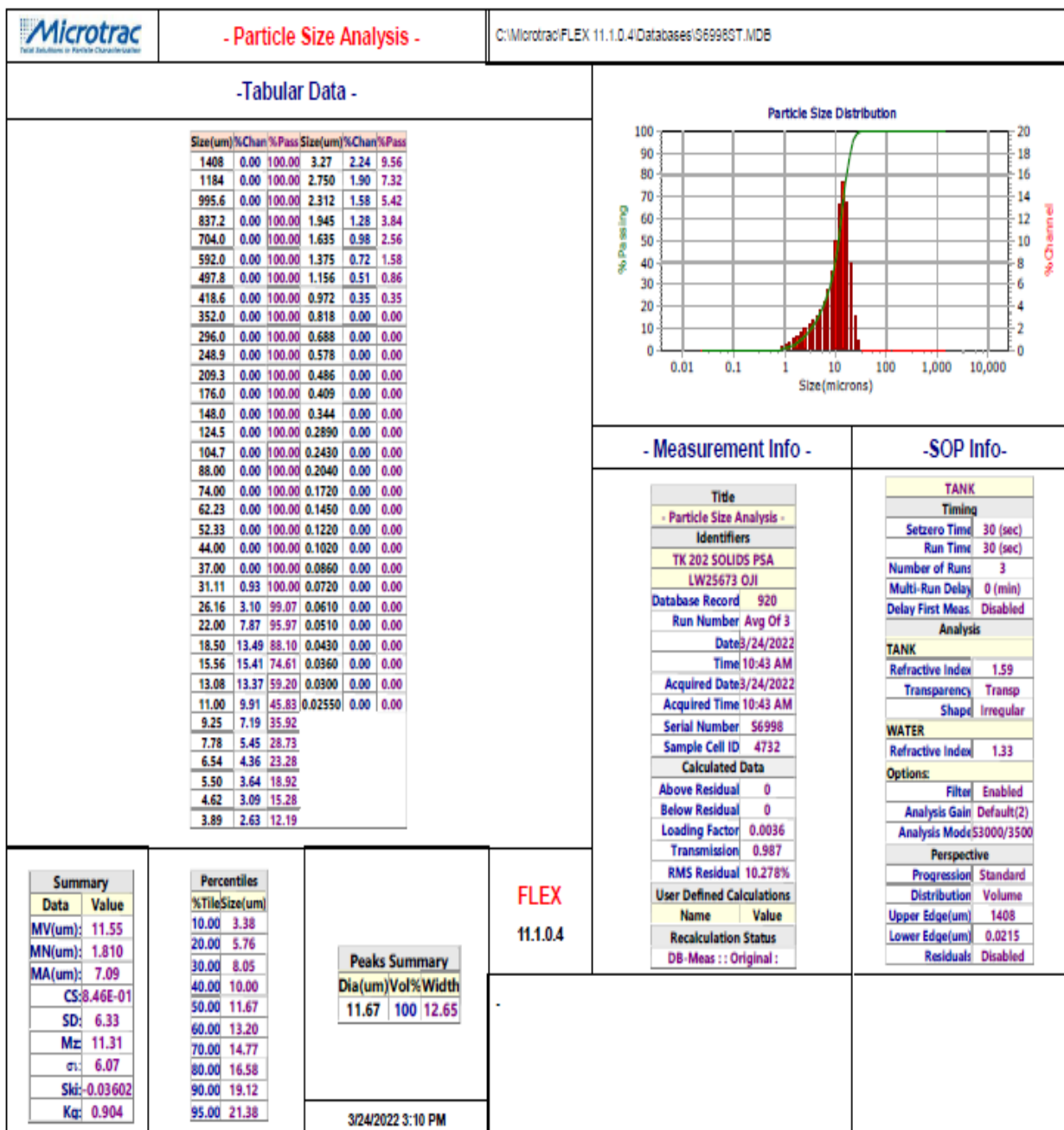


Figure 32. Particle size distribution of the March 2022 Tank 202 solids Acid Leached Residual Solids.

Table 3. Elemental composition for the March 2022 Tank 202 Acid Leachate Solids.

| Elemental composition | Concentration, mg/L | ^b TCLP Regulatory limit, mg/L | RCRA Code |
|------------------------------|----------------------------|-------------------------------------------------|------------------|
| Ag | < 0.002 | 5 | D011 |
| Al | 3.07 | na | na |
| B | < 0.012 | | na |
| Ba | 0.689 | 100 | D005 |
| Be | < 0.001 | na | na |
| Ca | 14.7 | na | na |
| Cd | 0.131 | 1 | D006 |
| Ce | < 0.122 | na | na |
| Co | 6.77 | na | na |
| Cr | 2.77 | 5 | D007 |
| Cu | 1.04 | na | na |
| Fe | 15.2 | na | na |
| Gd | < 0.004 | na | na |
| K | < 0.608 | na | na |
| La | < 0.008 | na | na |
| Li | < 0.524 | na | na |
| Mg | 4.85 | na | na |
| Mn | 1.54 | na | na |
| Mo | < 0.005 | na | na |
| Na | 236 | na | na |
| Ni | 3.39 | na | na |
| P | < 0.032 | na | na |
| Pb | < 0.256 | 5 | D008 |
| S | < 0.312 | na | na |
| Sb | < 0.020 | na | na |
| Si | 0.460 | na | na |
| Sn | < 0.125 | na | na |
| Sr | 1.36 | na | na |
| Th | < 0.139 | na | na |
| Ti | 52.4 | na | na |
| U | < 0.531 | na | na |
| V | < 0.025 | na | na |
| Zn | 0.388 | na | na |
| Zr | < 0.043 | na | na |

Liquid to solid phase ratio: 12.8 mL/g Tank 202 solids. ^bToxicity Characteristic Leaching Procedure [Environmental Protection Agency (EPA) method 1311].

6.0 Apparent buoyancy of organic solvent leached April 2022 Tank 202 Solids fraction in “mother liquor” and ¹H NMR/FT-IR characterization of organic emulsion layer

The solid fraction and filtrate (mother liquor) from the “as received” April 2022 Tank 202 slurry (Figure 33, insert A) was obtained by a liquid /solid separation using a 0.45 µm nylon Nalgene® filter membrane; about 180 mL of the “as-received” Tank 202 slurry was filtered through the Nalgene® membrane. The resulting solid fraction, as shown in Figure 33, insert B, was allowed to air-dry in the SRNL shielded Cells for about 48 hours before use.

About 7.5 grams of this wet Tank 202 solid fraction was put into a 50-mL capacity centrifuge tube already containing 26 mL of the organic solvent dichloromethane. The dichloromethane was used to strip organics from this April 2022 Tank 202 solids fraction material. The centrifuge tube and its contents were mechanically agitated for a total of 20 minutes and allowed to settle overnight in the Shielded Cell. The settled slurry phase separated or partitioned into three distinct layers (a solids layer at the bottom of the centrifuge tube, a near clear and transparent layer of dichloromethane with organic soluble species and a fluffy emulsion layer at the top) as shown in Figure 33, insert C. Thus, the leached solids settled at the bottom of the dichloromethane solvent and what appears to be organic emulsion layer is seen floating at the top of the solvent. The density of dichloromethane (DCM) is 1.33 g/mL. So, the density of the organic emulsion must be less than 1.33 g/mL and that of the solid layer at the bottom greater than or equal to 1.33 g/mL.

A slurry pipette was used to carefully remove and transfer nearly all the liquid phase dichloromethane and the organic emulsion into the 50 mL capacity centrifuge tube containing this dichloromethane leached Tank 202 solids into another container, leaving only the leached solids phase at the bottom of the 50 mL capacity centrifuge tube (Figure 33, insert C). About 13.4 grams of the DCM leached Tank 202 slurry was transferred into a 50 mL capacity graduated volumetric flask already filled to the 30 mL mark with the April 2022 Tank 202 filtrate or mother liquor.

The DCM leached Tank 202 April 2022 sample slurry in Tank 202 filtrate (mother liquor) is shown in Figure 34, insert A. A dispersed and diffused slurry was formed, which immediately started settling to the bottom of the graduated cylinder containing the mother liquor. No floating organic layer was present, which means the dichloromethane took out the insoluble organic components present in the original “as-received” Tank 202 solid fraction. The settling solids was monitored every hour for three hours and then after 24 hours as shown in Figure 34, inserts B, C, and D.

The DCM leached Tank 202 solids, as shown in the Figure 34, inserts C and D, settled to the bottom of the graduated cylinder, and did not show any signs of floating on the “mother liquor” after the leaching of the original Tank 202 solid fraction with the organic solvent dichloromethane. However, the organic emulsion layer that rose to the top after contacting the Tank 202 solids with DCM (see Figure 33 insert C and D) likely contained solids. Thus, some fraction of the solids remained buoyant even after stripping with DCM. Overall, the DCM was mostly effective in eliminating the buoyancy of the solids observed in the plant.

Working with similar samples from this batch of the Tank 202 samples, the plant had observed mercury bearing solids floating under certain conditions, which is contradictory to expectations based on bulk

density of the material. This floating or buoyancy behavior, as seen by the plant, maybe attributed to other surface effects or surface phenomena.

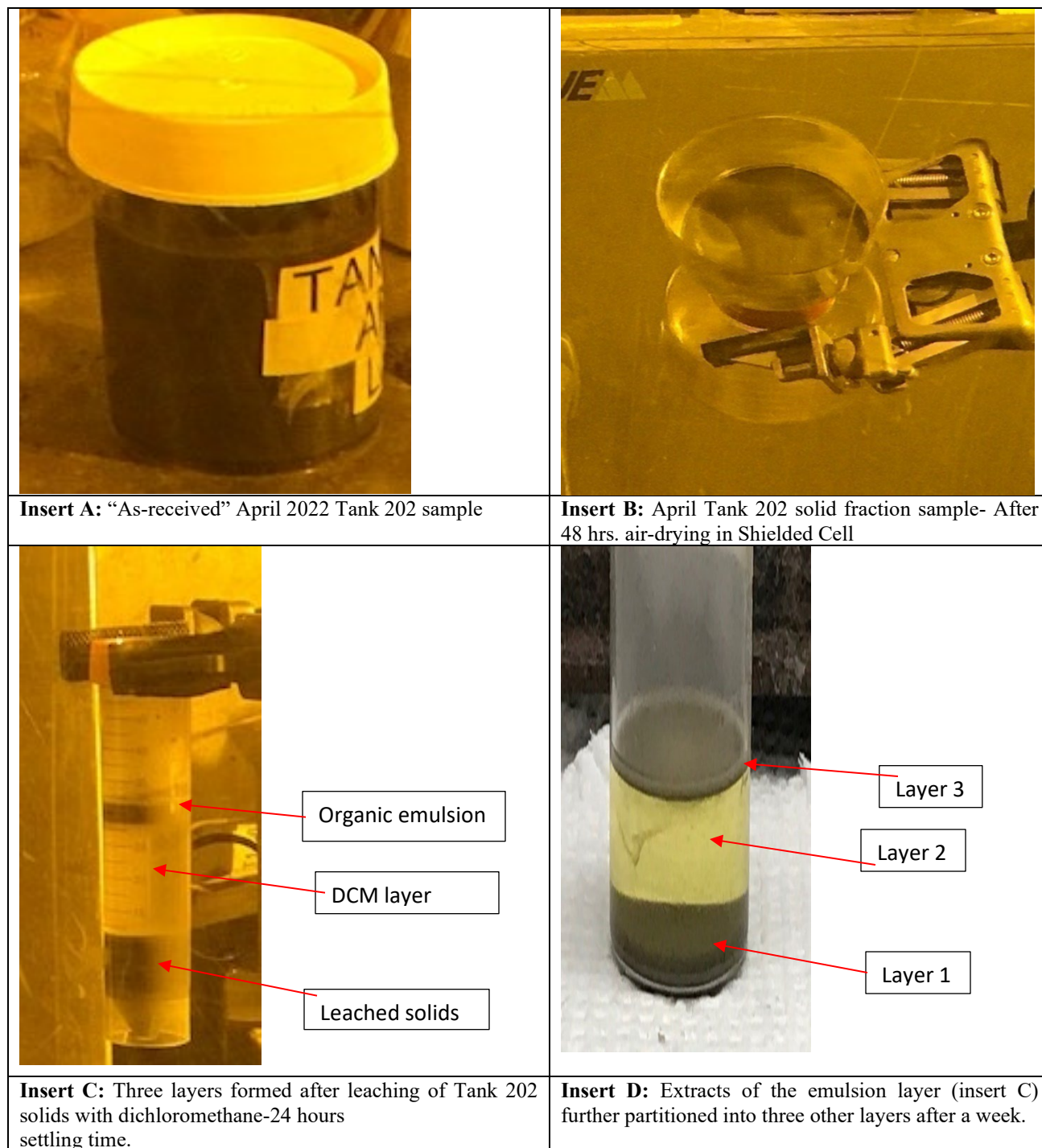


Figure 33. Post dichloromethane leaching of Tank 202 solids (April 2022 sample).

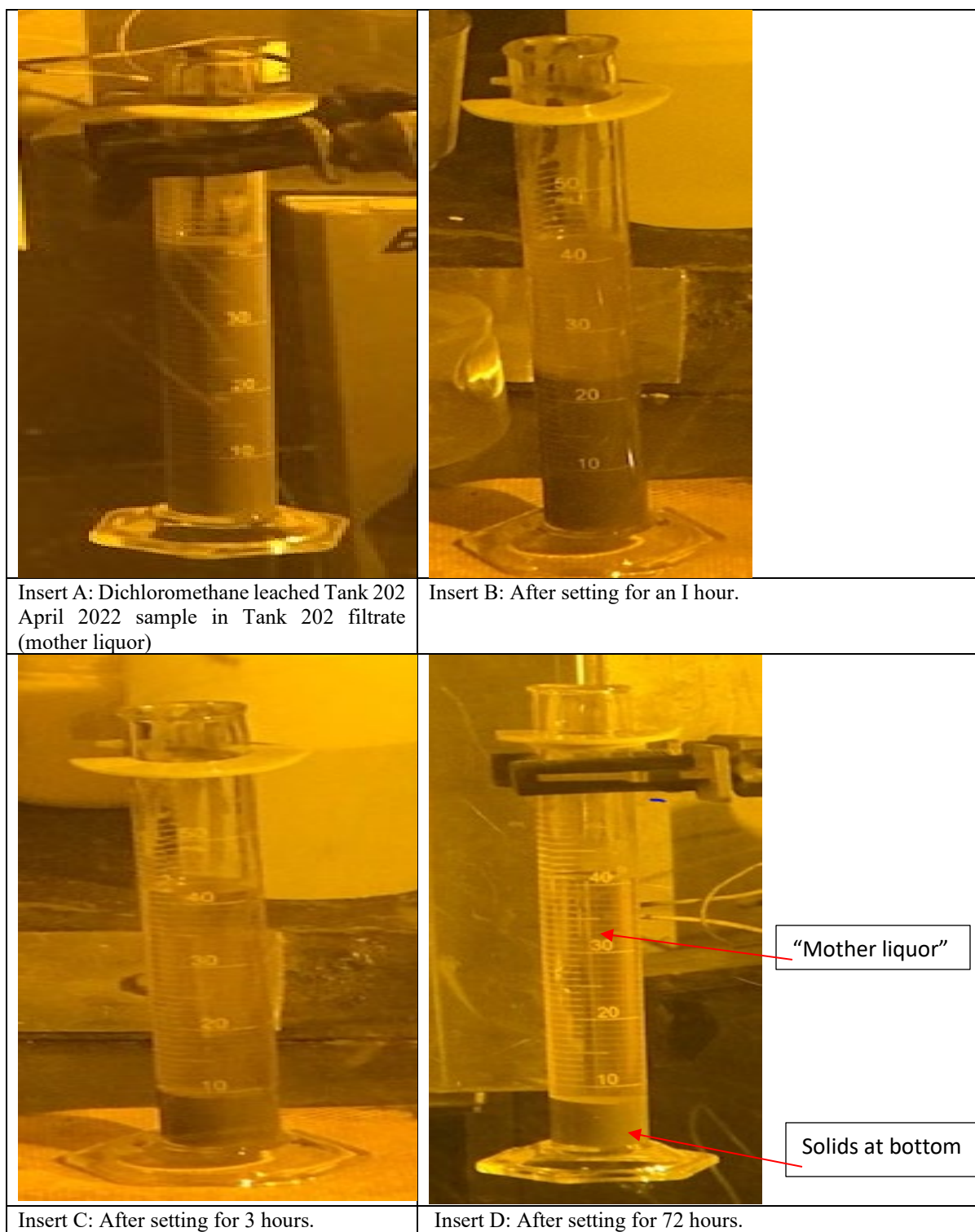


Figure 34. Apparent Buoyancy Test: Dichloromethane leached Tank 202 April 2022 sample in Tank 202 filtrate (Mother liquor).

6.1.1 ^1H NMR/FT-IR characterization of organic emulsion layer for the April 2022 Tank 202 sample

About a week after this dichloromethane leach, the emulsion layer extract (extract from Figure 33, insert C) sent for FT-IR and ^1H NMR characterizations had further partitioned into three other layers, as shown in Figure 33, insert D.

So, the FT-IR and ^1H NMR characterizations now also involved the use of the three separate layers in Figure 33, insert D. These three new partition layers may indicate that there at least three organic components in the emulsion layer.

The FT-IR spectra for this original emulsion layer (top layer) as seen in Figure 33, insert C, is presented in Figure 35. The FT-IR spectra for this emulsion layer shows that the layer is heterogenous and therefore needs a minimum of four spectra to account for all the identified species. The identified components include the modifier, and Isopar-L, which are caustic side solvent extraction components. The nitrate peaks are possible reaction products from acid cleaning in the plant, while the carboxylates may be decomposition products from the modifier (CS-7SB) or BobCalixC6.

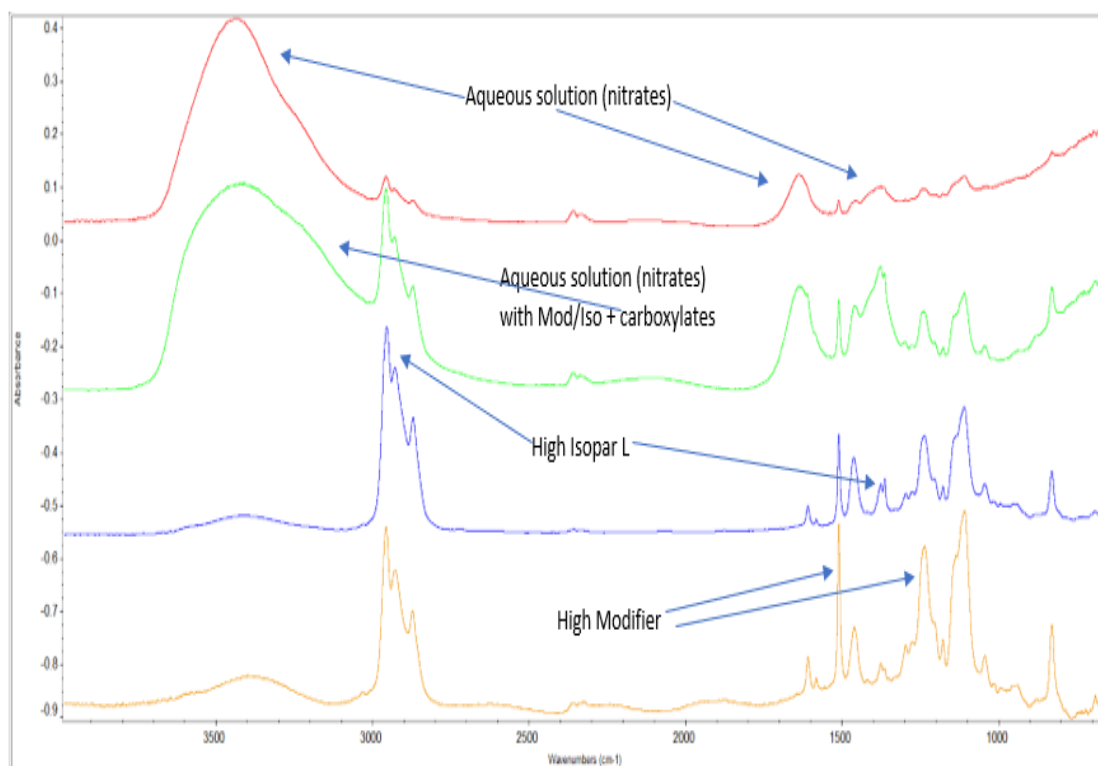


Figure 35. FT-IR spectra of the original emulsion layer (top layer) as seen in Figure 33, insert C.

Figure 36 shows the FT-IR spectra for the partitioned three-layer extract of the emulsion layer as seen in Figure 33, insert D. Since each of the three layers in Figure 33, insert D are not homogenous, a minimum of four spectra were needed to probe for all the identified species.

The bottom two FT-IR spectra in Figure 36 are spectra of the bottom layer in Figure 33, insert D with the modifier and Isopar-L the identified organics. The two top spectra in Figure 36 are those for the top layer in Figure 33, insert D showing the presence of nitrates, traces of water, and modifier with Isopar-L.

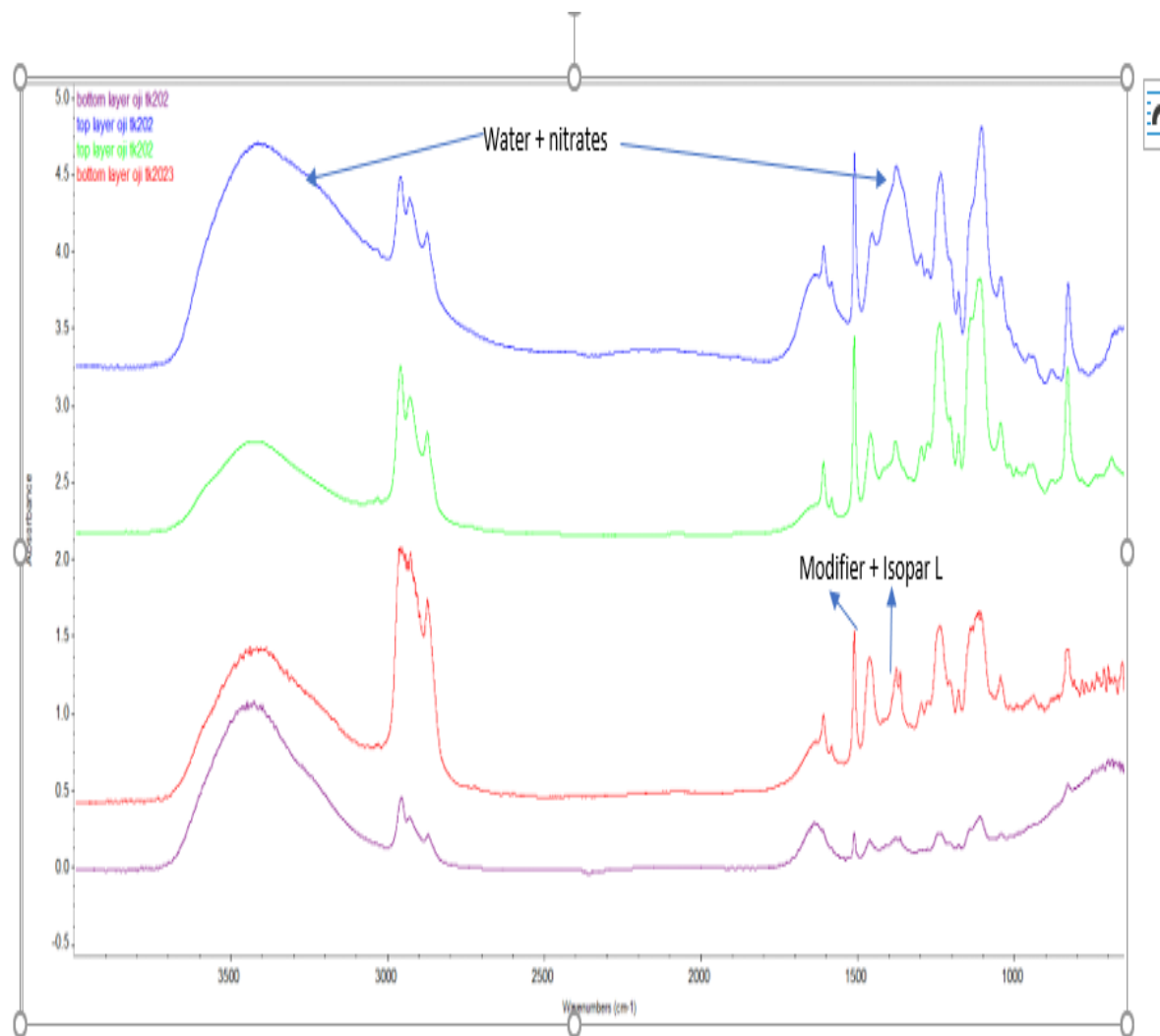


Figure 36. FT-IR spectra of the partitioned three-layer extract of the emulsion layer as seen in Figure 33, insert D.

The overlay ^1H NMR spectra in Figure 37 is from the yellow tinted partitioned layer (second layer) of the extracted emulsion layer as seen in Figure 33, insert D. This ^1H NMR overlay spectra are those for reference pure Isopar-L at the bottom of Figure 37, reference pure modifier in the middle and the Tank 202 yellow tinge solution of Figure 33, insert D at the top of the spectra overlay. The ^1H NMR identified organic and inorganic compounds in the yellow tinted partitioned region include aldehyde or carboxylic compounds, which may be decomposition products, the modifier with Isopar-L and the organic solvent, dichloromethane

used in the leaching process. The components of the Tank 202 yellow tinted layer may be soluble to a certain degree in dichloromethane organic solvent.

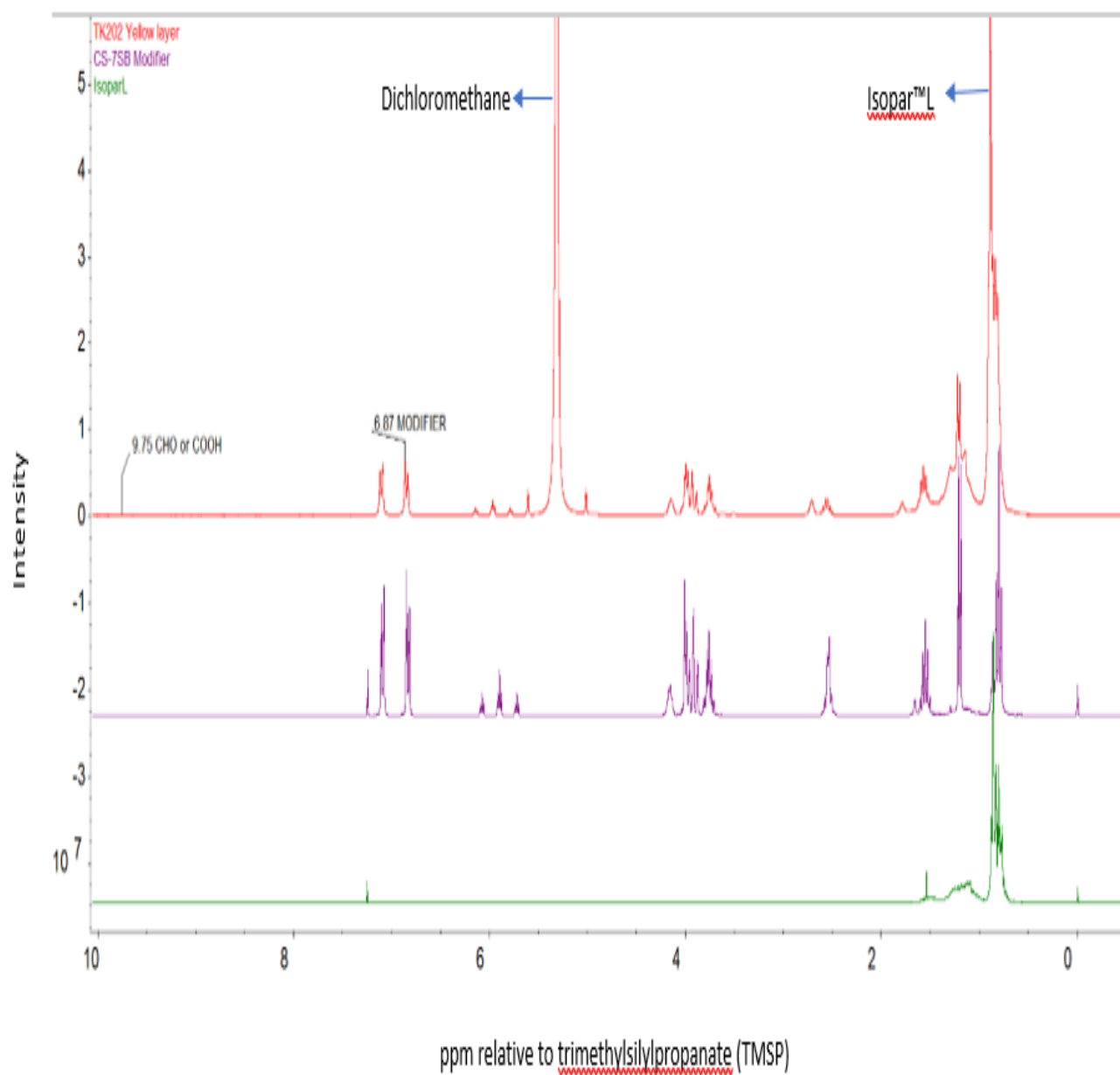


Figure 37. Overlay ^1H NMR spectrum for reference Isopar-L, reference modifier and Tank 202 yellow tinted partition layer (second layer) of the extracted emulsion layer as seen in Figure 33, insert D.

6.1.2 Elemental composition for the organic emulsion layer for the April 2022 Tank 202 sample

The organic emulsion layer with some interstitial liquids, as seen in Figure 33, insert C, was also aqua regia digested and analyzed for elemental composition by ICP-AES, DMA for total mercury, and ICP-MS to account for metals, if present, in the emulsion layer and the interstitial liquids.

The mass spectra data (ICP-MS) for the digested emulsion layer is presented in Appendix D2. The elements of interest and their measured concentrations include W [7.28E+01 mg/L (6.62E+01 ug/g)], and Pb [8.90E-01 mg/L (8.09E-01 ug/g)].

Table 4. Elemental composition for the April 2022 Tank 202 Emulsion Layer.

| Elemental composition | Ug/g | Concentration, mg/L | ^b TCLP Regulatory limit, mg/L | RCRA Code |
|-----------------------|------------|---------------------|------------------------------------------|-----------|
| Ag | < 1.36E-01 | < 1.50E-01 | 5 | D011 |
| Al | 1.08E+01 | 1.19E+01 | na | na |
| B | 1.80E+00 | 1.98E+00 | 100 | na |
| Ba | 1.04E+00 | 1.14E+00 | na | D005 |
| Be | < 7.03E-03 | < 7.73E-03 | na | na |
| Ca | 1.82E+01 | 2.00E+01 | na | na |
| Cd | 1.88E-01 | 2.07E-01 | 1 | D006 |
| Ce | < 8.32E-01 | < 9.15E-01 | na | na |
| Co | 1.04E+01 | 1.14E+01 | na | na |
| Cr | 1.61E+01 | 1.77E+01 | 5 | D007 |
| Cu | 1.59E+00 | 1.75E+00 | na | na |
| Fe | 1.12E+02 | 1.23E+02 | na | na |
| Gd | < 2.18E-01 | < 2.40E-01 | na | na |
| K | < 2.70E+00 | < 2.97E+00 | na | na |
| La | < 1.50E-02 | < 1.65E-02 | na | na |
| Li | < 5.33E-01 | < 5.86E-01 | na | na |
| Mg | 6.65E+00 | 7.32E+00 | na | na |
| Mn | 2.65E+00 | 2.92E+00 | na | na |
| Mo | 6.36E-01 | 7.00E-01 | na | na |
| Na | 5.49E+02 | 6.04E+02 | na | na |
| Ni | 9.07E+00 | 9.98E+00 | na | na |
| P | < 1.48E+00 | < 1.63E+00 | na | na |
| Pb* | 8.09E-01 | 8.90E-01 | 5 | D008 |
| S | 3.32E+00 | 3.65E+00 | na | na |
| Sb | < 2.21E-01 | < 2.43E-01 | na | na |
| Si | 2.01E+01 | 2.21E+01 | na | na |
| Sn | < 8.49E-01 | < 9.34E-01 | na | na |
| Sr | 1.55E+00 | 1.71E+00 | na | na |
| Th | < 9.44E-01 | < 1.04E+00 | na | na |
| Ti | 5.62E+02 | 6.18E+02 | na | na |
| U | < 1.46E+00 | < 1.61E+00 | na | na |
| V | < 1.70E-01 | < 1.87E-01 | na | na |
| Zn | 8.38E-01 | 9.22E-01 | na | na |
| Zr | 4.22E-01 | 4.64E-01 | na | na |
| W* | 6.62E+01 | 7.28E+01 | na | na |
| Hg-total | 1.60E+03 | 1.76E+03 | 0.2 | D009 |

* W and Pb data from ICP-MS (Appendix D2)

The April 2022 Tank 202 emulsion layer and interstitial fluid elemental composition is presented in Table 4. The concentrations for select elements, namely Al, Cd, Fe, Cr, Na, Ni, S, Ti, Zn, W and Hg are 1.19E+01mg/L, 2.07E-01 mg/L, 1.77E+01mg/L, 1.23E+02 mg/L, 6.04E+02 mg/L, 9.98E+00 mg/L, 3.65E+00 mg/L, 6.18E+02 mg/L, 9.22E-01 mg/L, 7.40E+01 mg/L, and 1.76E+03 mg/L, respectively. Most of the elemental components of the April 2022 Tank 202 solids fraction are also present in measurable quantities in the emulsion layer and interstitial liquids, although at relatively lower concentrations (compare Table 4 and Table 5).

6.1.3 Tank 202 solids fraction in water and dichloromethane

As shown in Figure 38, inserts A and B, the April 2022 Tank 202 sample solid fraction was immiscible with water and did not disperse in water either at a phase ratio of 5.8 mL/g solid, and no attempt was made to mechanically dissolve/disperse the solids in water. The immiscibility of the Tank 202 sample solid fraction with water is probably because of the high mercury and organic material content of the solid fraction at 14.2 weight percent total mercury. However, with the addition of dichloromethane (DCM), to this immiscible Tank 202 solids and water combination, the April 2022 Tank 202 solid fraction easily dispersed/dissociated to form a brown slurry as shown in Figure 38, insert C. The water layer was displaced to the top layer by the DCM/Tank 202 slurry mixture. Figure 38, insert D shows the post 24 hour settling of the water, Tank 202 slurry and DCM mixture. After settling for 24 hours, without any mechanical mixing or agitation, the mixture partitioned into five visible layers as shown in Figure 38, insert D: a thin layer of floating organic emulsion at the top of the water layer, water layer, a thin layer of organic emulsion floating on top of the DCM layer, DCM layer, and Tank 202 solid fraction slurry at the bottom.

The thin layer of floating organic emulsion on water is obviously not soluble in water, and not soluble in DCM and less dense than water and DCM. The thin layer of organic emulsion floating on top of the DCM layer is not water or DCM soluble but less dense than DCM and denser than water.

The set up in Figure 38, insert D was mechanically mixed with a slurry pipette as shown in Figure 39, insert A, and left over the weekend (96 hours) and later for one week. After 96 hours, the mixture once again partitioned itself into the same five unique layers, which were even more pronounced after one week as shown in Figure 39 insert B. As seen earlier in Figure 38, insert D, the five layers were a thin layer of floating organic emulsion on top of the water layer, the water layer, a thin layer of organic emulsion floating on top of the dichloromethane (DCM) layer, DCM layer and Tank 202 solid slurry at the bottom (Figure 39 insert B).

As earlier described for Figure 16 and Table 2, the air-dried organic emulsion layer from the December 2021 Tank 202 sample also indicate that the dried organic emulsion layer shows trapped inorganic double anion salts like nitrates and carbonates and multi cations and their oxides. Therefore, the thin layer of floating organic emulsions on top of the water and between the DCM and water layers, as presented in Figures 38 and 39, are probably CSSX solvents components and decomposition organic products containing trapped traces of inorganic oxides (such as HgO, TiO₂ and Fe₃O₄).

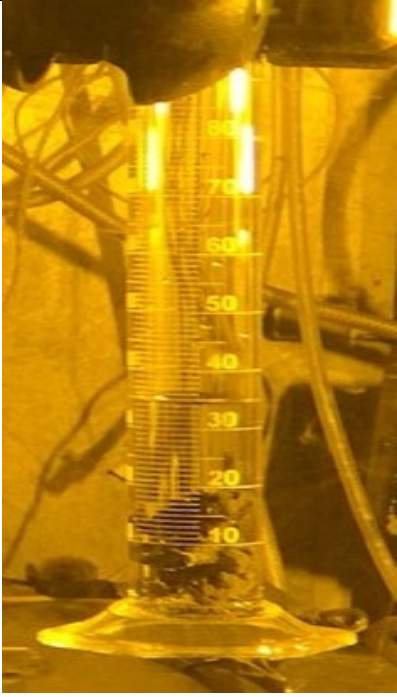
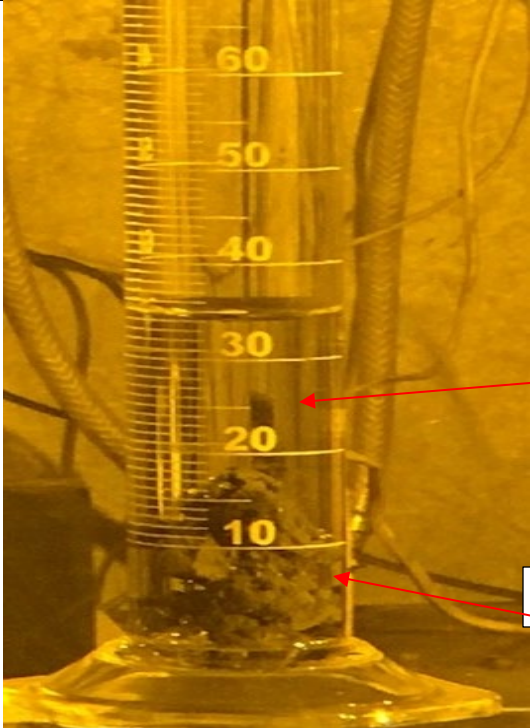
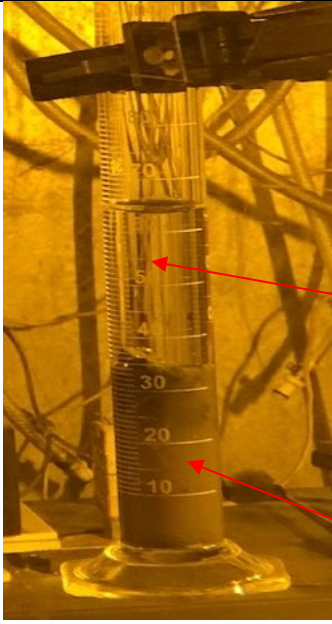
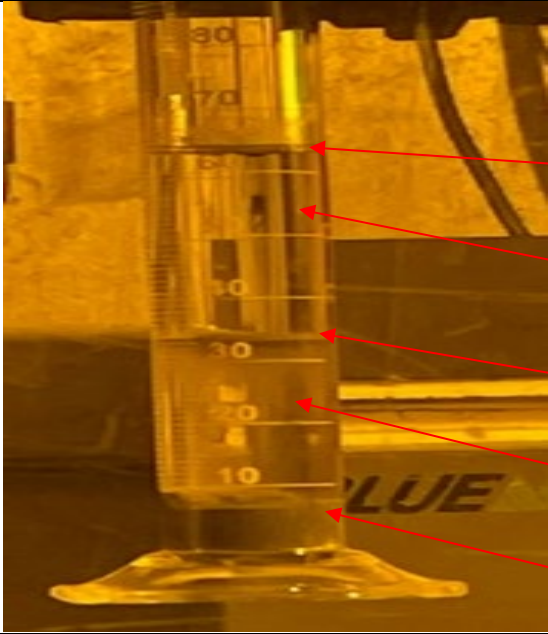
| | |
|--------------------------------------------------------------------------------------------------------------------------|---------------------------------------------------------------------------------------------------------------------------------------------------------------------------------|
|  |  <p>Water layer</p> <p>Immiscible solids</p> |
| <p>Insert A: Tank 202 solid fraction was immiscible with water with the addition of water.</p> | <p>Insert B: After 24 hours in water: No dissolution of solids in water; no dissolution in water.</p> |
|  <p>Water</p> <p>DCM-solids-slurry</p> |  <p>Layer 5</p> <p>Layer 4-water</p> <p>Layer 3</p> <p>Layer 2-DCM</p> <p>Layer 1-solids</p> |
| <p>Insert C: Addition of dichloromethane to solids in water. Tank 202 solids dissolves to form a slurry in DCM.</p> | <p>Insert D: Addition of dichloromethane to solids in water after 24 hours settling time. Five distinct layers are formed.</p> |

Figure 38. April 2022 Tank 202 solids fraction in water and dichloromethane without agitation.

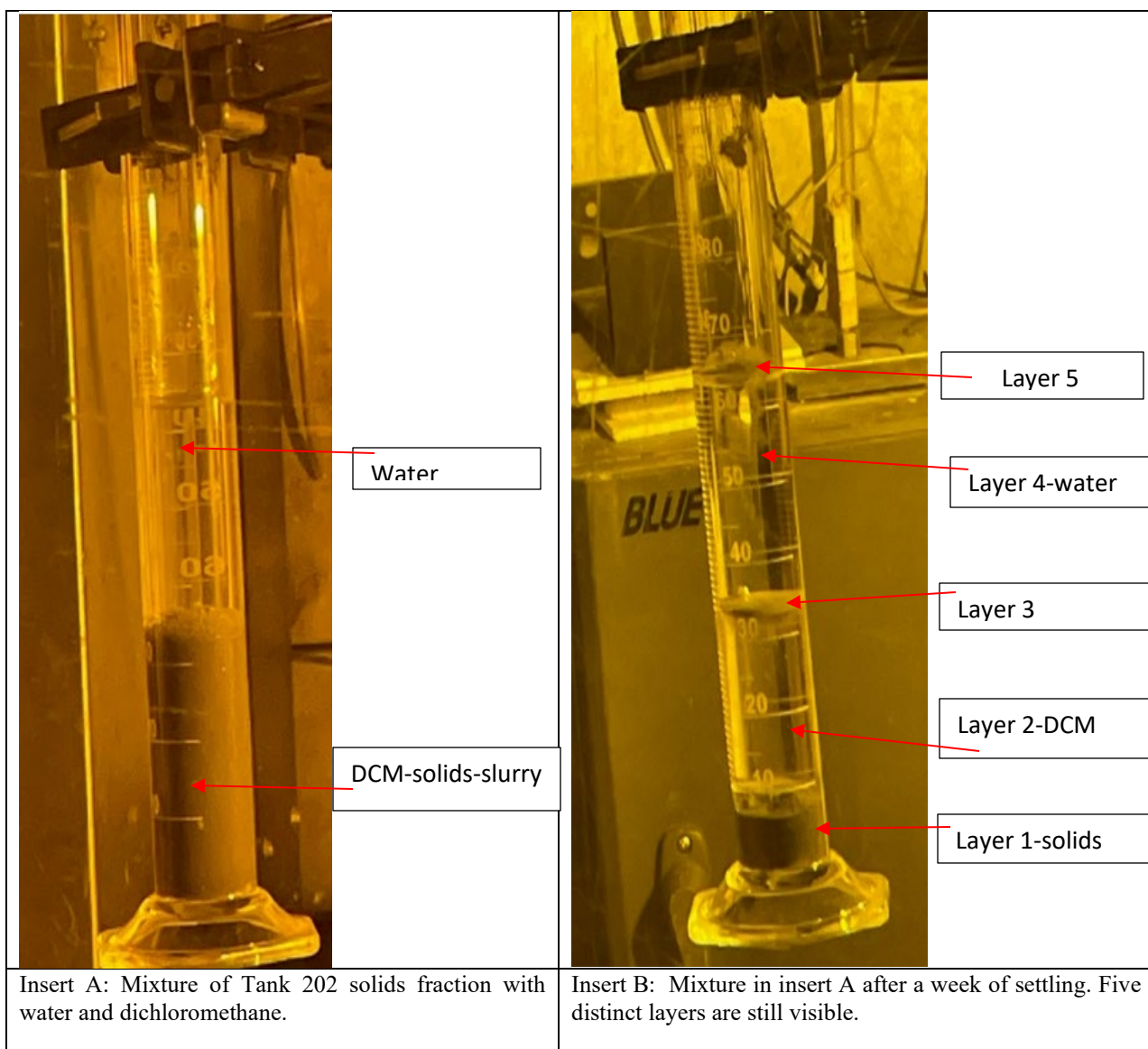


Figure 39. April 2022 Tank 202 solids fraction in water and dichloromethane with mixing and agitation.

7.0 Miscellaneous analysis of the “as-received” March 2022 Tank 202 Sample-Elemental Composition

The March 2022 Tank 202 “as-received” filtrate was not analyzed for elemental composition by ICP-AES because the sample had the consistency of vegetable oil due to the presence of significant amount of caustic side extraction (CSSX) solvent and thus would not mix with 2% HNO₃ acid diluent, which is used in ICP-AES sample preparation for analysis. The March 2022 Tank 202 solid fraction sample, as shown in Figure 2, insert C, was a “wet cake” coming from the solid/liquid separation of the “as-received” sample. This “wet cake” was acid digested and analyzed for elemental compositions by ICP-AES, ICP-MS for As and Se, and DMA for total mercury. The elemental and RCRA analytical results for this “as-received” March 2022 Tank 202 wet cake solid fraction is presented in Table 5. The density of the “as-received” Tank 202 (March 2022 sample) was not determined in this characterization of the material and thus an approximate density of 1.1 mg/L was also used in the AQR digestion conversions from µg/g to mg/L.

The RCRA metals for the March 2022 Tank 202 sample are presented in Table 5, and all but three of them were above RCRA/TCLP limit. The concentrations for Ba, Cd, Cr, Pb, and total mercury in the Tank 202 sample were all higher than their RCRA limits and measured 2.24E+02 mg/L, 3.74E+01 mg/L, 4.24E+03 mg/L, 1.73E+02 mg/L, and 1.56E+05 mg/L, respectively. The RCRA/TCLP limits for these metals (Ba, Cd, Cr, Pb, and total mercury) are 100 mg/L, 1.0 mg/L, 5 mg/L, 5 mg/L and 0.2 mg/L, respectively. Only Ag (2.76E+00 mg/L), As (5.62E-01 mg/L), and Se (<2.73E-01 mg/l) were below their RCRA limit requirement of 5 mg/L, 5 mg/L and 1.0 mg/L, respectively.

Meanwhile, it is worth noting that the weight percent total mercury in the “as-received” Tank March 2022 Tank 202 “wet” cake sample is relatively high at 14.20 wt.% (155,839 mg/L) when compared to the mercury concentration in the December 2021 Tank 201 sample at 4.44 wt.% (4.89E+04 mg/L) total mercury. The concentration for total mercury in the December 2021 Tank 202 sample (liquid portion) was only 49.1 mg/L.

In general, it is empirically acknowledged that transition metals are present in tank samples as oxides of those metals. At these levels of mercury and select metal concentrations in the “as-received” March 2022 Tank 202 Sample (Mercury at 1.56E+05 mg/L, titanium at 7.83E+04 mg/L, Iron at 2.73E+04 mg/L, zinc at 1.52E+02 mg/L, copper at 3.53E+03 mg/L, chromium at 4.24E+03 mg/L and aluminum at 2.54E+03 mg/L), the formation of submicron transition metal oxide particles, especially mercuric oxide (HgO), titanium oxide (TiO₂); possibly an MST decomposition product, and iron oxides/hydroxides (Fe₃O₄/Fe₂O₃) are possible.

The mercury and titanium SEM/EDX patterns in Figures 5, and 6 for the December 2021 Tank 201 sample, Figure 14 for the December 2021 Tank 202 dry organic emulsion layer, Figures 22-24 for the acid-leached March 2022 Tank 202 sample, and Figures 30 -32 for the “as-received” March 2022 Tank 202 sample, match the literature SEM/EDX patterns for mercuric oxide and titanium oxides.^{2, 3, 4} In the case of HgO, the particle size for HgO synthesized in organic/aqueous media¹ are indicated in the cited literatures as being in the nanoparticle size range. Since this organic/aqueous media is similar to the SWPF tank media, it can be concluded that the HgO formed in the SWPF tanks are also in the submicron range, if not in the nanoparticle range. Similarly, the iron oxide SEM/EDX patterns for the cited figures above for the three SWPF tank samples match the literature SEM/EDX patterns for iron oxide.^{4, 5}

Table 5. Elemental composition and RCRA metals for the “as-received” March 2022 Tank 202 solids

| Elemental composition | Concentration ug/g-solid | [†] Wt.% | Concentration, mg/L | [‡] TCLP Regulatory limit, mg/L | RCRA Code |
|-----------------------|--------------------------|-------------------|---------------------|------------------------------------------|-----------|
| Ag | 2.76E+00 | 2.76E-04 | 3.03E+00 | 5 | D011 |
| Al | 2.31E+03 | 2.31E-01 | 2.54E+03 | na | na |
| B | <2.44E+00 | <2.44E-04 | <2.68E+00 | | na |
| Ba | 2.04E+02 | 2.04E-02 | 2.24E+02 | 100 | D005 |
| Be | <2.56E-01 | <2.56E-05 | <2.82E-01 | na | na |
| Ca | 3.37E+03 | 3.37E-01 | 3.71E+03 | na | na |
| Cd | 3.40E+01 | 3.40E-03 | 3.74E+01 | 1 | D006 |
| Ce | <4.18E+01 | <4.18E-03 | <4.60E+01 | na | na |
| Co | 1.91E+03 | 1.91E-01 | 2.10E+03 | na | na |
| Cr | 3.85E+03 | 3.85E-01 | 4.24E+03 | 5 | D007 |
| Cu | 3.21E+02 | 3.21E-02 | 3.53E+02 | na | na |
| Fe | 24800 | 2.48E+00 | 2.73E+04 | na | na |
| Gd | <3.16E+00 | <3.16E-04 | <3.48E+00 | na | na |
| K | <9.82E+01 | <9.82E-03 | <1.08E+02 | na | na |
| La | <5.66E+00 | <5.66E-04 | <6.23E+00 | na | na |
| Li | <1.13E+02 | <1.13E-02 | <1.24E+02 | na | na |
| Mg | 1.21E+03 | 1.21E-01 | 1.33E+03 | na | na |
| Mn | 6.70E+02 | 6.70E-02 | 7.37E+02 | na | na |
| Mo | 7.67E+01 | 7.67E-03 | 8.44E+01 | na | na |
| Na | 3.74E+04 | 3.74E+00 | 4.11E+04 | na | na |
| Ni | 2.18E+03 | 2.18E-01 | 2.40E+03 | na | na |
| P | <2.75E+02 | <7.84E-04 | <8.62E+00 | na | na |
| Pb | 1.60E+02 | 1.60E-02 | 1.76E+02 | 5 | D008 |
| S | 2.90E+02 | 2.90E-02 | 3.19E+02 | na | na |
| Sb | <9.76E+00 | <9.76E-04 | <1.07E+01 | na | na |
| Si | 7.28E+02 | 7.28E-02 | 8.01E+02 | na | na |
| Sn | <3.09E+01 | <3.09E-03 | <3.40E+01 | na | na |
| Sr | 3.34E+02 | 3.34E-02 | 3.67E+02 | na | na |
| Th | <3.44E+01 | <3.44E-03 | <3.78E+01 | na | na |
| Ti | 7.12E+04 | 7.12E+00 | 7.83E+04 | na | na |
| U | <2.66E+02 | <2.66E-02 | <2.93E+02 | na | na |
| V | <1.02E+01 | <1.02E-03 | <1.12E+01 | na | na |
| Zn | 1.38E+02 | 1.38E-02 | 1.52E+02 | na | na |
| Zr | 5.12E+01 | 5.12E-03 | 5.63E+01 | na | na |
| W | 5.35E+02 | 5.35E-02 | 5.89E+02 | na | na |
| Hg _{total} | 1.42E+05 | 1.42E+01 | 1.56E+05 | 0.2 | D009 |
| As | 5.11E-01 | 5.11E-05 | 5.62E-01 | 5 | D004 |
| Se | < 2.48E-01 | <2.48E-05 | <2.73E-01 | 1 | D010 |

*It is assumed that the density of the Tank 201 sludge is 1.1 g/mL, @10000 ug/g-solid = 1 Wt.%, na = not applicable.

[‡]Toxicity Characteristic Leaching Procedure [Environmental Protection Agency (EPA) method 1311].

[†] 10000 ug/g solid = 1 wt. %

The “as-received” March 202 Tank 202 sample was different from the “as-received” December 2021 Tank 201 sample in the following ways.

- The liquid portion or fraction of the “as-received” March 2022 Tank 202 sample contained more organic components (CSSX solvents) when compared to the “as-received” December 2021 Tank 201 sample, which contained no liquid fraction at all. Only the December 2021 Tank 202 sample contained appreciable aqueous liquid phase.
- The molar ratios for several select metals (Na/Ti, Na/Al, Na/Fe, Ti/Al, and Al/Fe), as shown in Table 6, were measurably different between the two SWPF tank sample types (December 2021 Tank 201 sample and the March 2022 Tank 202 sample). For example, the Na/Ti, Na/Al, Na/Fe, and Ti/Al molar ratios in the March 2022 Tank 202 were 1.09, 19, 3.66 and 17.37, respectively. The corresponding element molar ratios for the December 2021 Tank 201 samples were significantly different and lower at 0.204, 0.684, 2.10 and 3.36, respectively.
- The concentrations for elemental sodium ($4.11\text{E}+04$ mg/L), titanium ($7.83\text{E}+04$ mg/L), Aluminum ($2.54\text{E}+03$ mg/L) and the RCRA metal were relatively different in the March 2022 Tank 202 sample than in the December 2021 Tank 201 sample, where the above select elements measured $1.97\text{E}+03$ mg/L, $2.01\text{E}+04$ mg/L, and $3.38\text{E}+03$ mg/L, respectively.

To confirm the actual concentrations of select elements, those with upper limit values in ICP-AES analysis, such as Ag and Pb and W (not normally seen in the elemental chemistry of these samples), which were not quantitatively measured by ICP-AES as in revision 1 of this report,⁷ it was necessary to acid digest the March 2022 Tank 202 solids fraction and analyze the resulting solution by ICP-MS as shown in Appendix D.

The concentrations for Ag, Pb, and W are based on the atomic masses of the stable isotopes, which are masses 107 and 109 for Ag, masses 206, 207, and 208 for Pb and masses 183, and 184 for W. Thus, the concentrations for Ag, Pb and W, as shown in Table 5, are calculated as 3.03 mg/L (2.76 µg/g), 176 mg/L (160 µg/g), and 589 mg/L (535 µg/g), respectively. Again, it is assumed that the density of the “as-received” solid fraction for the March 2022 Tank 202 sample is at least 1.1 mg/L.

The ICP-MS data for the March 2022 Tank 202 solids characterization shows the presence of tungsten at a concentration of 620 mg/L and therefore confirms the existence of tungsten and tungsten mineral (WC) in the Tank 202 samples, which were previously identified in the XRD and SEM/EDX characterization results for the previous December 2021 Tank 202 (Figures 15) and March 2022 Tank 202 samples (Figures 19, 20, 22 and 23).

Table 6. Elemental composition comparison between the December 2021 Tank 201 and March 2022 Tank 202 samples

| Ratio | Molar ratio: “As- received” Tank 201 Dec. 2021 sample | Molar ratio: “As- received” Tank 202-March sample |
|--------------|------------------------------------------------------------------|--------------------------------------------------------------|
| Na/Ti | 0.204 | 1.09 |
| Na/Al | 0.684 | 19.0 |
| Na/Fe | 2.10 | 3.66 |
| Ti/Al | 3.36 | 17.37 |
| Ti/Fe | 10.30 | 3.35 |
| Al/Fe | 3.07 | 0.19 |

The summary information for the characterization of these three SWPF tank samples, December 2021 Tank 201, and the two Tank 202 samples (December 2021, and March 2022 Tank 202 samples) are presented in Table 7. The April 2022 Tank 202 sample was only used for the buoyancy test and limited FT-IR and ^1H NMR characterizations. This April 2022 Tank 202 sample was never characterized in detail as the other samples.

Apart from the simple sodium minerals, which are found in all these samples, the unique identified XRD mineral gibbsite is present in both the December 2021 Tank 201 and the March 2022 Tank 202 samples. However, no gibbsite mineral was identified in the caustic December 2021 Tank 202 aqueous sample or the organic emulsion layer of the December 2021 Tank 202 sample. This is expected because gibbsite is soluble in a high pH environment⁸ but precipitates out in environment where the pH lies between 4 and 8.5. Therefore, the presence of gibbsite in the December 2021 Tank 201 and the March 2022 Tank 202 solids may indicate that those solid residues were generated from acid cleaning process with nitric acid, which would lower the pH of the resulting residues.

Other minerals such as titanium oxide (TiO_2) are present in the XRD spectra for the Tank 201 sample but can only be confirmed to be present in the Tank 202 samples because of the presence of elemental titanium in these sample. Tungsten carbide (WC), and elemental W were identified in the XRD/SEM/EDX spectra for the Tank 202 samples but not in the Tank 201 sample.

The SEM/EDX and elemental composition analytical results are essentially similar but not identical in terms of individual elemental concentrations in the December 2021 Tank 201 and March 2022 Tank 202 samples, although there are measurable quantities of W in the Tank 202 samples and traces of Cu in the Tank 201.

The modifier, gibbsite and ordinary grease were identified in all the FT-IR characterized samples for the December 2021 Tank 201, and the March 2022 Tank 202 samples along with the modifier decomposition products (Sec. butyl phenol, Carbonates, and nitrates). The December 2022 Tank 202 sample FT-IR characterization showed the presence of detectable amounts of carbonates and nitrates.

Organic and water extracted components from the samples were used to identify those components, especially the organics, which are organic versus water soluble species.

As summarized in Table 7, the ^1H NMR spectra for the organic solvent (dichloromethane) extracted samples for the December 2021 Tank 201 and December 2021 Tank 202 samples identified the presence of the modifier in both samples. The March 2022 Tank 202 sample also contained the decomposition products (propylene glycol group, and ter-butyl alcohol) for the modifier. Ordinary grease was also identified in the December 2021 Tank 201 sample and the March 2022 Tank 202 sample. The source of this ordinary grease from both the FT-IR and ^1H NMR spectra in these samples has not yet been established.

The ^1H NMR spectra for the water extracted samples (December 2021 Tank 201, December 2021 Tank 202, and the samples March 2022 Tank 202 sample) identified the presence of the modifier in the December 2021 Tank 201 and March 2022 Tank 202 samples. The presence of the modifier in the December 2021 Tank 202 emulsion and liquid phase were below detection limit, although the presence of BobCalix and other decomposition products (Sec. butyl phenol, formate, and aliphatic fluorides) were identified in this water extract. The decomposition products identified in the ^1H NMR spectra for the December 2021 Tank 202 emulsion and the March 2022 Tank 202 water extracts include sec. butyl phenol and acetic acid/acetone, respectively.

In general, the modifier and BobCalix, if present in the tank sample, are soluble in dichloromethane but partially soluble in water with all their radiolytic decomposition products.

There were no significant differences in the particle size distribution between the December 2021 Tank 201 and the March 2022 Tank 202 samples.

Table 7. Summary Information on December 2021 Tank 201 and March 2022 Tank 202 Samples

| Analyses | December 2021 Tank 201 | December 2021 Tank 202 emulsion ^s or liquid phase | March 2022 Tank 202 sample (acid leached sample) |
|------------------------------|----------------------------------------------------------------------------------------------|--------------------------------------------------------------------------------------------------------------------------------------------------------------------------------------|----------------------------------------------------------------------------------------------|
| Density | Not determined | 1.05 g/mL | Not determined |
| pH | Not applicable | ≥ 14 | Not applicable |
| XRD mineralogy | Gibbsite [$\text{Al}(\text{OH})_3$], titanium oxide (TiO_2), and sodium nitrate | Sodium nitrate (NaNO_3), thermonitrite ($\text{Na}_2\text{CO}_3 \cdot \text{H}_2\text{O}$) and trona ($\text{Na}_3\text{H}(\text{CO}_3)_2 \cdot 2\text{H}_2\text{O}$) | Tungsten carbide (WC), gibbsite [$\text{Al}(\text{OH})_3$], and quartz (SiO_2). |
| SEM/EDX elemental | Mg, F, Na, Al, Si, Hg, Ti, Fe, and Cu | F, Na, Al, Mg, Si, Hg, Ca, Ti, Fe, and W | F, Na, Al, Mg, Si, Hg, Cr, Ca, Ti, Fe, and W |
| Elemental composition | Al, Ba, Ca, Cd, Co, Cr, Fe, Mg, Mn, Mo, Na, Ni, P, S, Si, Ti, U, Zn and Zr. | Al, Ba, Ca, Co, Cr, Fe, Ma, Mn, Na, S, Si, Sr, Ti, and Zn | Al, Ba, Ca, Cd, Co, Cr, Fe, Mg, Mn, Mo, Na, Ni, P, S, Si, Ti, U, Zn and Zr. |
| RCRA metals | Cd, Cr, Pb, and Hg | Hg | Ba, Cd, Cr, Pb, and Hg |
| FT-IR organics | Modifier, ordinary grease, gibbsite, carbonates, nitrates | Carbonates, nitrates Below detection limits for modifier | Modifier, ordinary grease Sec. butyl phenol |
| NMR organics | | | |
| • Organic solvent extraction | Modifier, ordinary grease | Modifier | propylene glycol group, grease, and ter-butyl alcohol |
| • Water extraction | Modifier, sec. butyl phenol | Sec. butyl phenol, formate, BobCalix, aliphatic fluorides | Modifier, acetic acid, and acetone |
| Particle Size Analysis (PSA) | 2.75-31.11 μ , mean at 14.79 μ (SD = 4.87 μ and highest peak (mode) = 18.5 μ | Sub-micron particles in liquid phase. | 0.97-31.11 μ , mean at 11.6 μ (SD = 6.3 μ , and highest peak (mode) = 15.6 μ |

^s Tank 202 air-dried organic emulsion used for FT-IR and ^1H NMR analyses, Tank 202 wet emulsion used for XRD and SEM/EDX characterizations, and Tank 202 liquid portion used for ICP-AES for elementals and RCRA metals.

7.1.1 Data quality presentations for FT-IR and ^1H NMR based organic analyses

As earlier mentioned, gibbsite material was used as the control for the preparation of FT-IR samples in the SRNL shielded cells, especially for those samples which required overnight preparation of samples such as the air-drying of the Tank 202 emulsion sample for about 96 hours. The FT-IR spectra for gibbsite control, which was exposed to the Shielded Cell environment at the same time as the sample of interest (Tank 202 air dried sample), and the unexposed gibbsite control are shown in Appendix C. In the three FT-IR spectra, the gibbsite control material exposed in the shielded cell, shows the existence of extra organic peaks which match those of Shielded Cell oxidized oil grease and cellulose. These extra organic peaks from the Shielded Cell environment were below instrument detection limits for any of the Tank 201 and Tank 202 samples characterized by FT-IR or ^1H NMR.

8.0 Conclusions

The Salt Waste Processing Facility (SWPF) Tank 201 and Tank 202 samples have been characterized using X-ray diffraction (XRD), scanning electron microscope/energy dispersive x-ray (SEM/EDX), particle size analysis (PSA-Microtrac), Fourier transform-infrared (FT-IR) and proton nuclear magnetic resonance (^1H NMR) spectroscopic techniques to characterize and identify organic and inorganic components in Tanks 201 and 202 as part of efforts to understand the problems occurring at SWPF due to the presence of solids in the recovered solvent.

The key characterization results from the Tank 201 and Tank 202 includes the following.

- The December 2021 Tank 201 sample, collected from the Tank 201 decontaminated salt solution coalescer, was a small amount of grey slurry (paste), with no observed free-standing liquid, while the December 2021 Tank 202 sample, came in a glass vial with two phases: a liquid layer at the bottom and a floating organic emulsion layer at the top.
- The lower liquid phase of the December 2021 Tank 202 sample was a caustic solution with a pH of 14 or greater (pH is ≥ 14) and a density of 1.05 g/mL (0.32 %RSD).
- The March and April 2022 Tank 202 samples were slurry samples, which eventually settled to a solid fraction and a liquid fraction, consisting of mostly caustic side solvent extraction solvent at the top.
- XRD data for the December 2021 Tank 201 and Tank 202 samples show the presence of both amorphous and crystalline mineral phases. For the Tank 201 sample, the identified crystalline minerals include titanium oxide (TiO_2), bayerite [$\text{Al}(\text{OH})_3$], and sodium nitrate (NaNO_3). The identified crystalline minerals in the Tank 202 air-dried organic emulsion were sodium nitrate (NaNO_3), thermonitrite ($\text{Na}_2\text{CO}_3 \cdot \text{H}_2\text{O}$), and trona ($\text{Na}_3\text{H}(\text{CO}_3)_2 \cdot 2\text{H}_2\text{O}$).
- The SEM/EDX elemental compositions for the December 2021 Tank 201 sample include F (seen almost everywhere and believed to be coming from the modifier), Hg, and Ti, from many locations within the SEM photo images. Additionally, elements found in previous SWPF samples Na, Al, Si, Fe, and Cu are present with Fe and Cu only in relatively small amounts. The predominant SEM/EDX elements present in the December 2021 Tank 202 sample were F, Na, Al, Mg, Si, Hg, Ca, Ti, Fe, and W (tungsten).
- The XRD mineral content for both the March 2022 acid leached Tank 202 solids and the “as-received” March 2022 Tank 202 solids were identical and showed the presence of gibbsite, quartz, and tungsten carbide.
- The principal SEM/EDX elemental compositions for the March 2022 Tank 202 sample also include F, Na, Al, Mg, Si, Hg, Cr, Ca, Ti, Fe, and W.
- The presence elemental tungsten (W) and tungsten mineral (tungsten carbide) in the Tank 202 samples (December 2021, and March 2022 samples) were also confirmed by SEM/EDX, XRD and

ICP-MS characterizations and the source of this elemental tungsten or its carbide mineral is not known.

- The particle size distribution for the December 2021 Tank 201 solids show a near gaussian distribution of particles with particle sizes ranging from 2.75 microns to 31.11 microns and the mean particle size at 14.8 microns, with the most abundant particle size being the 18.5 microns. The particle size distribution for the March 2022 Tank 202 acid leached residual solids samples were like that of the December 2021 Tank 201 sample. The particle size distribution also showed a near gaussian distribution of particles with the particle range from 0.972 to 31.11 microns. The mode or highest peak in the distribution is 15.56 microns and the mean particle size of 11.56 micron (SD = 6.33 microns).
- The particle size characterization for the December 2021 Tank 202 liquid portion indicated that no measurable particles were detected in the liquid, which means the particles present, if any, were below the instrument detection limit of 0.243 microns.
- Three of the RCRA elements (Cd, at 5.95 mg/L, Cr at 337 mg/L and Hg at 4.89E+04 mg /L) for the December 2021 Tank 201 sample were above their RCRA limits of 1.0 mg/L, 5 mg/L, and 0.2 mg/L, respectively.
- Of the eight RCRA monitored metals (As, Ba, Cd, Cr, Pb, Hg, Se, Ag), only total mercury at a concentration of 49.1 mg/L was above the RCRA metals concentration limits of 0.2 mg/L in the December 2021 Tank 202 liquid sample portion.
- All but three of the RCRA metals for the March 2022 Tank 202 sample were above RCRA/TCLP limit. The concentrations for Ba, Cd, Cr, Pb, and total mercury in the March 2022 Tank 202 sample were all higher than their RCRA limits and measured 2.24E+02 mg/L, 3.74E+01 mg/L, 4.24E+03 mg/L, < 3.03E+02 mg/L, and 1.56E+05 mg/L, respectively. The RCRA limits for these metals (Ba, Cd, Cr, Pb, and total mercury) are 100 mg/L, 1.0 mg/L, 5 mg/L, 5 mg/L and 0.2 mg/L, respectively. Only Ag (< 7.85E-01 mg/L), As (5.62E-01 mg/L), and Se (< 2.73E-01 mg/l) were below the RCRA limit requirement of 5 mg/L, 5 mg/L and 1.0 mg/L, respectively.
- Based on the elemental concentrations and molar ratios for select elements (Na/Ti, Na/Al, Na/Fe, Ti/Al, Ti/Fe and Al/Fe), the December 2021 Tank 201 sample solids is different from the March 2022 Tank 202 sample solids.
- Infrared (FT-IR) characterization of the December 2021 Tank 201 identified the presence of inorganic compounds, mainly bayerite/ gibbsite ($\text{Al}(\text{OH})_3$), carbonates, and nitrates, while the FT-IR characterization of the December 2021 Tank 202 air-dried organic emulsion sample identified a mixture of multi-cations (Na, Ca, Mg, Fe and Al) and double anions salts (CO_3^{2-} , NO_3^-).
- The ^1H NMR characterization of the December 2021 Tank 201 sample confirmed the presence of two main organic components. These organic compounds include the modifier (Cs-7SB) and ordinary non silicon grease, while the identified ^1H NMR spectra components for the partially water-soluble organic components of the Tank 201 sample included the modifier and sec. butylphenol, which is a known radiolytic decomposition product of the modifier.
- The ^1H NMR characterization of the air-dried December 2021 Tank 202 emulsion sample, with chloroform extraction, identified mainly the modifier (Cs-7SB). ^1H NMR spectra for water extracted air-dried Tank 202 emulsion sample showed two water soluble components, mainly sec. butyl phenol, and formate. Additionally, traces of BOBCalixC6, and aliphatic fluorides were also identified. The sec. butyl phenol and formates are probably decomposition products from the modifier.
- The 1.0 M nitric acid leaching of the March 2022 Tank 202 sample did not show any measurable effect on the mineral structure of the identified minerals tungsten carbide (WC), gibbsite [$\text{Al}(\text{OH})_3$], and quartz (SiO_2).
- The three Tanks 201 and Tank 202 samples (December Tank 201, December Tank 202, and March 2022 Tank 202) are different in their XRD patterns and mineralogy. The March 2022 Tank 202 sample contained more crystalline minerals and thus less amorphous phases.

- The XRD spectrum for the acid leached March Tank 202 solid fraction showed a smaller background shift due to the presence amorphous minerals when compared to the background shift in the XRD spectrum for the “as-received” March 2022 Tank 202 solid fraction, which would seem to indicate that the amorphous layers (organic layers) of the Tank 202 sample may be degraded in the acid leaching process.
- The ^1H NMR spectra for the nitric acid leached March 2022 Tank 202 solids fraction unexpectedly showed that the 1.0 M nitric acid leaching of the March 2022 Tank 202 solid fraction resulted in significant modification/degradation of the molecular structure of the Cs-7SB modifier. The fluorinated tails of the molecule and the ter-butyl groups were now missing with the nitric acid leaching of the Tank 202 solid fraction. This observation is contrary to other study results, based on simulant salt solutions, which indicate marginal degradation of the modifier at 30 and 60 °C for extended contact times. At this time, it is uncertain what causes the degradation of solvent components (Cs-7SB modifier) in nitric acid; however, it is possible that the degradation observed in nitric acid leaching is due to irregular chemistry (i.e., transition metal catalytic reactions).
- Three components were identified in the FT-IR data for nitric acid leached March 2022 Tank 202 residual solids, and these include the modifier, sec. butyl phenol (a decomposition product) and heavy metal nitrates (possibly from the nitric acid leaching) and carbonates.
- The ^1H NMR spectra for the organic (dichloromethane) leached March 2022 Tank 202 sample showed mainly decomposition products for the modifier and BobcalixC6, which includes propylene glycol group, grease, and ter-butyl alcohol, while the ^1H NMR spectra for the water extracted March 2022 Tank 202 sample identified the presence of the modifier and decomposition products, sec. butyl phenol and acetic acid/ acetone.
- The SEM/EDX identified elemental compositions for the acid leached March 2022 Tank 202 sample is not different from that of the “as- received” March 2022 Tank 202. The principal elemental compositions are similar and include F, Na, W, Ti, Fe, Al, Si, and total Hg.
- The leaching of the organic components in the April 2022 Tank 202 sample with dichloromethane resulted in the formation of an organic emulsion layer, which floated on the dichloromethane organic solvent and a slurry solids layer at the bottom of the container.
- The elemental components for the “as-received” April 2022 Tank 202 solids fraction are also present in measurable quantities in the organic emulsion layer and interstitial liquids, although in relatively lower concentrations. The concentrations for select elements, namely Al, Cd, Fe, Cr, Na, Ni, S, Ti, Zn, W and Hg are 1.19E+01mg/L, 2.07E-01 mg/L, 1.77E+01mg/l, 1.23E+02 mg/L, 6.04E+02 mg/L, 9.98E+00 mg/L, 3.65E+00 mg/L, 6.18E+02 mg/L, 9.22E-01 mg/L, 7.40E+01 mg/L, and 1.76E+03 mg/L, respectively.
- The April 2022 Tank 202 organic solvent leached solids, when introduced into a 50 mL capacity graduated cylinder containing Tank 202 filtrate (mother liquor) did not show any signs of floating and readily sank to the bottom of the graduated cylinder. This confirms that the organic solvent leached Tank 202 solids density was greater than the density of the mother liquor.
- The April 2022 Tank 202 solid fraction was immiscible with water probably due to the high mercury and organic material content of the solids fraction.
- The blending of water with the April 2022 Tank 202 solid fraction sample and dichloromethane, after 24 hours of settling of the mixture, resulted in the formation of two extra phases: an organic phase on top of the water (possibly an organic decomposition product), and an organic phase at the water-dichloromethane interface layer and considered to be the modifier or decomposition products.

The main insoluble inorganic submicron particles identified in the SWPF Tanks 201, and 202 samples include mercuric oxide (HgO), titanium oxide (TiO_2), iron oxides/hydroxides ($\text{Fe}_3\text{O}_4/\text{Fe}_2\text{O}_3$), gibbsite [$(\text{Al}(\text{OH})_3)$], zinc oxide (ZnO), and even tungsten carbide (WC). These inorganic particles are not only present in the solid and liquid fractions of these Tank 201 and Tank 202 samples, but also in the organic

emulsions in each SWPF tank samples sent for characterization. Mercuric oxide (HgO), titanium oxide (TiO₂) and iron oxides/hydroxides (Fe₃O₄/Fe₂O₃), particles are the most abundant particles based on their weight percent composition in each sample. These insoluble inorganic submicron particles may be responsible for the occasional plugging of the SWPF crossflow filtration system.

Aqueous media soluble salts, mostly sodium salts identified in these tank samples, include sodium nitrate, sodium carbonate, and sodium bicarbonate, while the caustic side solvent extraction organic compounds identified include the modifier (Cs-7B), BobCalixC6, Isopar-L, and radiolytic decomposition products including formates, sec. butyl phenol, fluorinated aliphatic compounds, acetic acid, acetone, and propylene ether.

The aqueous chemistry for the SWPF tank contents suggests that insoluble mercuric oxide particles (HgO), and transition metal particles (Fe₃O₄ and TiO₂), which can foul the crossflow filtrations systems, may be readily formed in the SWPF tanks. Thus, since the potential for the formation of these insoluble mercury submicron particles, especially mercuric oxide, and titanium oxide exists in the SWPF tanks, it is recommended that both the mercury and monosodium titanate (MST) loadings in the feeds be evaluated to determine if it is possible to lower their concentrations/quantity to minimize the formation of HgO and TiO₂.

9.0 Quality Assurance

The SWPF defined scope for SRNL, as shown in attachment A, details the nature of the work to be performed with SWPF Tank 201 and Tank 202 samples. The requested safety classification for this scope is production support (PS) classification; a Safety Significant Class does not apply to this work. Equipment with a General Service functional classification comprises the analytical measurement systems used to collect data for these characterizations. Standards used to calibrate these systems were purchased at level 2 with a certificate of analysis. Chemicals and reagents used in testing and sample preparation are purchased at levels 2 or 3 and standards are uniquely identified and traceable to NIST or equivalent per 1Q, 2-7 section 5.2.3.

To match the requested PS classification, the reports, calculations, and technical memoranda issued from this testing received technical review by design check (E7 Manual Procedure 2.60, Section 5.3). This document, including all calculations, was reviewed by Design Verification by Document Review^{9.10} SRNL documents the extent and type of review using the SRNL Technical Report Design Checklist contained in WSRC-IM-2002-00011, Rev. 2. The experimental work, the analyses, and peer checks all comply with the customer quality assurance (QA) requirements.

10.0 References

- (1) Peter V. Bonnesen, Frederick V. Sloop, Jr., and Nancy L. Engle, “Stability of the Caustic-Side Solvent Extraction (CSSX) Process Solvent: Effect of High Nitrite on Solvent Nitration,” ORNL/TM-2002/115, July 2002.
- (2) Ehab A. Abdelrahman, R. M. Hegazy, “Facile Synthesis of HgO Nanoparticles Using Hydrothermal Method for Efficient Photocatalytic Degradation of Crystal Violet Dye Under UV and Sunlight Irradiation” *Journal of Inorganic and Organometallic Polymers and Materials* <https://doi.org/10.1007/s10904-018-1005-6>.
- (3) Alireza Mohadesi, Mehdi ranjbar, and S.M. Hosseinpour-Mashkani, “solvent-free synthesis of mercury oxide nanoparticles by simple thermal decomposition method,” *Superlattices and Microstructure* 66 (2014) 48-53.
- (4) Elham Jalali, Shahab Maghsoudi, and Ebrahim Noroozian, “A novel method for biosynthesis of different polymorphs of TiO₂ nanoparticles as a protector for *Bacillus thuringiensis* from Ultraviolet” *Scientific Reports* | (2020) 10:426 | <https://doi.org/10.1038/s41598-019-57407-6>.
- (5) K. Patel, Sandip Mandal, Tapswani Padhi, Manoj Kumar sahu, “Synthesis of Magnetic Iron-oxide Nanoparticle through Micro emulsion for Environmental Application,” https://www.researchgate.net/figure/Figure-3-SEM-Image-and-EDX-spectrum-of-Magnetic-iron-oxide-nanoparticle_fig3_276265147.
- (6) Buzuayehu Abebe and H. C. Ananda Murthy, “Synthesis and Characterization of Ti-Fe Oxide Nanomaterials for Lead Removal,” *Journal of Nanomaterials* Volume 2018, Article ID 9651039, 10 pages <https://doi.org/10.1155/2018/9651039>.
- (7) L. N. Oji, and F. Fondeur “Characterization of the Soluble and Insoluble Portions of Solids from the Salt Waste Processing Facility Tank 201 and Tank 202 Samples,” SRNL-STI-2022-00145, Revision 1, May 2022.
- (8) Jacob G. Reynolds, Jacob K. McCoskey, and Daniel L. Herting, “Gibbsite Solubility in Hanford Nuclear Waste Approached from above and below Saturation,” DOI: 10.1021/acs.iecr.6b00743, *Ind. Eng. Chem. Res.* 2016, 55, 5465–5473.
- (9) “Technical Reviews”, Manual E7, Procedure 2.60, Revision 18, December 2, 2019.
- (10) “Savannah River National Laboratory Technical Report Design Check Guidelines,” WSRC-IM-2002-00011, Revision 2, August 2004.

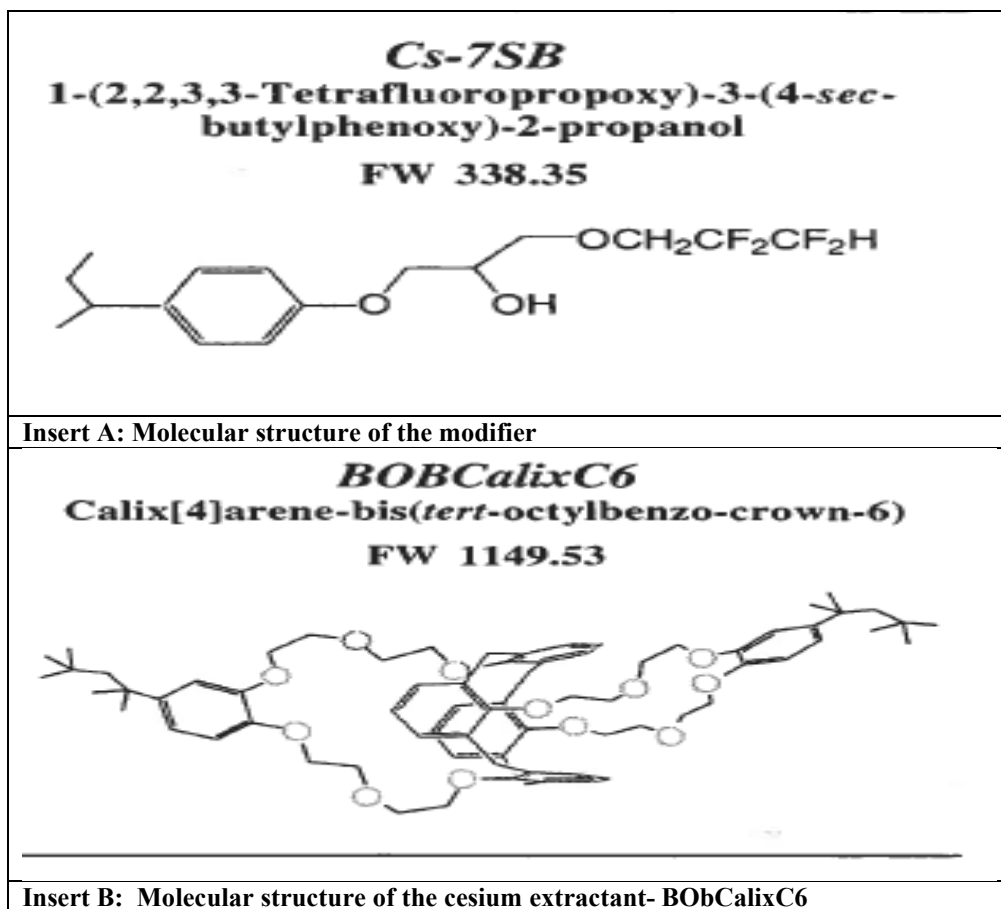
Appendix A: SRNL Scope for the Characterization of the soluble and insoluble portions of solids from SWPF Tank 201 and Tank 202 samples.

SRNL Scope

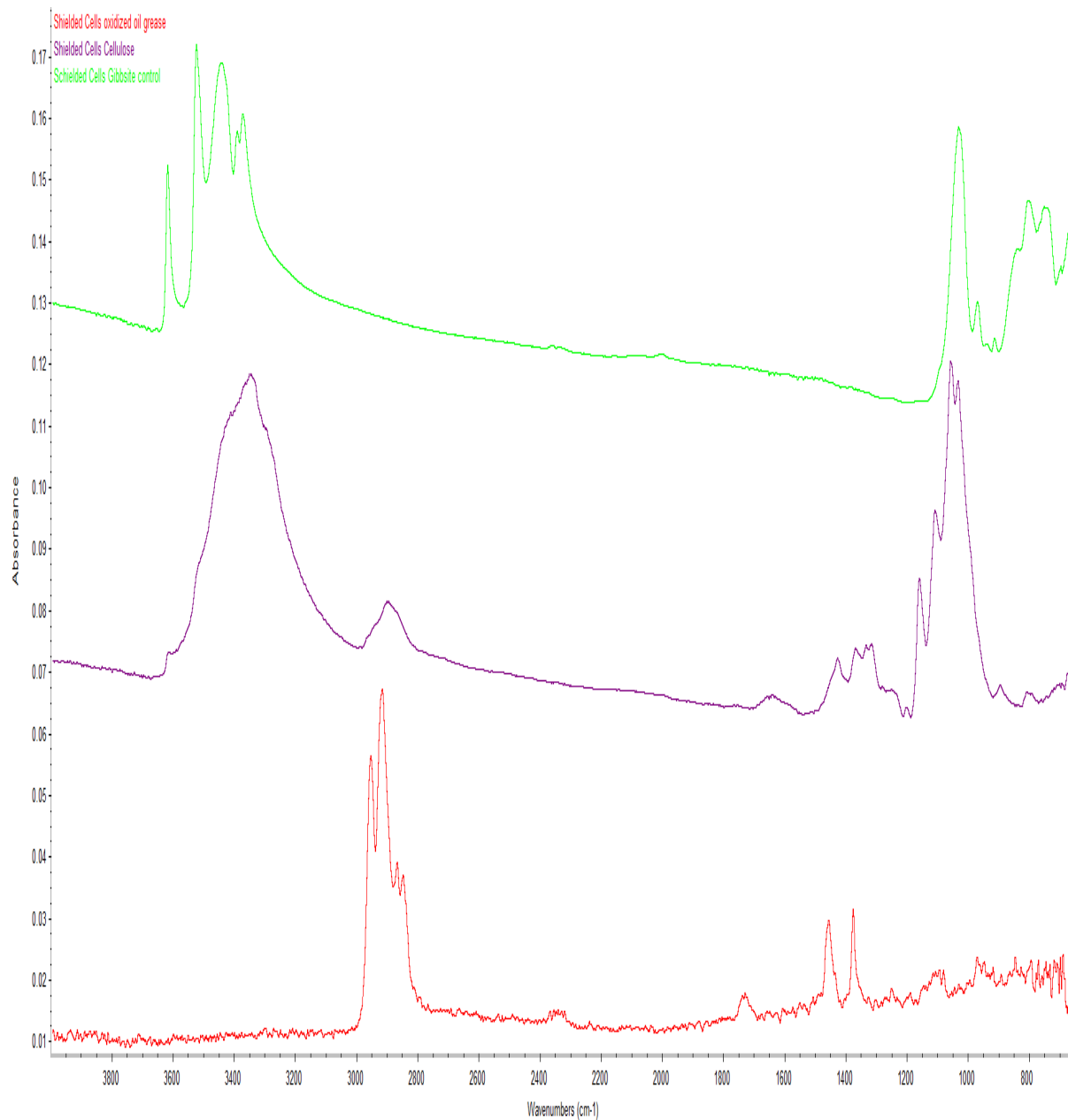
1. Characterize the soluble and insoluble portions of solids from TK-208 (Solvent Drain Tank). The SWPF Lab will prepare the samples by decanting as much liquid as practical.
 - a. Raw solids
 - i. SEM-EDS – Size and elemental composition
 - ii. XRD – Crystalline/semi-crystalline structure
 - iii. FTIR – Structural/Molecular composition
 - iv. Microtrac – solids may be suspended in a simulant salt solution for analyses
 - b. Acid leachate
 - i. Leach solids in nitric acid
 - ii. ICP-ES or ICP-AES for elemental composition of leachate
 - c. Residual solids
 - i. SEM-EDS – Size and elemental composition
 - ii. XRD – Crystalline/semi-crystalline structure
 - iii. FTIR – Structural/Molecular composition
 - iv. Microtrac – solids may be suspended in a simulant salt solution for PSA analyses
 - d. Evaluate mechanism of apparent buoyancy of solids including:
 - i. Filter solids to remove liquid
 - ii. Strip/leach organics from the solids using organic solvent. Phase ratio = 3.5 mL/g.
 - iii. After leaching, return solids to “mother liquor” (aqueous) and observe tendency to sink/rise.
 - iv. RCRA Metals and elemental analysis of solids (AQR digestion)
 - v. SEM/EDX for the solid fraction
 - e. Additional scope with April 2022 Tank 202 sample used for step (d(i)).
 - i. FT-IR & ^1H NMR characterization of thin emulsion layer from buoyancy test above (d(ii))
 - ii. To the wet cake solid fraction from filtering of the “as-received” sample, (d(i)), add water and report observation and then add DCM to mixture and report observations with shaking of the mixture. This will be a mixed settle observation. Phase ratio = 3.5 mL/g. Settling time of 24 hours for each test before final observation is made and Take pictures.
 - iii. To part of the wet cake solid fraction from filtering of the “as-received” sample above (d(i), leach with DCM and let it sit for 24 hours. Take pictures.
 - iv. Extract and digest (via Aqua Regia) the thin emulsion layer formed in test d(iii) above and characterize (ICP-ES for metals, and DMA for total Hg analysis).
2. Characterize the soluble and insoluble portions of solids from TK-201 (Decontaminated Salt Solution Coalescer).
 - a. Raw solids
 - i. SEM-EDS – Size and elemental composition
 - ii. XRD – Crystalline/semi-crystalline structure
 - iii. FTIR – Structural/Molecular composition
 - iv. Microtrac – solids may be suspended in a simulant salt solution for analyses
 - b. Acid leachate
 - i. Leach solids in nitric acid
 - ii. ICP-ES or ICP-AES
 - c. Residual solids
 - i. SEM-EDS – Size and elemental composition

- ii. XRD – Crystalline/semi-crystalline structure
 - iii. FTIR – Structural/Molecular composition
 - iv. Microtrac – solids may be suspended in a simulant salt solution for analyses
- d. Evaluate apparent buoyancy of solids including:
 - i. Mix solids in simulant salt solution and observe buoyancy
 - ii. Mix CSSX solvent in with simulant/solids mixture and observe buoyancy
 - iii. Strip solids of potential organics using suitable solvent (e.g., acetone, dichloromethane) and observe buoyancy in salt solution.

Appendix B. Molecular structure of Cs-7SB and BobCalixC6



Appendix C. FT-IR spectra for gibbsite control blanks showing the presence of extra organic peaks coming from the Shielded Cell oxidized oil grease (in red) and cellulose (in purple).



Appendix D. Mass Spectral Analyses of March 2022 Tank 202 Solid fraction.

| ICP-MS, m/z | Ug/g | mg/L | Likely element (s) |
|--------------------|-------------|-------------|---------------------------|
| 59 | 1.91E03 | 2.10E+03 | Co |
| 84 | 7.60E-01 | 8.36E-01 | Sr |
| 85 | 2.90E00 | 3.19E+00 | Rb |
| 86 | 2.98E01 | 3.28E+01 | Sr |
| 87 | 2.94E01 | 3.23E+01 | Rb, Sr |
| 88 | 2.67E02 | 2.94E+02 | Sr |
| 89 | 7.52E-01 | 8.27E-01 | Y |
| 90 | 1.43E01 | 1.57E+01 | Zr, Sr |
| 91 | 7.87E00 | 8.66E+00 | Zr |
| 92 | 1.66E01 | 1.83E+01 | Zr, Mo |
| 93 | 1.71E01 | 1.88E+01 | Nb |
| 94 | 1.47E01 | 1.62E+01 | Nb, Mo |
| 95 | 1.05E01 | 1.16E+01 | Mo |
| 96 | 1.54E01 | 1.69E+01 | Ru, Zr, Mo |
| 97 | 7.07E00 | 7.78E+00 | Mo, Tc |
| 98 | 1.50E01 | 1.65E+01 | Ru, Mo, Tc |
| 99 | 3.73E00 | 4.10E+00 | Tc, Ru |
| 100 | 7.58E00 | 8.34E+00 | Ru, Mo |
| 101 | 6.07E00 | 6.68E+00 | Ru |
| 102 | 5.53E00 | 6.08E+00 | Ru, Pd |
| 103 | 1.13E00 | 1.24E+00 | Rh |
| 104 | 3.45E00 | 3.80E+00 | Ru, Pd |
| 105 | 2.16E00 | 2.38E+00 | Pd |
| 106 | 2.25E00 | 2.48E+00 | Pd, Cd |
| 107 | 1.93E00 | 2.13E+00 | Ag |
| 108 | 7.81E-01 | 8.6E-01 | Pd, Cd |
| 109 | 8.61E-01 | 9.47E-01 | Ag |
| 110 | 3.63E00 | 3.99E+00 | Pd, Cd |
| 111 | 4.74E00 | 5.21E+00 | Cd |
| 112 | 9.17E00 | 1.01E+01 | Sn, Cd |
| 113 | 4.65E00 | 5.12E+00 | In, Cd |
| 114 | 1.12E01 | 1.23E+01 | Sn, Cd |
| 116 | 3.37E00 | 3.71E+00 | Sn, Cd |
| 117 | 5.40E-01 | 5.94E-01 | Sn |
| 118 | 1.64E00 | 1.80E+00 | Sn |
| 119 | 3.93E00 | 4.32E+00 | Sn |
| 120 | 2.25E00 | 2.48E+00 | Sn |
| 121 | <9.92E-02 | <1.09E-01 | Sb |
| 122 | 4.88E-01 | 5.37E-01 | Te, Sn |
| 123 | 4.61E-02 | 5.07E-02 | Sb, Te |
| 124 | 7.83E-01 | 8.61E-01 | Te, Sn |
| 125 | <1.98E-02 | <2.18E-02 | Sb, Te |
| 126 | 1.51E00 | 1.66E+00 | Te |
| 128 | <3.97E-02 | <4.37E-02 | Te |
| 130 | 1.01E00 | 1.11E+00 | Te |
| 133 | 3.14E01 | 3.45E+01 | Cs |
| 134 | 4.34E00 | 4.77E+00 | Ba, Cs |

Appendix D. Mass Spectral Analyses of March 2022 Tank 202 Solid fraction Continued.

| ICP-MS, m/z | Ug/g | mg/L | Likely element (s) |
|-------------|-----------|-----------|--------------------|
| 135 | 1.61E01 | 1.77E+01 | Ba, Cs |
| 136 | 1.50E01 | 1.65E+01 | Ce, Ba |
| 137 | 4.47E01 | 4.92E+01 | Cs, Ba, La |
| 138 | 1.31E02 | 1.44E+02 | Ba, La, Ce |
| 139 | 2.33E00 | 2.56E+00 | La |
| 140 | 2.07E00 | 2.28E+00 | Ce |
| 141 | 5.93E-01 | 6.52E-01 | Pr |
| 142 | 4.84E-01 | 5.32E-01 | Nd, Ce |
| 143 | 9.74E-02 | 1.07E-01 | Nd., Pm |
| 144 | 1.92E-01 | 2.11E-01 | Nd, Sm, Pm |
| 145 | 6.73E-02 | 7.40E-02 | Nd, Pm |
| 146 | 1.39E-01 | 1.53E-01 | Nd, Sm |
| 147 | 2.61E-02 | 2.87E-02 | Sm, Ti |
| 148 | 6.57E-02 | 7.23E-02 | Nd, Gd, Sm |
| 149 | 2.19E-02 | 2.41E-02 | Sm |
| 150 | 5.74E-02 | 6.31E-02 | Nd, Gd, Sm, Eu |
| 151 | <1.98E-02 | <2.18E-02 | Eu |
| 152 | 5.99E-02 | 6.59E-02 | Gd, Sm, Eu |
| 153 | 3.94E-02 | 4.33E-02 | Eu |
| 154 | 1.18E-01 | 1.30E-01 | Gd, Sm, Eu, Dy |
| 155 | 1.93E-01 | 2.12E-01 | Gd |
| 156 | 4.70E-02 | 5.17E-02 | Gd, Dy |
| 157 | 3.23E-02 | 3.55E-02 | Gd, Tb |
| 158 | 4.70E-02 | 5.17E-02 | Gd, Dy, Tb |
| 159 | 2.35E-02 | 2.59E-02 | Tb |
| 160 | 4.08E-02 | 4.49E-02 | Gd, Dy |
| 161 | 2.21E-02 | 2.43E-02 | Dy |
| 162 | 2.99E-02 | 3.29E-02 | Dy, Er |
| 163 | 2.86E-02 | 3.15E-02 | Dy, Ho |
| 164 | 3.43E-02 | 3.77E-02 | Dy, Er |
| 165 | 2.09E-02 | 2.30E-02 | Ho |
| 166 | 2.19E-02 | 2.41E-02 | Er, Ho |
| 167 | <1.98E-02 | <2.18E-02 | Er |
| 168 | <1.98E-02 | <2.18E-02 | Er, Yb |
| 169 | <1.98E-02 | <2.18E-02 | Tm |
| 170 | <1.98E-02 | <2.18E-02 | Er, Yb |
| 171 | <1.98E-02 | <2.18E-02 | Yb |
| 172 | <1.98E-02 | <2.18E-02 | Yb |
| 173 | <1.98E-02 | <2.18E-02 | Yb |
| 174 | 2.14E-02 | 2.35E-02 | Yb, Hf |
| 175 | <1.98E-02 | <2.18E-02 | Lu |
| 176 | 2.39E-02 | 2.63E-02 | Lu, Hf, Yb |
| 177 | 4.54E-02 | 4.99E-02 | Hf |
| 178 | 7.10E-02 | 7.81E-02 | Hf |
| 179 | 3.84E-02 | 4.22E-02 | Hf |
| 180 | 7.39E-01 | 8.13E-01 | Hf, W, Ta |
| 181 | 2.37E00 | 2.61E+00 | Ta |
| 182 | 1.35E02 | 1.49E+02 | Hf, W |

Appendix D. Mass Spectral Analyses of March 2022 Tank 202 Solid fraction Continued.

| ICP-MS, m/z | Ug/g | Mg/L | Likely element (s) |
|-------------|-----------|-----------|--------------------|
| 183 | 8.33E01 | 9.16E+01 | W |
| 184 | 1.51E02 | 1.66E+02 | W |
| 185 | <3.97E-02 | <4.37E-02 | Re |
| 186 | 1.94E02 | 2.13E+02 | Os, W |
| 187 | 2.18E-02 | 2.40E-02 | Re, Os |
| 188 | 1.98E-02 | <2.18E-02 | Os |
| 189 | 1.98E-02 | <2.18E-02 | Os |
| 191 | 3.89E-02 | 4.28E-02 | Ir |
| 193 | 6.96E-02 | 7.66E-02 | Ir, Pt |
| 194 | 1.74E-01 | 1.91E-01 | Pt |
| 195 | 1.79E-01 | 1.97E-01 | Pt |
| 196 | 1.03E02 | 1.13E+02 | Hg, Pt |
| 203 | 1.22E00 | 1.34E+00 | Tl |
| 205 | 1.85E00 | 2.04E+00 | Tl |
| 206 | 3.96E01 | 4.36E+01 | Pb |
| 207 | 3.44E01 | 3.78E+01 | Pb |
| 208 | 8.34E01 | 9.17E+01 | Pb |
| 229 | <1.98E-02 | <2.18E-02 | Th |
| 230 | <1.98E-02 | <2.18E-02 | Th |
| 232 | 1.31E00 | 1.44E+00 | Th, U |
| 233 | 9.13E-02 | 1.00E-01 | U |
| 234 | 6.34E-01 | 6.97E-01 | U |
| 235 | 4.62E00 | 5.08E+00 | U |
| 236 | 9.59E-01 | 1.05E+00 | U |
| 237 | 3.44E00 | 3.78E+00 | Np |
| 238 | 2.03E02 | 2.23E+02 | U, Pu |
| 239 | 3.71E01 | 4.08E+01 | Pu |
| 240 | 5.33E00 | 5.86E+00 | Pu |
| 241 | 3.59E-01 | 3.95E-01 | Pu, Am |
| 242 | 5.86E-01 | 6.45E-01 | Pu, Am |
| 243 | <1.98E-02 | <2.18E-02 | Pu, Cm |
| 244 | <1.98E-02 | <2.18E-02 | Pu, Cm |
| 245 | <1.98E-02 | <2.18E-02 | Cm |
| 246 | <1.98E-02 | <2.18E-02 | Cm |
| 247 | <1.98E-02 | <2.18E-02 | Cm, Bk |
| 248 | <3.97E-02 | <4.37E-02 | Cm |
| 249 | <1.98E-02 | <2.18E-02 | Cf |
| 250 | <1.98E-02 | <2.18E-02 | Cf |
| 251 | <1.98E-01 | <2.18E-01 | Cf |
| 252 | <5.95E-02 | <6.55E-02 | Cf, Cm |

Appendix D2. Mass Spectral Analyses of April 2022 Tank 202 Emulsion Layer.

| ICP-MS, m/z | Ug/g | mg/L | Likely element (s) |
|-------------|------------|------------|--------------------|
| 59 | 1.14E+01 | 1.26E+01 | Co |
| 84 | 3.48E-03 | 3.82E-03 | Sr |
| 85 | 1.51E-01 | 1.66E-01 | Rb |
| 86 | 1.45E-01 | 1.59E-01 | Sr |
| 87 | 4.16E-01 | 4.57E-01 | Rb, Sr |
| 88 | 1.37E+00 | 1.51E+00 | Sr |
| 89 | 3.99E-03 | 4.39E-03 | Y |
| 90 | 1.49E-01 | 1.64E-01 | Zr, Sr |
| 91 | 6.03E-02 | 6.64E-02 | Zr |
| 92 | 1.57E-01 | 1.73E-01 | Zr, Mo |
| 93 | 5.08E-01 | 5.58E-01 | Nb |
| 94 | 1.30E-01 | 1.44E-01 | Nb, Mo |
| 95 | 1.26E-01 | 1.39E-01 | Mo |
| 96 | 1.32E-01 | 1.45E-01 | Ru, Zr, Mo |
| 97 | 9.21E-02 | 1.01E-01 | Mo, Tc |
| 98 | 1.76E-01 | 1.93E-01 | Ru, Mo, Tc |
| 99 | 2.21E-02 | 2.43E-02 | Tc, Ru |
| 100 | 9.89E-02 | 1.09E-01 | Ru, Mo |
| 101 | 4.28E-02 | 4.71E-02 | Ru |
| 102 | 3.89E-02 | 4.28E-02 | Ru, Pd |
| 103 | 1.25E-02 | 1.37E-02 | Rh |
| 104 | 3.36E-02 | 3.69E-02 | Ru, Pd |
| 105 | 3.74E-02 | 4.12E-02 | Pd |
| 106 | 4.35E-02 | 4.78E-02 | Pd, Cd |
| 107 | < 6.81E-02 | < 7.50E-02 | Ag |
| 108 | < 4.09E-02 | < 4.50E-02 | Pd, Cd |
| 109 | < 6.81E-02 | < 7.50E-02 | Ag |
| 110 | 3.73E-02 | 4.10E-02 | Pd, Cd |
| 111 | 2.68E-02 | 2.95E-02 | Cd |
| 112 | 5.35E-02 | 5.89E-02 | Sn, Cd |
| 113 | 2.54E-02 | 2.79E-02 | In, Cd |
| 114 | 6.47E-02 | 7.11E-02 | Sn, Cd |
| 116 | 2.00E-02 | 2.20E-02 | Sn, Cd |
| 117 | 3.35E-03 | 3.69E-03 | Sn |
| 118 | 1.04E-02 | 1.15E-02 | Sn |
| 119 | 2.46E-02 | 2.71E-02 | Sn |
| 120 | 1.43E-02 | 1.57E-02 | Sn |
| 121 | 4.28E-03 | 4.71E-03 | Sb |
| 122 | 3.04E-03 | 3.35E-03 | Te, Sn |
| 123 | 3.21E-03 | 3.53E-03 | Sb, Te |
| 124 | 4.84E-03 | 5.33E-03 | Te, Sn |
| 125 | < 1.36E-03 | < 1.50E-03 | Sb, Te |
| 126 | 9.98E-03 | 1.10E-02 | Te |
| 128 | < 1.36E-03 | < 1.50E-03 | Te |
| 130 | 6.23E-03 | 6.86E-03 | Te |
| 133 | 2.35E+00 | 2.58E+00 | Cs |
| 134 | 2.28E-02 | 2.51E-02 | Ba, Cs |

Appendix D2. Mass Spectral Analyses of April 2022 Tank 202 Emulsion Layer- Continued.

| ICP-MS, m/z | Ug/g | mg/L | Likely element (s) |
|-------------|------------|------------|--------------------|
| 135 | 3.02E-01 | 3.32E-01 | Ba, Cs |
| 136 | 7.90E-02 | 8.69E-02 | Ce, Ba |
| 137 | 7.81E-01 | 8.60E-01 | Cs, Ba, La |
| 138 | 7.55E-01 | 8.30E-01 | Ba, La, Ce |
| 139 | 1.26E-02 | 1.39E-02 | La |
| 140 | 1.62E-02 | 1.78E-02 | Ce |
| 141 | 4.04E-03 | 4.45E-03 | Pr |
| 142 | 3.69E-03 | 4.06E-03 | Nd, Ce |
| 143 | < 1.36E-03 | < 1.50E-03 | Nd., Pm |
| 144 | 1.71E-03 | 1.88E-03 | Nd, Sm, Pm |
| 145 | < 1.36E-03 | < 1.50E-03 | Nd, Pm |
| 146 | < 1.36E-03 | < 1.50E-03 | Nd, Sm |
| 147 | < 1.36E-03 | < 1.50E-03 | Sm, Ti |
| 148 | < 1.36E-03 | < 1.50E-03 | Nd, Gd, Sm |
| 149 | < 1.36E-03 | < 1.50E-03 | Sm |
| 150 | < 1.36E-03 | < 1.50E-03 | Nd, Gd, Sm, Eu |
| 151 | < 1.36E-03 | < 1.50E-03 | Eu |
| 152 | < 1.36E-03 | < 1.50E-03 | Gd, Sm, Eu |
| 153 | < 1.36E-03 | < 1.50E-03 | Eu |
| 154 | < 1.36E-03 | < 1.50E-03 | Gd, Sm, Eu, Dy |
| 155 | 2.08E-03 | 2.29E-03 | Gd |
| 156 | < 1.36E-03 | < 1.50E-03 | Gd, Dy |
| 157 | < 1.36E-03 | < 1.50E-03 | Gd, Tb |
| 158 | < 1.36E-03 | < 1.50E-03 | Gd, Dy, Tb |
| 159 | < 1.36E-03 | < 1.50E-03 | Tb |
| 160 | < 1.36E-03 | < 1.50E-03 | Gd, Dy |
| 161 | < 1.36E-03 | < 1.50E-03 | Dy |
| 162 | < 1.36E-03 | < 1.50E-03 | Dy, Er |
| 163 | < 1.36E-03 | < 1.50E-03 | Dy, Ho |
| 164 | < 1.36E-03 | < 1.50E-03 | Dy, Er |
| 165 | < 1.36E-03 | < 1.50E-03 | Ho |
| 166 | < 1.36E-03 | < 1.50E-03 | Er, Ho |
| 167 | < 1.36E-03 | < 1.50E-03 | Er |
| 168 | < 1.36E-03 | < 1.50E-03 | Er, Yb |
| 169 | < 1.36E-03 | < 1.50E-03 | Tm |
| 170 | < 1.36E-03 | < 1.50E-03 | Er, Yb |
| 171 | < 1.36E-03 | < 1.50E-03 | Yb |
| 172 | < 1.36E-03 | < 1.50E-03 | Yb |
| 173 | < 1.36E-03 | < 1.50E-03 | Yb |
| 174 | < 1.36E-03 | < 1.50E-03 | Yb, Hf |
| 175 | < 1.36E-03 | < 1.50E-03 | Lu |
| 176 | < 1.36E-03 | < 1.50E-03 | Lu, Hf, Yb |
| 177 | 1.37E-03 | 1.50E-03 | Hf |
| 178 | 2.05E-03 | 2.26E-03 | Hf |
| 179 | < 1.36E-03 | < 1.50E-03 | Hf |
| 180 | 9.01E-02 | 9.91E-02 | Hf, W, Ta |
| 181 | 2.52E-02 | 2.77E-02 | Ta |
| 182 | 1.79E+01 | 1.97E+01 | Hf, W |

Appendix D2. Mass Spectral Analyses of April 2022 Tank 202 Emulsion Layer- Continued

| ICP-MS, m/z | Ug/g | Mg/L | Likely element (s) |
|-------------|------------|------------|--------------------|
| 183 | 9.41E+00 | 1.04E+01 | W |
| 184 | 2.05E+01 | 2.26E+01 | W |
| 185 | 2.03E-03 | 2.23E-03 | Re |
| 186 | 1.93E+01 | 2.13E+01 | Os, W |
| 187 | 2.24E-03 | 2.46E-03 | Re, Os |
| 188 | 6.38E-03 | 7.01E-03 | Os |
| 189 | 1.11E-02 | 1.22E-02 | Os |
| 191 | 1.52E-03 | 1.67E-03 | Ir |
| 193 | < 2.73E-03 | < 3.00E-03 | Ir, Pt |
| 194 | 6.33E-01 | 6.96E-01 | Pt |
| 195 | 3.77E+01 | 4.15E+01 | Pt |
| 196 | 3.09E-02 | 3.40E-02 | Hg, Pt |
| 203 | 1.81E+01 | 1.99E+01 | Tl |
| 205 | 3.40E-02 | 3.74E-02 | Tl |
| 206 | 2.69E-01 | 2.95E-01 | Pb |
| 207 | 2.32E-01 | 2.55E-01 | Pb |
| 208 | 5.61E-01 | 6.17E-01 | Pb |
| 229 | < 1.36E-03 | < 1.50E-03 | Th |
| 230 | < 1.36E-03 | < 1.50E-03 | Th |
| 232 | 2.13E-02 | 2.34E-02 | Th, U |
| 233 | < 1.36E-03 | < 1.50E-03 | U |
| 234 | 3.30E-03 | 3.63E-03 | U |
| 235 | 2.74E-02 | 3.01E-02 | U |
| 236 | 6.01E-03 | 6.61E-03 | U |
| 237 | 2.06E-02 | 2.26E-02 | Np |
| 238 | 1.34E+00 | 1.48E+00 | U, Pu |
| 239 | 2.75E-01 | 3.02E-01 | Pu |
| 240 | 3.58E-02 | 3.93E-02 | Pu |
| 241 | 2.42E-03 | 2.66E-03 | Pu, Am |
| 242 | 3.92E-03 | 4.31E-03 | Pu, Am |
| 243 | < 1.36E-03 | < 1.50E-03 | Pu, Cm |
| 244 | < 1.36E-03 | < 1.50E-03 | Pu, Cm |
| 245 | < 1.36E-03 | < 1.50E-03 | Cm |
| 246 | < 1.36E-03 | < 1.50E-03 | Cm |
| 247 | < 1.36E-03 | < 1.50E-03 | Cm, Bk |
| 248 | < 1.36E-03 | < 1.50E-03 | Cm |
| 249 | < 1.36E-03 | < 1.50E-03 | Cf |
| 250 | < 1.36E-03 | < 1.50E-03 | Cf |
| 251 | < 1.36E-03 | < 1.50E-03 | Cf |
| 252 | < 1.36E-03 | < 1.50E-03 | Cf, Cm |

Appendix E. Analytical Methods

FT-IR spectroscopy is the application of infra-red spectroscopy to identify chemical substances or functional groups (organic and inorganic materials) in solid, liquid, or gaseous forms. FT-IR spectroscopy is also used to characterize new materials or identify and verify known and unknown samples.

Proton Nuclear magnetic resonance (in this case proton ^1H NMR) is the application of nuclear magnetic resonance in ^1H NMR spectroscopy with respect to hydrogen-1 nuclei within the molecules of a substance, in order to determine the structure of its molecules.

Inductively coupled plasma atomic emission spectroscopy (ICP-AES) is an emission spectroscopy that identifies and quantifies the elemental composition of samples. ICP-AES is based on exciting the metal atoms/ions of the samples using a plasma and analyzing the emission wavelength of the electromagnetic radiation, which is typical of that metal or element of interest.

X-ray diffraction analysis (XRD) is a technique used in materials science to determine and identify the crystallographic structure of a material or mineral. XRD works by irradiating a material with incident X-rays and then measuring the intensities and scattering angles of the X-rays that leave the material.

Energy dispersive X-ray spectroscopy (EDX) is an analytical method for chemical characterization of materials. EDX systems are generally attached to an electron microscopy instrument such as transmission electron microscopy (TEM) or **scanning electron microscopy (SEM)**.

Particle size analysis (PSA) is laboratory techniques which determines the size range, and/or the average, or mean size of the particles in a powder or liquid sample.

Toxicity Characteristic Leaching Procedure (TCLP) is a leaching and chemical analysis process used to determine whether there are hazardous elements present in a solid waste [United States Environmental Protection Agency (EPA) method 1311]. The test simulates leaching through a landfill and can provide a rating that can prove if the solid waste is dangerous to the environment, such as determining if the waste is a hazardous waste by exhibiting the characteristic of toxicity. TCLP is designed to determine the mobility of both organic and inorganic analytes present in liquid, solid, and multiphasic wastes. This is usually used to determine if a waste may meet the definition of EPA Toxicity, that is, carrying a hazardous waste code under RCRA (40 CFR Part 261) of D004 through D052.

DISTRIBUTION LIST:

| Name | Electronic address |
|-------------------------|-------------------------------------------|
| <u>Alex Cozzi</u> | <u>alex.cozzi@srnl.doe.gov</u> |
| Boyd Wiedenman | <u>boyd.wiedenman@srnl.doe.gov</u> |
| <u>Sharon Marra</u> | <u>sharon.marra@srnl.doe.gov</u> |
| <u>Connie Herman</u> | <u>connie.herman@srnl.doe.gov</u> |
| <u>Frank Pennebaker</u> | <u>frank.pennebaker@srnl.doe.gov</u> |
| <u>Gregg Morgan</u> | <u>gregg.morgan@srnl.doe.gov</u> |
| <u>Terri Fellingner</u> | <u>terri.fellinger@srs.gov</u> |
| C. A. Nash | <u>charles.nash@srnl.doe.gov</u> |
| R. O. Voegtlen | <u>robert.voegtlen@srs.gov</u> |
| D. T. Wallace | <u>david.wallace@srs.gov</u> |
| Rachel Seeley | <u>Rachel.Seeley@srs.gov</u> |
| Christine Baker | <u>Christine.Baker@srs.gov</u> |
| Bill Holtzscheiter | <u>bill.holtzscheiter@srs.gov</u> |
| K. Taylor-Pashow | <u>kathryn.taylor-pashow@srnl.doe.gov</u> |
| J. Manna | <u>Joseph.Manna@srnl.doe.gov</u> |
| C.J. Martino | <u>chris.martino@srnl.doe.gov</u> |
| T. B. Peters | <u>thomas.peters@srnl.doe.gov</u> |
| J.E. Occhipinti | <u>John.Occhipinti@srs.gov</u> |
| B. L. Garcia-Diaz | <u>Brenda.Garcia-Diaz@srnl.doe.gov</u> |
| B. Lee | <u>brady.lee@srnl.doe.gov</u> |
| N. Peralta | <u>nixon.peralta@srs.gov</u> |
| C. J. Bannochie | <u>cj.bannochie@srnl.doe.gov</u> |
| J.G. Jackson, JR | <u>dennis.jackson@srnl.doe.gov</u> |
| S. J. Livermore | <u>sean.livermore@srs.gov</u> |
| R. T. McNew | <u>ryan.mcnew@srs.gov</u> |
| D. J. Baxter | <u>dylan.baxter@srs.gov</u> |
| A.I Silker | <u>aubrev.silker@srs.gov</u> |
| H. P. Boyd | <u>helen.boyd@srs.gov</u> |
| J. W. Ray | <u>jeff.ray@srs.gov</u> |
| J. D. Ledbetter | <u>jeremiah.ledbetter@srs.gov</u> |
| C. S. Weston | <u>christopher.weston@srs.gov</u> |
| M. L. Johnson | <u>mark-l.johnson@srs.gov</u> |
| F. Fondeur | <u>fernando.fondeur@srnl.doe.gov</u> |
| Keeli Fricks, | <u>keeli.fricks@srs.gov</u> |
| Alex Luzzatti | <u>Alexander.Luzzatti@srs.gov</u> |
| William F. Bates | <u>william.bates@srnl.doe.gov</u> |
| Mark Johnson | <u>mark-l.johnson@srs.gov</u> |
| C. J. Conner | <u>clifford.conner@srs.gov</u> |
| J. W. Schulte | <u>justin.schulte@srs.gov</u> |
| Wesley H. Woodham | <u>wesley.woodham@srnl.doe.gov</u> |